Université de Montréal

MicroRNA signature of tumor infiltrated CD8+ T lymphocytes under αPD-L1 immunotherapy treatment in the context of the melanoma murine model and the effects of miR-21 on the CD8+ T cells.

Unité académique de Microbiologie, infectiologie et immunologie, Faculté de Médecine

Mémoire présenté en vue de l'obtention du grade de Maîtrise ès sciences
en Microbiologie et Immunologie

Février 2022

Université de Montréal

Unité académique de Microbiologie, infectiologie et immunologie, Faculté de Médecine

---

Ce mémoire intitulé

MicroRNA signature of tumor infiltrated CD8+ T lymphocytes under αPD-L1 immunotherapy treatment in the context of the melanoma murine model and the effects of miR-21 on the CD8+ T cells.

Présenté par

Linda Castoun-Puckett

A été évalué par un jury composé des personnes suivantes

Jean-Sébastien Delisle

Président-rapporteur

Christopher E Rudd

Directeur de recherche

Étienne Gagnon

Membre du jury

Résumé

L'étude des microARNs (miARNs) en immuno-oncologie est devenue un sujet d'intérêt ayant le potentiel d'augmenter le rejet des tumeurs et d'aider les patients atteints du cancer. Les cellules T $CD8^+$ ont la capacité d'éliminer les cellules cancéreuses dans une tumeur. Le sujet que j'aborde dans ce mémoire est à propos de miARNs spécifiques exprimés suite au blocage par anticorps du point de contrôle immunitaire PD-1 ou son ligand PD-L1 (anti-PD-L1 ou αPD-L1) utilisé pour traiter des tumeurs. Par le biais de l'utilisation d'un modèle de blocage des points de contrôle immunitaire (BCI) αPD-L1 dans le mélanome B16 pour des souris C57BL/6j, mon travail a identifié plusieurs miARNs dans les cellules T $CD8^+$ infiltrant les tumeurs (TILs) dont l'expression différait entre les souris traitées et les souris non traitées. Parmi la liste des 50 miARNs identifiés, l'expression de mmu-miR-21a-5p et mmu-miR-155-5p a augmenté dans les $CD8^+$ TILs provenant du traitement αPD-L1. Les deux miARNs augmentés dans les cellules immunitaires ciblent des régulateurs immunitaires clé tels que Transforming Growth Factor β Receptor 2 (TGFBR2) et certains autres regulateurs. Parmi les cibles intéressantes, il est possible de diminuer l'expression de Programmed Death 1 (PD-1). Au niveau de la transcription, l'expression de Pdcd1 (gène de PD-1) était réduite. Lors des analyses de cytométrie, une augmentation de PD-1 fut observée sur les cellules T $CD8^+$ transduites avec miR-21 mimique. Cette augmentation de PD-1 a également été aperçue dans les cellules T $CD8^+$ après le transfert de cellules OT-I transduites avec miR-21 mimique. Mon travail a montré par le transfert des cellules T $CD8^+$ OT-I surexprimant miR-21 une régression du mélanome B16 et une augmentation de l'activité cytotoxique des cellules T $CD8^+$. De plus, le transfert des cellules OT-I transduites avec miR-21 mimique change le phénotype des cellules T $CD8^+$ et l'infiltration des $CD4^+$ dans les tumeurs. Ce projet a identifié un potentiel miARN dans la régulation du blocage des points de contrôle immunitaire αPD-1.

Mots-clé : microARN, miR-21, miR-155, Transfert de cellule adoptive (ACT), PD-1, $CD8^+$.

Abstract

The study of microRNAs (miRNAs) in immuno-oncology has become a topic of interest with the potential to increase tumor rejection and to help cancer patients. $CD8^+$ T cells are the population with the ability to eliminate cancer cells within a tumor. The question that I addressed in this thesis is whether specific miRNAs are engaged by anti (α)-PD-1 immune checkpoint blockade (ICB) in the rejection of cancer. By using a model of αPD-L1 ICB in the B16 melanoma in C57BL/6j mice, my work identified several specific miRNAs in tumor-infiltrated $CD8^+$ T cells (TILs) from treated versus untreated mice. Among 50 miRNAs, the expression of mmu-miR-21a-5p and mmu-miR-155-5p increased in $CD8^+$ TILs from αPD-L1 treatment. Importantly, the miRNAs are enriched in immune cells and target key mediators such as Transforming Growth Factor β Receptor 2 (TGFBR2) and other immune regulators. Amongst interesting targets, it could be possible to decrease the expression of Programmed Death 1 (PD-1). At the transcriptional level, the expression of Pdcd1 (PD-1 gene) was decreased. Confirmational FACS analysis showed an increase in PD-1 expression in CD8+ T cells transduced with the miR-21 mimic. This was also observed in $CD8^+$ T cells after cell transfer of OT-I cells transduced with miR-21 mimic into mice. Also, as would be expected for a key mediated of αPD-1 ICB, my work showed that the adoptive cell transfer of OT-I T-cells with altered miR-21 was more effective against B16 melanoma and increased the cytotoxic activity of CD8+ T-cells. In addition, the transfer of OT-I cells transduced with miR-21 mimic changed the phenotype of the $CD8^+$ T cells and the infiltration of $CD4^+$ in the tumor. This work has identified a putative miRNA in the regulation of αPD-1 immune checkpoint blockade.

Keywords: microRNA, miR-21, miR-155, adoptive cell transfer (ACT), PD-1, $CD8^+$.

Table des matières

List of Figures

List of Tables

List of Abbreviations

4E-BP1 (EIF4EBP2): Eukaryotic translate initiation factor 4E-binding protein 1

ACT: Adoptive cell transfer

ADAP: Arf-GAP with dual PH domain-containing protein

Ago: Argonaut

AICD: Activated immune cells death

AKT: RAC-alpha serine/threonine-protein kinase

AP-1: Activator protein 1

APC: Antigen-presenting cells

Arf-GAP: ADP-ribosylation factor GTPase-activating protein

Arp2/3: Actin Related Protein *2/*3

BAD: Bcl2-associated agonist of cell death

BCL: B-cell lymphoma

BLAST: Basic Local Alignment Search Tool

BVDV: Bovine viral diarrhea virus

CCR4-NOT: carbon catabolite repression 4–negative on TATA-less

CAF: Cancer-associated fibroblasts

CAF1: Chromatin assembly factor 1

CARMA1: Caspase recruitment domain-containing membrane-associated guanylate kinase protein-1

Ccd42: cell division cycle 42

cDNA: complementary DNA

DCP: Decapping

CHD: chromodomain helicase DNA-binding protein

CREB: cAMP response element-binding protein

CTL: Control

CTLA-4: Cytotoxic T-lymphocyte antigen-4

DAG: Diacylglycerol

DBNL: Drebrin-like protein

DC: Dendritic cell

DGCR8: DiGeorge syndrome critical region gene 8

DNMT: DNA (cytosine-5)-methyltransferase

DNA: Deoxyribonucleic acid

dLN: draining lymph node

DUSP10: Dual-specificity phosphatase 10

E. coli: Escherichia coli

EDC3: Enhancer of mRNA-decapping protein 3

eIF: eukaryotic initiation factor

ER: Endoplasmic reticulum

EOMES: Eomesodermin

FACS: fluorescence-activated cell sorting

FasL: Fas ligand

FBS: Fetal Bovine Serum

FBXO11: F-Box Protein 11

FERMT3: FERM Domain Containing Kindlin 3

FOSL2: Fos-related antigen 2

Foxo1: Forkhead Box O1

FZD5: Frizzled Class Receptor 5

GADS: GRB2 related adaptor protein downstream of Shc

GATAD: GATA zinc finger domain containing protein

Grb-2: Growth factor receptor-bound protein 2

GSK3β: Glycogen synthase kinase-3β

GzmB: Granzyme B

GW182: Protein Gawky

HDAC: Histone deacetylases

HIF-1α: Hypoxia-inducible factor 1α

HK: Hexokinase

HRK: Harakiri

ICOS: inducible T cell co-stimulator

IFN: Interferon

IL: Interleukin

IRF: Interferon regulatory factor

IP: intraperitoneal

IP3: inositol 1,4,5-trisphosphate

IKBKE: Inhibitor of Nuclear Factor Kappa B Kinase Subunit Epsilon

IKK: inhibitor of nuclear factor-κB kinase

INPP5D/SHIP1: Src homology 2 (SH2) domain containing inositol polyphosphate 5-phosphatase 1

ITAM: Immunoreceptor tyrosine-based activation motif

ITIM: immunoreceptor tyrosine-based inhibition motif

ITK: IL-2-inducible T-cell kinase

ITSM: immunoreceptor tyrosine-based switch motif

JAK: Janus Kinase

JARID2: jumonji, AT rich interactive domain 2

KLF6: Kruppel Like Factor 6

KLRG1: Killer cell lectin-like receptor subfamily G member 1

KO: Knockout

LAG3: Lymphocytes-activation gene 3

LAT: Linker for the activation of T cells

LB: Luria Broth

Lck: Lymphocyte-specific protein tyrosine kinase

LCMV: lymphocytic choriomeningitis virus

LDH: Lactate dehydrogenase

LEF: Lymphoid Enhancer Binding Factor

LFA-1: Lymphocyte function-associated antigen 1

Malt1: Mucosa-associated lymphoid tissue lymphoma translocation protein 1

MAPK: Mitogen-activated protein Kinase

MAP2K: Mitogen-activated protein Kinase Kinase

MAP3K: Mitogen-activated protein Kinase Kinase Kinase

MDB: methyl-CpG-binding domain

MDM2: Mouse double minute 2 homolog

MFI: Mean fluorescence intensity

MHC I: Major histocompatibility complex class I

mLST8: mammalian lethal with SEC13 *protein* 8

MPEC: Memory precursor effector cells

mRNA: Messenger RNA

miRNA: microRNA

MTA: Metastasis-associated *protein*

MTOC: microtubule-organizing center

mTORC: mammalian target of rapamycin complex

NCBI: National Center for Biotechnology Information

Nck1: non-catalytic region of tyrosine kinase adaptor protein 1

NFAT: Nuclear factor of activated T-cells

NF-κB: nuclear factor-kappa B

NR4A: nuclear receptor 4A

NuRD: nucleosome remodeling and deacetylase

ORAI1: ORAI Calcium Release-Activated Calcium Modulator 1

OVA: ovalbumin

pb: pair base

PBS: phosphate-buffered saline

PKC: Protein kinase C

PDCD4: Programmed Cell Death 4

PD-1: Programmed death-1

PD-L1: Programmed death-Ligand 1

PDK1: phosphoinositide-dependent kinase-1

PELI1: Pellino E3 Ubiquitin Protein Ligase 1

PFA: Paraformaldehyde

PI3K: Phosphoinositide 3-kinase

PIK3R1 (p85α): Phosphoinositide-3-Kinase Regulatory Subunit 1

PIP2: Phosphatidylinositol 4,5-bisphosphate

PIP3: Phosphatidylinositol (3,4,5) trisphosphate

PLC-γ1: Phospholipase C γ1

PLEKHA1: Pleckstrin Homology Domain Containing A1

PKC- ζ: protein kinase C ζ

PRAS40: proline-rich Akt substrate of 40 kDa

Prf: Perforin

pri-miRNA: primary miRNA

PTEN: Phosphatase and TENsin homolog

PTPN2: Protein Tyrosine Phosphatase Non-Receptor Type 2

Rac1: Ras-related C3 botulinum toxin substrate 1

RasGRP1: RAS guanyl-releasing protein 1

RBBP: Retinoblastoma-binding protein

rh: human recombinant

RISC: RNA-induced silencing complex

RITS: RNA-induced transcriptional silencing

qPCR: quantitative polymerase chain reaction

RNA: ribonucleic acid

RNA pol II: RNA polymerase II

RNA pol III: RNA polymerase III

RT: Reverse Transcription

SATB1: special AT binding protein 1

shRNA: short hairpin RNA

SHP: Src-homology 2 domain (SH2)-containing protein tyrosine phosphatase

SKAP1: Src Kinase Associated Phosphoprotein 1

SLEC: Short live effector cells

SLP-76: SH2 domain-containing leukocyte protein of 76kDa

SMAC/DIABLO: Second mitochondria-derived activator of caspase/direct inhibitor of apoptosis-binding protein with LOw pI

SMAD: Suppressor of Mothers Against Decapentaplegic

SMURF: SMAD Specific E3 Ubiquitin Protein Ligase

SOCE: Store-operated calcium entry

SOCS: Suppressor of cytokine signal

SOS: Son of Sevenless

SPY: speedy/RINGO cell cycle regulator family member A

SPRY: Sprouty

STAT: Transducer and activator of transcription

STIM1: stromal interaction molecule 1

TAB2: TGF-beta activated kinase 1 binding protein 2

TAC: Transcriptome Analysis Console

TCR: T cell receptor

TCF: T cell-specific transcription factor

TIAM1: T-cell lymphoma invasion and metastasis 1

TIGIT: T cell immunoreceptor with Ig and ITIM domains

TIM-3: T cell immunoglobulin, and mucin-domain-containing-3

TME: Tumoral microenvironment

TGF-β1: Transformation growth factor-β 1

TGFBR: Transformation growth factor-β receptor

TOX: Thymocyte selection-associated high mobility group box protein TOX

TNF: Tumor necrosis factor

TRAIL: TNF-related apoptosis-inducing ligand

Tex: exhausted T cell

TF: Transcription factor

TRAF3: TNF receptor-associated factor 3

TRBP: TAR RNA-binding protein

TSC: tuberous sclerosis complex

TYK: Tyrosine kinase 2

UTR: Untranslated Transcribed Region

VAV1: Vav Guanine Nucleotide Exchange Factor 1

WASP: Wiskott-Aldrich Syndrome protein

WT: Wild-type

YAP: Yes-associated protein

ZAP-70: Zeta-chain-associated protein kinase 70

I dedicate this Master's thesis to my mother and family for supporting me in my highs and lows to nurture me into the person I'm today.

Remerciement

First, I would like to thank my research director, Dr. Christopher E. Rudd, for his support, guidance and all the scientific knowledge I received from him during this M. Sc interesting project. I'm also very grateful to my program director, Dr. George Saztmari, for his help and advice in the past year. And a special thanks to my jury's members, Dr. Jean-Sébastian Delisle and Dr. Étienne Gagnon, for their availability, accurate correction and encouragement. Finally, I wish to thank all my colleagues in the lab, helping me with my technics learning, especially, Dr. François Santinon, Dr. Tu Hien Thai, Dr. Alexandra Kazanova, Dr. Xueyang Guo, Dr. Yufeng Gao, Dr. Janna Krueger, Dr. Catherine Ménard, Dr. Meriem Bachsais, Dr. Stephanie Thurmond, Andres Oroya, and Shirisha Cherukommu.

Chapter 1: Introduction

1.1. T-cell signaling pathways

The activation of the T cells is regulated by three signals. Firstly, the interaction between their T cell receptor (TCR) and the major histocompatibility complex class I (MHC I) presenting the antigen from the dendritic cells (DC), followed by the interaction of the co-receptor, such as CD28 from the T cell and CD80/CD86 from the antigen-presenting cell (APC), and finally, the cytokine released by the $CD4^+$ T cell, the DC and the $CD8^+$ T cells [1,2].

In the tumor microenvironment (TME), the inhibitory pathways of PD-1 and TGF-β/SMAD are activated to prevent a proper effector activity, such as the cytotoxicity activity of the $CD8^+$ T cells and the pro-inflammatory cytokine production by the T cells [3].

1.1.1 TCR complex/CD8 signaling pathway

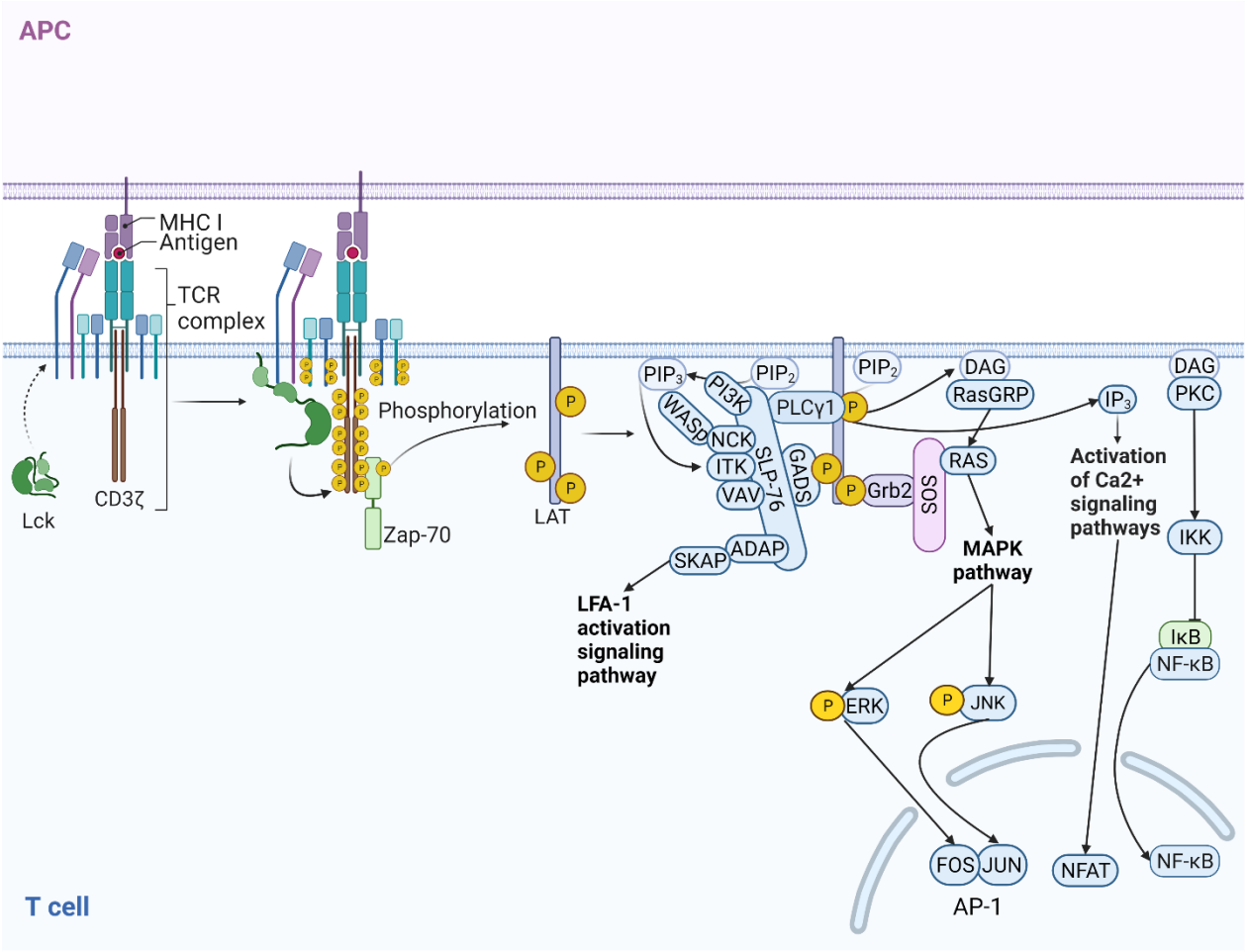

Created with BioRender.com

Figure 1: TCR signaling pathway for activating T cell.

The activation of the $CD8^+$ T cells is initiated by the recognition of the antigen and the MHC I and the TCR by the affinity between the antigen and the TCR. As first shown by the Rudd lab, the co-receptors CD4 and CD8 bind to the protein-tyrosine kinase $p56^{lck}$ which phosphorylates the antigen receptors in the initiation of a protein-tyrosine phosphorylation cascade [4,5]. In the model, during antigen presentation, the co-receptors bring $p56^{lck}$ into proximity of the CD3 and TCR-ζ chains due to their recognition of non-polymorphic regions of MHC antigens presenting peptide antigen [6]. The Bolen/Veillette labs at the NIH found similar findings in mice and further showed that ligation of CD4 and CD8 could activate $p56^{lck}$ [7], although this model has been recently challenged [8,9]. This

interaction releases then phosphorylates immunoreceptor tyrosine-based activation motifs (ITAMs) of each CD3ζ as well as the two ITAMs of each CD3ε and CD3δ. A precondition also involves the release of cytoplasmic tails from localization to the inner face of the plasma membrane [10]. A large proportion of Lck is found in their active form (pY394) inside the cytoplasm. The inactive form Lck (pY505) can be changed by the recruitment of Lck to the intracellular domain of CD45, a phosphatase, and the integration in the cytoplasmic membrane. Afterward, Lck autophosphorylate the activation residue Y394 [2,11,12]. The phosphorylation of CD3ζ then results in the recruitment of Zeta-chain-associated protein kinase 70 (ZAP-70) [11].

Downstream, the kinase $p56^{lck}$ and ZAP-70 can phosphorylate adaptor proteins needed to integrate proximal signals with the activation of effector functions [13]. ZAP-70 phosphorylates the Linker for the activation of T cells (LAT), on the residue Y132, Y171, and Y191 [14]. Each phosphorylate residue recruits three proteins including two adaptor proteins, Growth factor receptor-bound protein 2 (Grb-2) and Grb-2 related adaptor protein downstream of Shc (GADS), as well as the Phospholipase C γ1 (PLC-γ1) [5,12,15-17].

GADS recruits the large protein SH2 domain-containing leukocyte protein of *76kDa* (SLP-76) and interacts with multiple proteins. They are responsible for the reorganization of the actin network, the adherence of the T cell to the APC or the target cell, along with the survival and the activation of the T cell [18]. The interaction between the different proteins and SLP-76 requires the phosphorylation of three tyrosine residues, Y113, Y128, and Y145 by ZAP-70 [5,18,19].

The actin reorganization is regulated by the adaptor proteins, the non-catalytic region of tyrosine kinase adaptor protein 1 (Nck1) and Vav Guanine Nucleotide Exchange Factor 1 (VAV1). Nck1 regulates the actin network through the Wiskott-Aldrich Syndrome protein (WASP) followed by Actin Related Protein 2/3 (Arp2/3). Also, VAV1 has a Rho-GTPase activity causing the activation of cell division cycle 42 (Cdc42) by replacing the GDP into a GTP molecule. It is essential for the activation of WASP. The Cdc42/ Ras-related C3 botulinum toxin substrate 1 (Rac1) complex mediates the polymerization of the actin to the cytoplasmic membrane [20-22]. The polymorphism change is essential during the migration of the $CD8^+$ T cells to the inflammation site. The migration is mediated by the

chemokine gradient in the blood vessel as well as the expression of the different selectin on the endothelial cells [23]. After the adherence of the cells to the blood vessel by the interaction of the integrin and the selectin, the T cell has a morphology change enabling the start of transendothelial migration by the mechanism of diapedesis. The mechanism is based on the presence of pore between the endothelial cells caused by the large influx of liquid in the inflammation site. The T cell will modify its membrane structure through the localization of the F-actin movement to pass through the blood vessel walls [24].

The survival of the $CD8^+$ T cells is regulated by the PI3K/AKT signaling pathway. The interaction of PI3K protein to SLP-76 wasn't confirmed due to the similitude between the interaction domain of PI3K and the one of SLP-76 [25]. The PI3K/AKT pathway is mainly activated by the co-receptor CD28. The interaction between the p85 subunit of PI3K protein and SLP-76, as well as the closeness between the kinase and the membrane, initiates the transformation of phosphatidylinositol 4,5-bisphosphate (PIP2) into phosphatidylinositol (3,4,5) trisphosphate (PIP3), two phospholipids. This initiation results in a full protein cascade of two signaling pathways. Firstly, the PIP3 activates the protein RAC-alpha serine/threonine-protein kinase (AKT) and assures the survival of the T cell [26]. Also, PIP3 activates IL-2-inducible T-cell kinase (ITK) resulting in the activation of PLC-γ1 [27]. The phospholipase catalyzes the hydrolysis of PIP2 into diacylglycerol (DAG) and inositol 1,4,5-trisphosphate (IP_3). DAG is a membrane lipid that interacts with RAS guanyl-releasing protein 1 (RasGRP1) triggering the Mitogen-activated protein kinase (MAPK) pathway and PKC protein initiating the NF-κB pathway while IP3 engages the calcium signaling pathway. Each signaling pathway is essential for the activation of the T cell and the liberation of three TFs that regulates the expression of the effector molecules and other TFs needed for the T-cell polarization [1,2].

The activation of the Activation protein 1 (AP-1), TF, needs the expression of Fos and the phosphorylation of c-Jun by the MAP Kinase pathway. The initiation of the pathway by the production of DAG recruits the RasGRP protein to the membrane to activate Ras that is bound to Son of Sevenless (SOS) which, in turn, binds to Grb2 and LAT. The activation of Ras creates a chain reaction of phosphorylation. Afterward, the MAPK kinase kinase (MAP3K), Raf, is phosphorylated resulting in the phosphorylation of

MAPK kinase (MAP2K), Mek, followed by the phosphorylation of Erk who activates the TF Elk-1 that upregulates the expression of FOS. The activation of c-Jun is catalyzed by pJNK. Its phosphorylation is caused by MKK4 or MKK7 (MAP2K). Those kinases are activated by MEKK1 and other MAPKs. After the phosphorylation of c-Jun, it'll bind to Fos creating the TF, AP-1. It is needed to expand the activated $CD8^+$ T cells and the production of IFN-γ and TNF-α. The other target gene of AP-1 includes the TF, T-bet, Blimp-1, and EOMES. Also, the AP-1 complex upregulates the expression of multiple inhibitory receptors, including PD-1 and TIM-3 [28].

The second TF, NFAT, is activated by the influx of Ca^{2+} in the $CD8^+$ T cells. The interaction of IP_3 with its receptor, IP_3R, localized on the smooth endoplasmic reticulum (ER) liberates the calcium ion in the cytoplasm. This action is recognized by another smooth ER transmembrane protein, stromal interaction molecule 1 (STIM1), which will cluster together. This change of configuration will activate ORAI1, Ca^{2+} channel, through its subunit Store-operated calcium entry (SOCE) [29,30]. It'll create a large influx of Ca^{2+} in the cells. The ions will bind to calmodulin to change its conformation and assuring its binding to the calcineurin. This action will activate the phosphatase activity of the calcineurin which will dephosphorylate NFAT and activate it. This TF is responsible for the expression of a cytotoxic molecule, such as GzmB, as well as the expression of exhaustion markers, such as Thymocyte selection-associated high mobility group box protein (TOX) and NR4A. Also, NFAT oligomerizes with AP-1 to assure the expression of IL-2, IFN-γ, and TNF-α [28].

The third TF NF-κB is activated by the degradation of IκB. Not only does DAG activates the AP-1 pathway, but it also recruits protein kinase C (PKC). The kinase phosphorylates the inhibitor of nuclear factor-κB kinase (IKK) that, in turn, phosphorylates IκB. The reaction causes the polyubiquitin of IκB and frees NF-κB to translocate into the nucleus [1]. Once inside the nucleus, the TF regulates the expression of the different chemokine receptors as well as the multiple cytokines important for the differentiation of the T cell. It's also responsible for the expression of other activator co-receptors, including inducible T cell co-stimulator (ICOS), and activator markers, CD69 and CD44 [31-34].

1.1.1.1 LFA-1 activation pathway and function in T-cell activation

The maintenance of the interaction between the T cell and the APC or the target cell is important in their activation or their effector function. It is mediated by the activation of Lymphocyte function-associated antigen 1 (LFA-1). The pathway is initiated by the interaction of ADP-ribosylation factor GTPase-activating protein (Arf-GAP) with dual PH domain-containing protein (ADAP) on the SH2 domain of SLP-76. This results in the recruitment of Src Kinase Associated Phosphoprotein 1 (SKAP1) to ADAP followed by RapL, and Rap1 connection between Skap1 and LFA-1. It causes a conformation change resulting in the activation of the integrin [5,35]. Moreover, other adhesion molecules are involved in the T cell activation such as LFA-2, very late antigen-1 (VLA-1), and VLA-2 [36].

1.1.2 CD28 signaling pathway

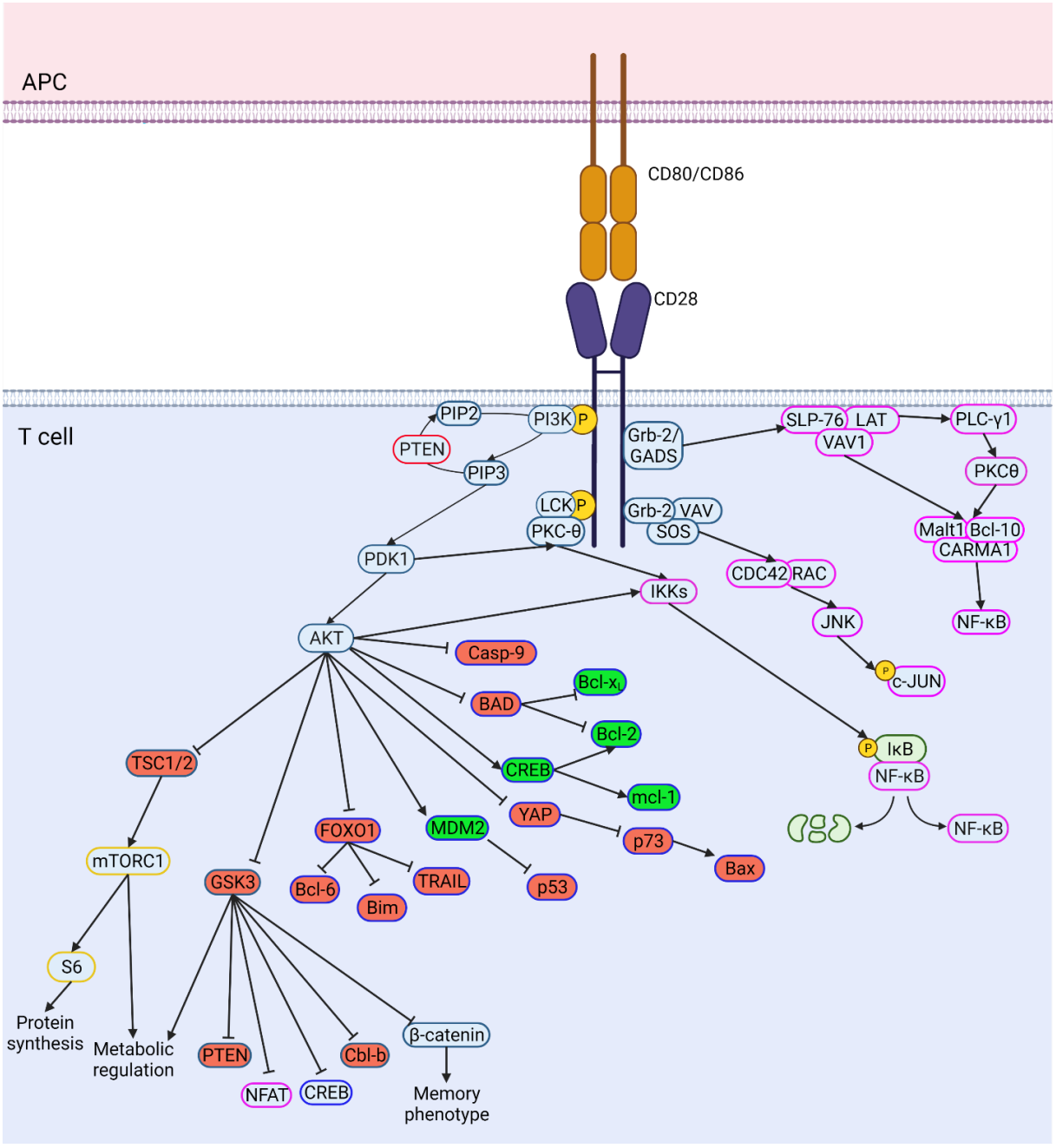

Created with BioRender.com

Figure 2: CD28/PI3K/AKT survival and activation signaling pathway.

The interaction between CD28 and its ligand, CD80 or CD86, results in the recruitment of different proteins to its unphosphorylated and/or phosphorylated motifs. The phosphorylation of the three tyrosine is mediated by Lck, Itk, and Fyn. These kinases

are recruited to an unphosphorylated motif of the cytoplasmic tail. Until now, PI3K, Lck, Itk, Fyn, Grb-2/SOS and GADS recognize the two binding site on CD28, YMNM and PYAP [5,37]. As explained above, PI3K is responsible to catalyse the transformation of PIP2 into PIP3. This reaction can be reversed by the Phosphatase and TENsin homolog (PTEN) which inhibits the activation of AKT. The interaction of Grb-2/SOS and GADS to CD28 strengthens the activation signaling pathway and the translocation of the TF, AP-1, and NF-Kb. The activation of c-JUN, a subunit of AP-1, is mediated by its phosphorylation caused by JNK. The activation of the MAPK pathway, permitting the activation of AP-1, is induced by the recruitment of VAV and SOS to Grb-2 [37]. This interaction will activate Cdc42/RAC complex. Cdc42 has been identified to have a Rho GTPase enzyme activity. Because of this kinase activity, Cdc42 is essential to activate RasGRP kinase in the phosphorylation of Ras followed by the activation of the MAPK pathway [38].

CD28 regulates the activation of the NF-κB through the phosphorylation of phosphoinositide-dependent kinase-1 (PDK1) by PIP3 and the recruitment of GADS or Grb-2 to its cytoplasmic tails. The interaction of the adaptor protein to the tails would increase the activation of SLP-76, VAV to LAT resulting in the activation of PKCθ. This kinase is needed for the phosphorylation and activation of Caspase recruitment domain-containing membrane-associated guanylate kinase protein-1 (CARMA1), a scaffold protein essential for the activation of NF-κB by the activation of the IKK kinase. This reaction will result in the recruitment of Mucosa-associated lymphoid tissue lymphoma translocation protein 1 (Malt1) and Bcl-10 to phosphorylated CARMA1. Moreover, IKK phosphorylation can be mediated by AKT increasing the activation of NF-κB [39-41].

The phosphorylation of AKT T308 and S473 mediated by PDK1 and mTORC2, respectively, results in the activation of a different signaling pathway. Phosphorylated (p) AKT regulates the apoptosis and activation pathway. And also controls the protein synthesis, metabolic changes and memory phenotype by phosphorylating its multiple target proteins. The phosphorylated residue on the target protein could be activated or inhibited [42-45].

The regulation of survival is mediated by the inhibition of Caspase-9, Bcl2-associated agonist of cell death (BAD) pro-apoptotic activity and Yes-associated protein

(YAP) and FOXO1 translocation into the nucleus [26,43,44]. In the infection model Bovine viral diarrhea virus (BVDV), the phosphorylation of Caspase-9 through pAKT reduces the cleaved form of Casp-9 and Casp-3 in the T cell resulting in the reduction of caspase-mediated apoptosis [45]. Also, in the hepatocellular tumor cells, Huh7, the increase of PTEN expression and, subsequently, the reduction of pAKT releases the cytochrome-c and increases the active form of Casp-9 and Casp-3 in the cytoplasm. This reaction leads to the apoptosis of the tumor cells [46]. The precise signaling pathway of AKT in the caspase-mediated apoptosis is unclear due to its effect on the release of cytochrome-c from the mitochondria. The apoptosis mediated by BAD cumulated on the mitochondria external membrane releases cytochrome-c and activates Casp-9 and Casp-3 [26]. The phosphorylation of BAD mediated by AKT results in its liberation in the cytoplasm and the neutralization of its pro-apoptotic activity. Its phosphorylation permits the liberation of Bcl-2 and Bcl-x_L into the cytoplasm [47]. The liberation of Bcl-2 and Bcl-x_L causes their insertion into the mitochondria outer membrane and prevents the formation of Bax cytochrome-c Second mitochondria-derived activator of caspase/direct inhibitor of apoptosis-binding protein with LOw pI (SMAC/DIABLO) functional pore [48]. Regarding the function of YAP in apoptosis, its phosphorylation reduces the affinity of YAP to p73, a pro-apoptotic TF, causing a reduction of p73 translocation into the nucleus and the reduction of pro-apoptotic molecules expression such as Bax [26,49].

The regulation of FOXO1 translocation into the nucleus affects the expression of pro-apoptotic molecules. Its phosphorylation by AKT causes a reduction in its translocation [50,51]. This TF is responsible for the upregulation of TNF-related apoptosis-inducing ligand (TRAIL), Bim and Bcl-6. TRAIL is a member of the TNF receptor along with Fas and FasL. The activation of TRAIL results in the cleavage of Casp-8 followed by Casp-3 [52]. Bcl-6 downregulates the expression of the Bcl-x_L gene increasing the apoptosis of the cell. Also, the inhibition of Bim expression decreases the formation of Bax cytochrome-c SMAC/DIABLO [48].

In addition, AKT upregulates the expression and the pro-survival activity of cAMP response element-binding protein (CREB) and Mouse double minute 2 homolog (MDM2) [26,53,54]. CREB contains three phosphorylation sites, S129, S133 and S142. The

phosphorylation of S133 mediated by AKT and other kinases increases the affinity between the TF and the promoter of different genes regulating the activation and helping the survival of the T cell [55,56]. The phosphorylation of the two other sites results in the decrease of the target gene's expression. In the activation of the target gene, CREB regulates the expression of variates receptors and IL in the T cell. It has been identified in the interaction of the TF and the promoter of IL-2, CD25/IL-2Rα and IL-2Rγ which are essential for the proliferation of the activated T cells and their survival [57]. Also, CREB is responsible for the upregulation of two pro-survival molecules, Bcl-2 and Mcl-1. Mcl-1 has the same mechanism as Bcl-2 in the inhibition of the cytochrome-c released from the mitochondria as explained above [58,59]. However, the alternative splicing of Mcl-1 messenger RNA (mRNA) results in the creation of two isoform proteins. Mcl-1_L has been identified to be an anti-apoptotic molecule while Mcl-1_S has a pro-apoptosis characteristic by inhibiting the activity of Mcl-1_L. Mcl-1_S is only composed of the BH3 domain similar to pro-apoptotic molecules like BAD. This switch of alternative splicing has not been identified in the T cell but was confirmed in the cell line MCL-7 through the Knockdown of splicing proteins [59].

The third responsibility of the AKT/PKB signaling pathway is the regulation of the metabolism and protein production during the $CD8^+$ T cell activation. The regulation of the metabolism is through the activation of mTORC1 and the inhibition of GSK-3. The activation of the mTORC1 complex is regulated by two proteins, tuberous sclerosis complex (TSC) 1 and TSC2. Although the mechanism is unknown, the phosphorylation of those two proteins by AKT results in the recuperation of the mTORC1 complex activity [26]. The complex is composed of mTOR, Raptor, mammalian lethal with SEC13 *protein* 8 (mLST8) and proline-rich Akt substrate of 40 kDa (PRAS40). The complex regulates the protein synthesis through the phosphorylation of S6K and 4EBP1 [60]. S6K activation through its phosphorylation results in the phosphorylation of the ribosomal protein, S6 [61]. The function of pS6 is controversial in the initiation of the translation. Many studies showed that by removing the phosphorylation sites of the protein or knockout the expression, the translation is increased within the cells. However, S6K1/2 and pS6 are needed for ribosomal biogenesis [62]. The ribosomal protein, S6, is still useful in the initiation of the translation [63]. The initiation of the translation includes the recruitment of the eukaryotic

initiation factors (eIF) complex to the 5'cap of the mRNA. The formation of the complex on the cap is regulated by the phosphorylation of Eukaryotic translate initiation factor 4E-binding protein 1 (4E-BP1) and the eIF4 subunit, eIF4E. The phosphorylation of the 4E-BP1 by mTORC1 and other kinases, such as Glycogen synthase kinase-3β (GSK3β) and ERK, results in the liberation of eIF4E from the inhibitory protein. To assure the binding of the initiation factor protein to the 5'cap, eIF4E has to be phosphorylated by the MAPK proteins, MNK1 and MNK2 [64,65]. The regulation of the protein synthesis is essential for T cell proliferation as well as the production of the effector molecules, receptors,à and TFs needed for the activation and differentiation.

The implication of the AKT signaling pathway helps the regulation of the metabolism. The two main regulators are GSK3 and mTORC1 [65,66]. As the name suggested, one of the functions of GSK3 is the regulation of the glycogen/glucose metabolism within the cell. The phosphorylation of GSK3 through AKT inhibits its kinase activity. The kinase targets different proteins implicated in other signaling pathways causing their inactivation or activation [65]. For metabolism regulation, GSK3 inhibits the glucose uptake through the downregulation of GLUT1, a glucose transport,à and hexokinase 2 (HK2) expression, a catalysator of glucose transformation into Glucose-6-Phosphate [67,68]. Also, GSK3 negatively regulates glutamine metabolism,à and lipid biogenesis [65,69]. The other target of GSK3 is implicated in the phenotype differentiation, the regulation of AKT activation and the survival of the cells. The effects of GSK3 on the memory phenotype are mediated by the Wnt pathway. The inhibition of GSK3 kinase activity leads to the accumulation of β-Catenin in the nucleus. This enhances the expression of memory markers by increasing the DNA binding stabilization of TFs, such as TCF1 and LEF1 [69,70]. In the T cell, Cbl-b regulates their activation and their tolerance toward their antigen. The inhibition of GSK3 through its phosphorylation causes the increase of Cbl-b ubiquitination and degradation [70]. Furthermore, GSK3 regulates negatively the TF, NFAT and CREB. It also inhibits PTEN activity by its phosphorylation [71].

1.1.3 Cytokine signaling pathway

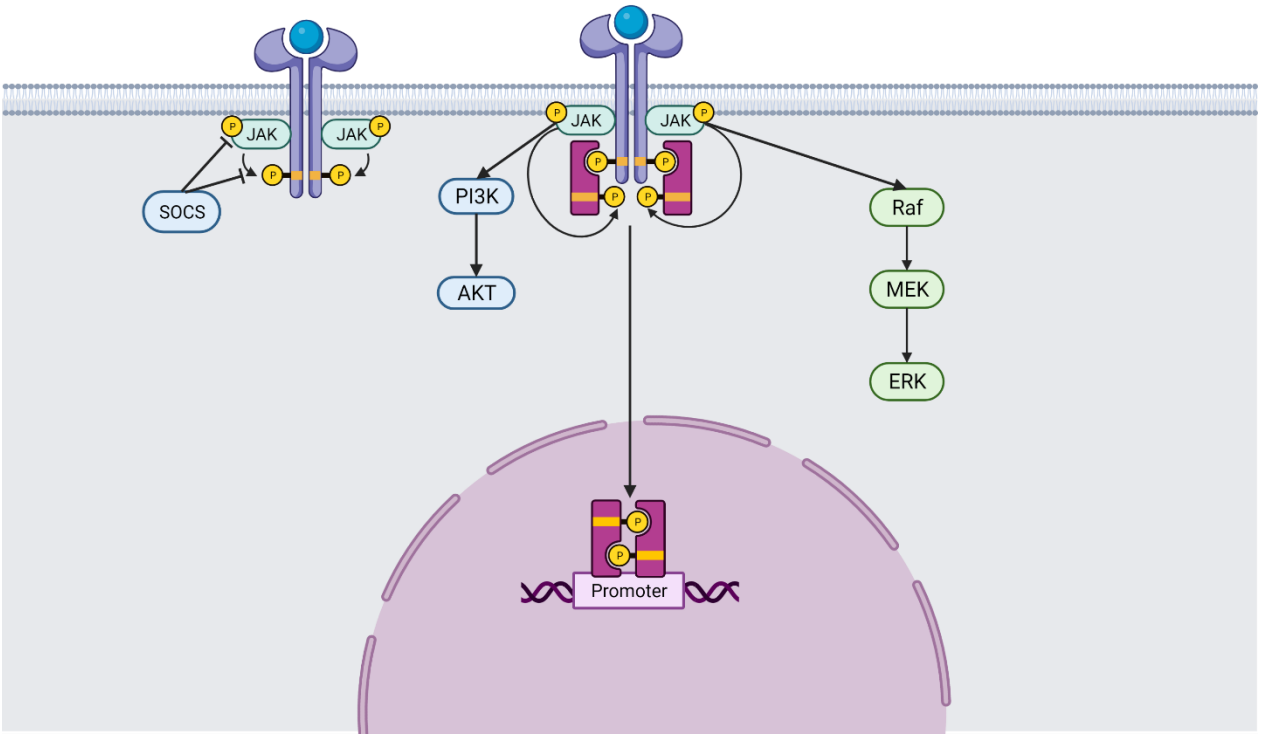

Created with BioRender.com

Figure 3: JAK/STAT signaling pathway.

The interaction between the cytokine, the interleukin, the interferon and the growth factor to their receptors mediates different functions in the activation of T-cells and their differentiation into their subset (Fig.1) [72-75]. The signaling pathway is initiated through the binding of the cytokine to its receptor. It results in the recruitment of Janus kinases (JAKs) and the initiation of their transphosphorylation activity. The activated JAKs phosphorylate the Tyr residue on the tails and the recruitment of the TF, STAT [76]. The proximities of the STAT proteins to the JAK kinases enable the phosphorylation and the dimerization of STAT. Once dimerized, STAT will be translocated in the nucleus. Also, activated JAKs and phosphorylated receptors recruit adaptor proteins, Grb-2 and SOS. This strengthens the signaling pathway of MAPK and PI3K/AKT[77].

The regulation of the JAK/STAT pathway is mediated by the Suppressor of cytokine signaling (SOCS) family protein and SHP protein. Depending on the repressor proteins, SOCS bind to either the phosphorylated JAK protein or the unphosphorylated site of the receptor. This causes the inhibition of STAT recruitment. Additionally, SOCS reduces the activation of MAPK and PI3K signaling pathways. The main mechanism of JAK inhibition by SOCS1 is the ubiquitination of JAK and transportation to the proteasome. As for SOCS3, it directly binds to the phosphorylation and STAT recruitment site on the cytoplasmic tail of the receptor [78].

1.1.4 PD-1 signaling pathway

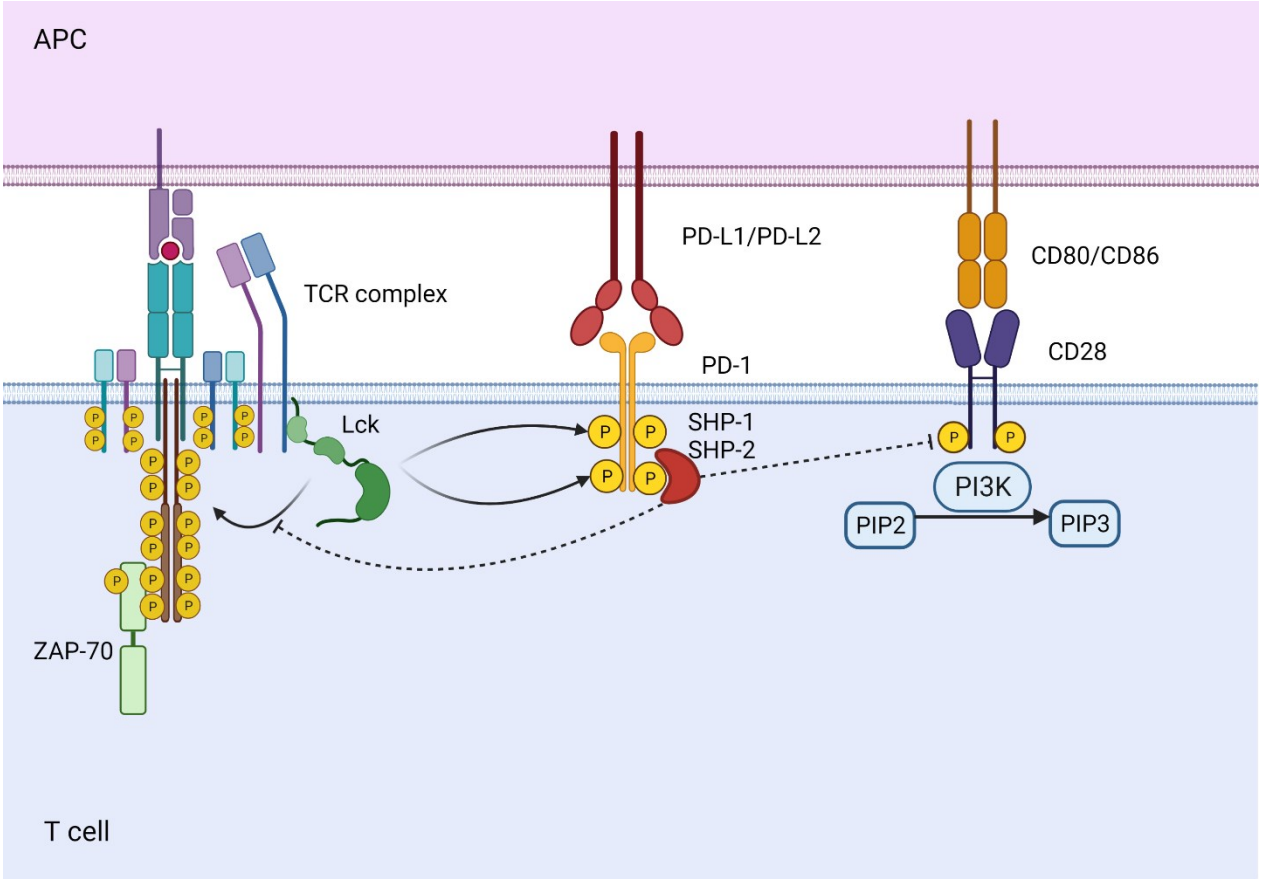

Created with BioRender.com

Figure 4: Inhibitory effects of PD-1 on the TCR signaling and CD28.

The expression of PD-1 on the surface of T cell has always been identified with low cytotoxicity activity and proliferation. The development of anti-PD-1 and anti-Programmed cell death-Ligand 1 (αPD-L1) immunotherapies was revolutionary in the treatment of cancer. By the use of the antibodies, the T cells expressing an intermediate level of PD-1 on their surface can regain the cytolytic activity and cytokine production [79].

The activation of PD-1 signaling in the activated T cells affects different important pathways for the cell cycle, the production of pro-inflammatory molecules, the metabolism and gene transcriptions. The engagement of PD-1 with its ligands will inhibit the PI3K/AKT/mTOR, and MAPK signaling pathway [80,81]. There is the possibility of inhibiting the uptake of Ca^{2+} in the cells, reducing the activation of NFAT and, overall, the T cell. The effects on the Ca^{2+} uptake through the PD-1 were proved to be in an expression level-

dependent manner [82]. However, the mechanism is not well-defined. One study showed an effect on the phosphorylation of Lck and the TCR complex, while another study showed a direct effect on the phosphorylation of CD28 [83,84]. After the interaction of PD-L1 to PD-1, the immunoreceptor tyrosine-based inhibition motif (ITIM) and the immunoreceptor tyrosine-based switch motif (ITSM) are phosphorylated by Lck and Fyn [85]. Afterward, the proteins mediating the inhibitory effects of PD-1, Src-homology 2 domain (SH2)-containing protein tyrosine phosphatase (SHP)-1 and SHP-2, on the multiple signaling pathways are recruited and activated through their conformation changes to liberate their phosphatase domain [86,87]. Regarding the function of SHP-2, various research showed the importance of phosphatase on the activation of the TCR and its phosphorylation. In the mice model Shp-2 KO, the T cell activation is depleted compared to the wild-type (WT) mice because of a low level of pERK and a low production level of IL-2. Also, the interaction of SHP-2 to the cytoplasmic tail of PD-1 does not need its phosphorylation or its interaction with the ligand [87,88]. However, the interaction strengthens the recruitment. Contrarily, Guarda lab showed that SHP-2 was not the main inhibitory signaling pathway of PD-1 in the chronic infectious disease, LCMV clone 13 and CD4-cre SHP-2 flox/flox mice [89]. The PD-1 inhibitor signaling pathway could be mediated by the other protein identified in the signalosome. Among the protein, SHP-1 and SHP-2 are present with Grb-2, Drebrin-like protein (DBNL), FERM Domain Containing Kindlin 3 (FERMT3), ZAP70 and INPP5D/SHIP1 [88].

1.1.5 TGF-β/SMAD pathway

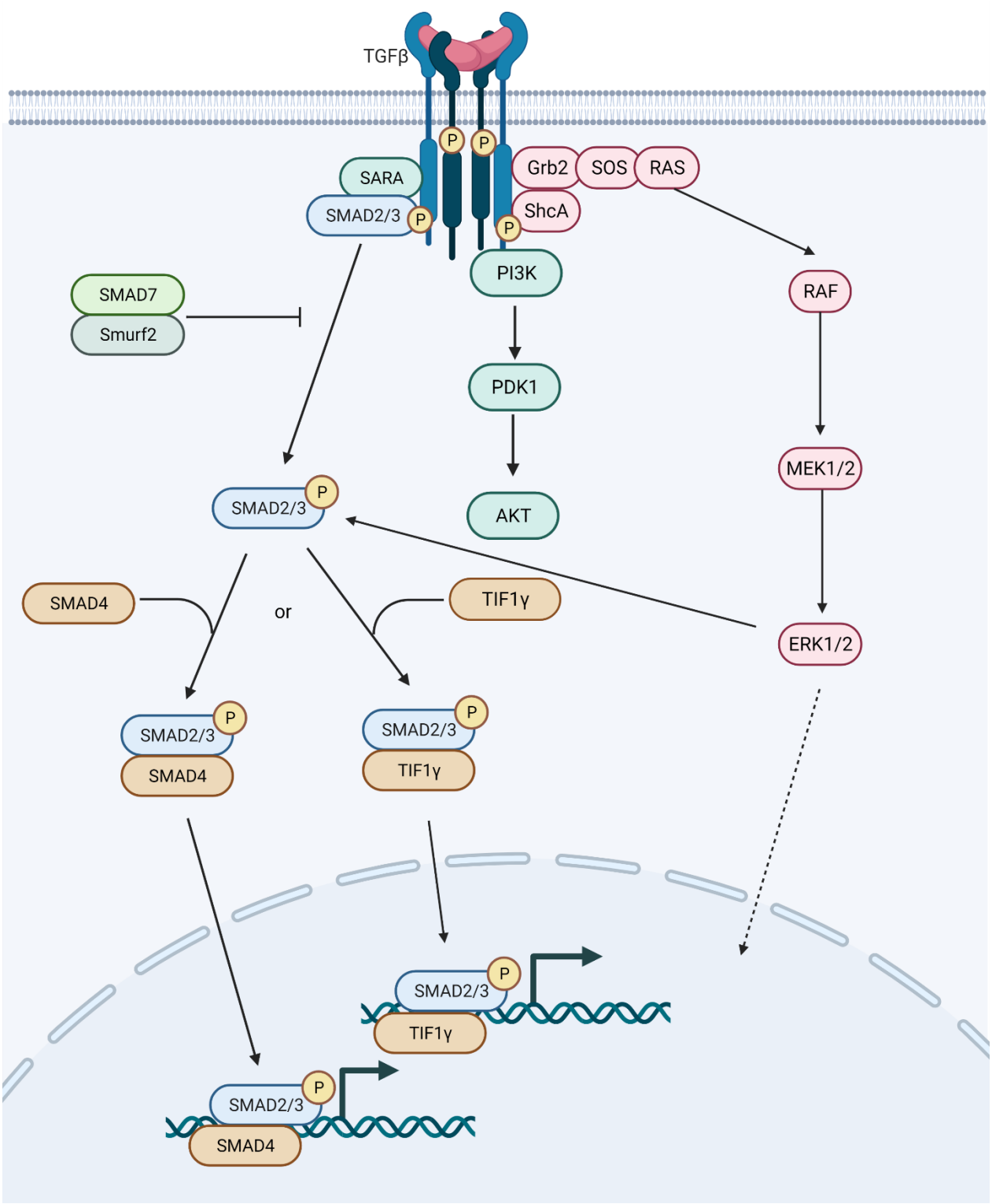

Created with BioRender.com

Figure 5: TGF-β1/SMAD signaling pathway.

The signaling of the Transformation growth factor-β 1 (TGF-β1) pathway regulates the expressions of multiple genes and the phenotype of the different immune cells, the cancer cells and environment cells, such as the Cancer-associated fibroblasts (CAF) [90,91]. The main function of TGF-β1 is the maintenance of homeostasis and immune tolerance. The cytokine is expressed in healthy tissues by the somatic cells and the regulatory T cells. In the immunosuppressive tumoral microenvironment (TME), the high expression of TGF-β1 suppresses the cytotoxic activity of $CD8^+$ T cells by targeting the transcription of important genes regulating their activity. Suppressor of Mothers Against Decapentaplegic (SMAD) 2/3/4 complex interacts with multiple promoters of the following genes: EOMES, T-BET, STAT4, IL-2, PRF, GZMB, special A-T binding protein 1 (STAB1), MYC, P21Cip1 and P27KIP1. Except for P21Cip1 and P27KIP1, the SMAD complex will repress the expression of the other genes [92].

The effects of TGF-β1 on the $CD8^+$ T cells are known to be suppressive. The knockdown of TGFBR2 expression at the surface of the cytotoxic T lymphocytes in a tumor model will reject the tumor and amplify the cytotoxic activity of the cells through an increase of Prf1, GzmA, GzmB, IFN-γ, c-Myc and IL-2 production as well as the expression of FasL to the surface. Also, TGF-β1 reduces the proliferation of the T cells by the upregulation of p21Cip1 and p27KIP1, two inhibitors of the cell cycle [93].

The regulation of gene transcription can be mediated by different mechanisms: chromatin remodeling and DNA methylation. The suppression of the gene transcription is mediated by the deacetylation and the methylation of the histone. Also, the methylation of DNA by the *de novo* process or the maintenance. Each mechanism is mediated by a different DNA methyltransferase, DNA (cytosine-5)-methyltransferase (DNMT) 3A/B for *de novo* and DNMT1 for the maintenance after the mitosis [94]. The engagement of the TGF-β/SMAD pathway can increase the expression of PD-1 through the suppression of SATB1 by the binding of SMAD3 to its promotor. The interaction of SATB1 with the promotor of PDCD1 will result in the recruitment of the NuRD complex [94-96]. This complex is composed of different DNA and histone binding proteins: chromodomain helicase DNA-binding protein (CHD) 4, MTA1/2/3, methyl-CpG-binding domain (MDB) 2, MDB3, Histone deacetylases (HDAC) 1/2, GATA zinc finger domain containing protein (GATAD) 2A/B

and Retinoblastoma-binding protein (RBBP) 4/7. Each has a function regarding the repression of genes containing the binding sites of GATAD2A/B and MTA1/2/3 at the promotor region. This interaction is strengthened by MBD3 with SATB1 [96]. The CHD4 subunit is known to have a helicase activity facilitating the remodeling of the chromatin. He is also responsible to recruit the DNA methyltransferase, DNMT1 and DNMT3B [97]. As for HDAC1/2, they are both histone deacetylases which are important to repress the chromatin and reduce the availability of the gene to the RNA polymerase. And, the RBBP4/7 function isn't fully known. Many papers suggest a structural function in the stabilization of the complex with the histone [96].

The activation of the Transformation growth factor-β receptor (TGFBR) II/I complex after the binding with TGF-β1 will initiate the autophosphorylation of the cytoplasmic tail of TGFBRII follow by the phosphorylation of TGFBRI tails. By the agglomeration of the four receptors (two TGFBRII and two TGFBRI), the kinase SARA is recruited along with SMAD2/3 to assure the activation of the dimer. The process can be inhibited by SMAD7 and/or SMAD Specific E3 Ubiquitin Protein Ligase (SMURF) 2 through its binding to the interaction site on the TGFBRI, blocking the site to the other SMAD proteins [98,99].

The complex of TGFBRI/II can induce SMAD independent signaling pathways. In the T cell, the MAPK and the PI3K/AKT pathways can be activated with the interaction of TGFBRII and I with its cytokine. The cytoplasmic domain of TGFBRI/II does contain the binding site of Grb-2 and ShcA that will initiate the MAPK cascade and the activation of pErk and pJNK. They can activate the SMAD2/3/4 complex by their phosphorylation and bypass the inhibitory effects of SMAD7 and SMURF2. The initiation of PI3K/AKT signaling is independent of the SMAD and the MAPK pathway [99].

1.2. Immune system

The immune system has the function to protect the host from infection which could be caused by bacteria, viruses, fungus and protozoa. Its strategies are either the prevention by using anatomic barriers, or the elimination of the pathogen through innate and adaptative immunity. The innate immune response is the first response against the presence of non-self antigen from a pathogen. It is composed of the complement system, innate immunity, antibody-mediated immunity (humoral immunity), cell-mediated immunity (T cell immunity) and phagocytosis [100,101].

During the inflammatory response, multiple immune cells are recruited to the inflammation site. In the first stage, macrophages and monocytes located at the inflammation site are active to produce cytokine and chemokine to recruit neutrophils followed by the dendritic cell (DC) and T cells [100]. Once the pathogen is eliminated, the inflammation is resolved by clearing the neutrophil, the pro-inflammatory cytokines, short-live T cells and B cells with a return of the tissue homeostasis [102]. In an immune response, the antigen-presenting cells (APC) activate different T cell populations, including $CD8^+$ T lymphocytes.

During the T cell development in the thymus, the thymocytes undergoes multiple development stages from double negative (DN) 1 to single positive (SP). Starting from DN1 to DN4, the thymocytes develop their TCR before the expression of the coreceptor CD4 and CD8 during the double positive (DP) stage. It is after this stage that the T cells differentiate into the $CD4^+$ T helper cells and the $CD8^+$ T cytolytic cells. Each has an important function in the immune system [103].

The $CD4^+$ T helper cells are essential for the modulation of the $CD8^+$ T cell activation and differentiations. They promote the types of cytokines produced and the immune response (humoral or cell-mediated immunity) depending on their differentiation, Th1 or Th2 [103]. Also, the $CD4^+$ T cell is essential for the dendritic cell's full activation and licensing. This interaction permits a switch in the DC and the presentation of MHC class I with the antigen for the $CD8^+$ T cells activation [104].

1.2.1 CD8$^+$ T cells

CD8$^+$ T cells, also known as cytotoxic T lymphocytes, have been identified to be the soldiers of the immune system. They kill and eliminate abnormal cells, such as infected cells or cancer cells. CD8$^+$ T cells are activated by APCs and helped by CD4$^+$ T cells with antigen recognition and activation via the T cell receptor (TCR) with additional signals from the co-receptor and the cytokine signaling pathways [105]. They can migrate toward the inflammation site by following the chemokine gradient and the presence of integrins on the surface of endothelial cells from the blood vessel [100]. After the CD8$^+$ T cells have reached the infection or tumor site, they'll interact with the target cells expressing peptide antigen. During this interaction, effector CD8$^+$ T cells cause the apoptosis of the target cells. The death of the target cell can result from the liberation of the granzyme B (GzmB) and perforin (Prf) vesicle from the cytotoxic T lymphocytes or the interaction of Fas Ligand (FasL) from the CD8$^+$ T cell with Fas receptor on the target cell [105].

Upon encountering antigen and becoming activated, the CD8$^+$ T cells can be polarized into Tc1, Tc2, Tc9, Tc22 and Tc17 subsets depending on the presence of cytokine during the activation (Fig. 1) [72]. The differentiation between the memory cells (central memory, effector memory) and the effector cells depends on the affinity between the antigen and the TCR and the time of interaction during the activation as well as the uneven distribution of certain transcription factors (TFs) during the clonal expansion [106,107]. After the activation, the effector T cell can be differentiated further into exhausted T cells (progeniture Tex then terminally Tex) by chronic overexposure to their antigen (Fig. 2). In the diversity of CD8$^+$ T cells subsets, effector Tc1 cells are responsible for the strong cytotoxic activity and protection of healthy cells [108].

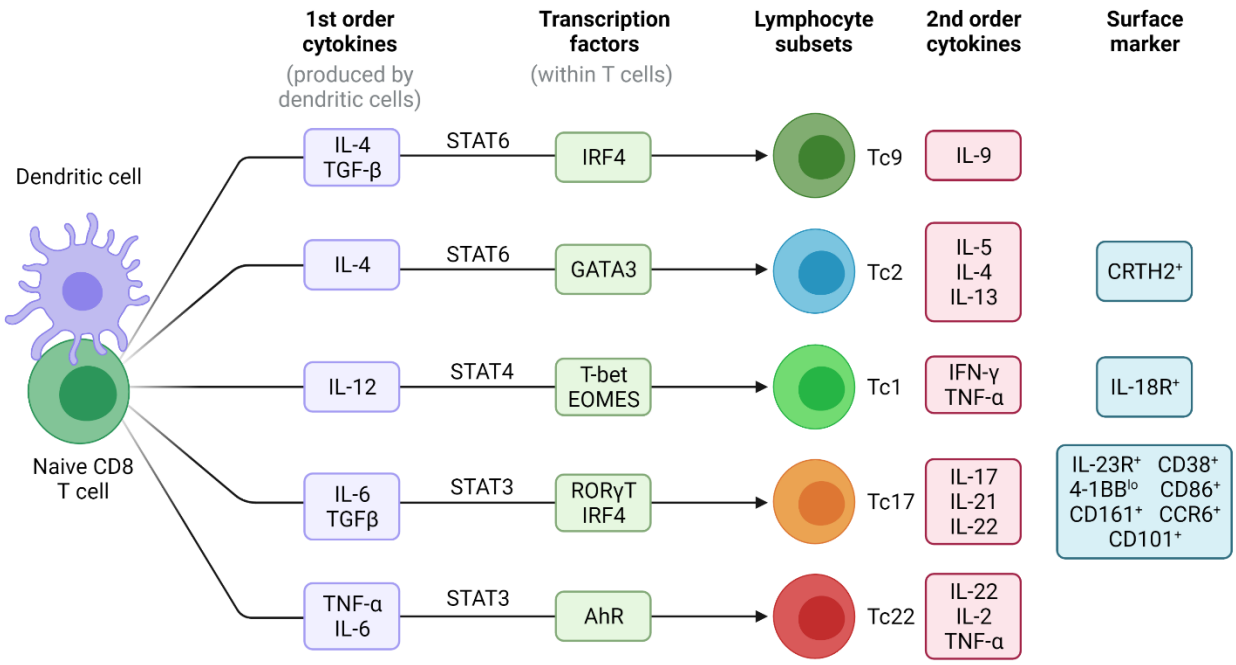

Figure 6: CD8⁺ T cell subsets. The polarization of the active CD8⁺ T cells is mediated by the presence of cytokine produced by the DC and the activation of specified STAT protein. They, in turn, will upregulate the expression of new TF within the CD8⁺ T cells finalizing the polarization into a subpopulation. Created with Biorender.

1.2.1.1 Effector Tc1 CD8⁺ T cells

The effectors Tc1 subset has been identified to have high cytotoxic activity and are commonly known as cytotoxic T lymphocytes. They are the subset essential for eliminating the intracellular infected cells and the tumoral cells. Their differentiation is mediated by interleukin (IL)-12 and a strong interaction between the TCR and the antigen [108]. The activation of its pathway results in the translocation of transducer and activator of transcription (STAT) 4, STAT5, T-bet, Blimp-1, interferon regulatory factor (IRF) 4 and Id2 in the nucleus causing a high expression of effector molecules such as perforin (Prf), granzyme B (GzmB), interferon (IFN)-γ and tumor necrosis factor (TNF-α). During the activation of the CD8⁺ T cells, IRF4 mainly regulates the differentiation of effector and memory T cells, their proliferation and their survival. A high IRF4 translocation induces the cell into short live effector cells (SLEC) while its low translocation induces the memory precursor effector cells (MPEC). The memory precursor TF signatures included T cell-specific transcription factor (TCF) 1, Lymphoid Enhancer Binding Factor (LEF-) 1,

Eomesodermin (EOMES) and Bcl-6 [72,108]. Additionally, IRF4 contributes to reprogramming metabolism of activated cells by directly affecting hypoxia-inducible factor 1α (HIF-1α), Forkhead Box O1 (Foxo1) and glucose transporters Glut1 and Glut3 expression [109]. This switch of metabolism toward aerobic glycolysis promotes the effector phenotype. It has been identified that IL-12 and IL-2 promote the effector phenotype by the activation of the phosphoinositide 3-kinase (PI3K) pathway as well as the STAT4 pathway increasing T-bet and Id2 expression. Furthermore, IL-2 suppresses the expression of Id3 and B-cell lymphoma (BCL)-6 responsible for promoting memory phenotype.

Once activated, the effector cells have polyfunctionality and high cytotoxic activity. The activation induces an expansion of the effector cells through the upregulation of CD25 and the production of IL-2 as an autocrine signal. The signaling pathway increases the expression of cyclins and anti-apoptotic proteins such as Bcl-2/BcL-xl and the metabolism needed to sustain proliferation. In this context, a second signal is provided by CD28 and its engagement of mediators such as PI3K and the adaptor Grb-2 as elucidated by the Rudd lab and others followed by induction of the CD40 and cytokine pathways [110]. A key function of the pro-inflammatory cytokines IFN-γ and TNF-α is to increase their cytotoxic activity via the upregulation of GzmB [111,112]. Also, IFN-γ upregulates TNF-related apoptosis-inducing ligand (TRAIL). Although IFN-γ is important to the cytotoxic activity and affects the target cells, tumoral cells and infected cells, TNF-α has a broader effect on $CD8^+$ T cells in the early phase of the immune response and the ending of the immune response [111,112]. The interaction of TNF-α and its receptor on the $CD8^+$ T cells will increase their proliferation and survival. It is followed by an increase in GzmB secretion and the production of IFN-γ. However, TNF-α mediates the induction of Activated immune cell death (AICD) to terminate the response and cause the $CD8^+$ T cell apoptosis [111,112]. The dual function of TNF-α in the activation, survival, proliferation and apoptosis is related to the receptor and the phase in the T cell activation and differentiation. The activation of the TNFR2 pathway is needed to reduce the T cell activation threshold in the early TCR-mediated activation phase and the proliferation [113,114]. The relation between the AICD and the TNFR2 is connected to the degradation of TRAF2 in the cells and the activation of NF-κB. In the TNFR2 -/- mouse model, TRAF2 intracellular level was maintained compared

to WT in the presence of TNF-α. Furthermore, NF-κB regulates multiples survivals genes. As explained in the TCR complex/CD8 signaling pathway section, IκBα blocks the translocation of NF-κB into the nucleus. The phosphorylation of IκBα releases the NF-κB and IκBα is degraded. The phosphorylated form of IκBα is increased in the TNFR2 -/- model showing the influence of TNF receptors in the survival of the activated T cells and AICD [115].

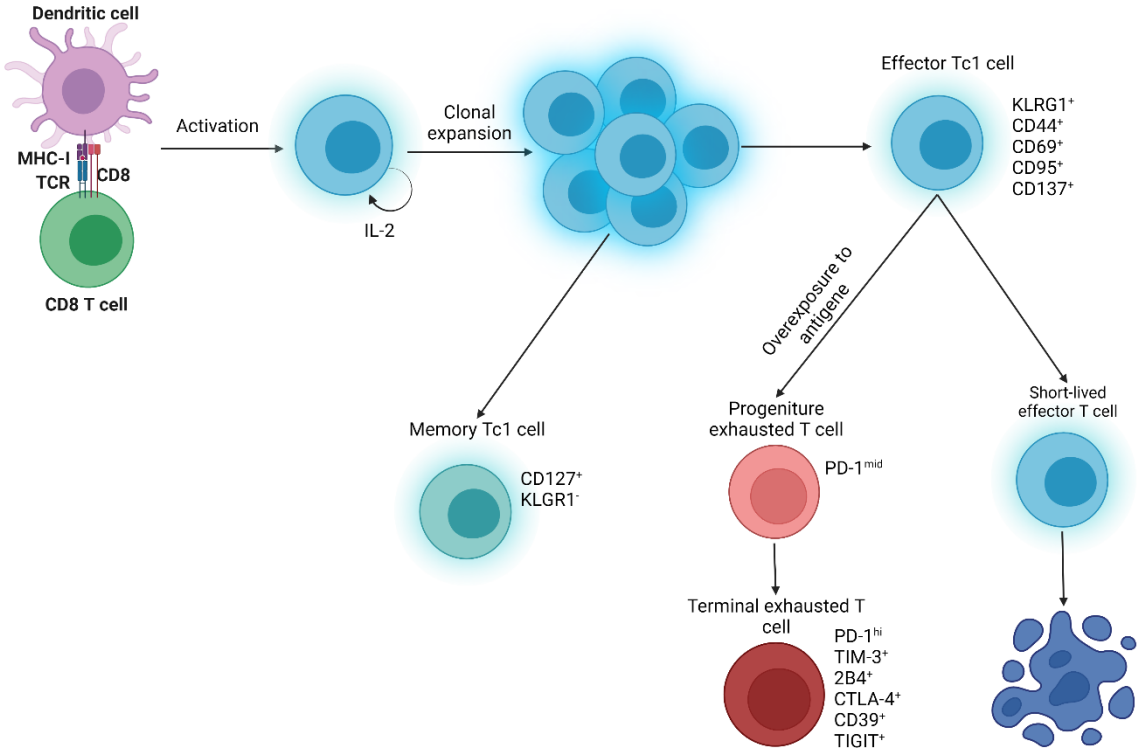

Created with BioRender.com

Figure 7: CD8+ T cells activation and differentiation.

1.2.1.2 Tc1 memory CD8+ T cells

As discussed in the previous section, the generation of memory T cells depends on the strength of the TCR signal and the presence of certain cytokines, such as IL-6 and IL-21, as well as the asymmetric division during the initial expansion of active CD8+ T cells

[116]. Through the interaction of the cytokine with its receptor, STAT3 is activated causing an increase in the suppressor of cytokine signals (SOCS) 1 and 3. Moreover, the IL-21 signaling pathway increases the expression of TCF1, LEF-1, EOMES and Bcl-6 which are TF and anti-apoptotic proteins related to the memory $CD8^+$ T cells [72,108]. Asymmetric division of the mother cell caused by a concentration of the cytoskeleton factor tubulin allows the asymmetric localization of signaling proteins, T-bet, Il-2 receptor α (CD25), protein kinase C ζ (PKC-ζ), CD3 to one side of the mitotic $CD8^+$ T cells [107]. As discussed in the effector Tc1 cells, those markers influence the $CD8^+$ T cells into Teff. So, by concentrating the molecule on one side of the dividing T cells, one of the daughter cells will have a memory phenotype while the other daughter cell will have the effector phenotype.

1.2.1.3 Exhausted $CD8^+$ T cells

In situations where chronic exposure to antigen is encountered, $CD8^+$ T cells become dysfunctional and exhausted [117]. This population is seen in the tumoral microenvironment and chronic infection where the $CD8^+$ T cells are unable to clear their antigen [106]. This subset is recognized through the expression of inhibitory receptors, such as Programmed cell death-1 (PD-1), cytotoxic T-lymphocyte antigen-4 (CTLA-4), Lymphocytes-activation gene 3 (LAG-3), 2B4 (CD244), T cell immunoglobulin and mucin-domain-containing-3 (TIM-3) and T cell immunoreceptor with Ig and ITIM domains (TIGIT) [118-120]. The overexposure to the antigen recognized by the TCR will initiate the changing phenotype of the effector Tc1 into progenitor exhausted T cells. They are recognized by an intermediate expression of PD-1 and the absence of the other inhibitory receptor [121].

Furthermore, exhausted T cells are separated into different categories depending on the surface expression level of PD-1 [122]. While the $PD\text{-}1^{mid}$ $CD8^+$ T cells are known to be progenitor exhausted T cells whose activity can be recovered after restimulation and resting from their antigen [122]. $PD\text{-}1^{hi}$ $CD8^+$ T cells are terminally exhausted T cells whose fate is cellular death after the elimination of the antigen without the possibility of reactivation. During the exhaustion of the T cells, they will go through multiple stages with different marker expression variations, such as PD-1, TCF-1, KLRG1, TIM-3 and CD69. In the early stages of Tex, the stem-like $CD8^+$ T cells precursor (or pre-Tex) will have a

low to mid surface expression of PD-1 along with high expression of TCF-1, a TF of memory T cells. Furthermore, the treatment αPD-1 blockade affects only the pre-Tex promoting the regain of the $CD8^+$ T cell polyfunctionality [123,124]. Before the T cells become terminally dysfunctional, the pre-Tex have an effector-like transitory phenotype. Those $CD8^+$ T cells proliferate rapidly and produce GzmB. However, they lose rapidly their effector-like function and become terminally exhausted T cell [120]. The phenotype difference between the three subsets of exhausted T cells has been studied in multiple chronic infection and tumoral models. In the hepatocellular carcinoma model, PD-1^{hi} $CD8^+$ T cells exhibit a high level of the other inhibitor receptor while PD-1^- and PD-1^{mid} T cells didn't express the other inhibitory receptor [122].

While effector $CD8^+$ T cell has high cytotoxic activity with polyfunctionality, their inability to clear their antigen results in the loss of function. Exhausted $CD8^+$ T cells exhibit a reduction of IL-2, IFN-γ and TNF-α production. In the context of the tumoral microenvironment (TME), the $CD8^+$ tumor-infiltrated T lymphocytes (TILs) can produce a normal level of GzmB and Prf [125]. However, they show defects in the localization of $GzmB^+$ and Prf^+ vesicles to the immunological synapse due to defective microtubule-organizing center (MTOC) mobilization [125]. Also, exhausted TILs have shown low phosphor-activation of $p56^{lck}$ which results in a decrease of pCD3ζ and pErk localization to the immune synapse [126]. Another group has shown the effect of PD-1 on the phosphorylation of CD28 on tyrosine of the motif YMNM and PYAP [83].

1.3. microRNAs

microRNAs are small non-coding RNA molecule of a size of approximative 22 nucleotides with the ability to bind to mRNA and inhibits the translation of the coding protein [127-129].

1.3.1 microRNA biogenesis

The localization of miRNA within the genome is different. There is miRNA localized in the intron of coding genes, while others are intergenic (Fig. 8). The initiation of miRNA biogenesis is their transcription by RNA polymerase II (pol II) or RNA polymerase III (pol III). To produce the primary (pri-) miRNA, the miRNA origin is responsible for the variation

in the initiation of the process. miRNA provided from the intron is expressed after the transcription of the gene by the RNA pol II and the removal of the intron through the splicing of the pre-mRNA by the spliceosome. As for intergenic miRNA, they are transcript mainly by RNA pol II. Some miRNA can be synthesized by the RNA pol III [128]. After the transcription, the pri-miRNA takes a hairpin form to be recognized by the Drosha and DiGeorge syndrome critical region gene 8 (DGCR8) protein, the microprocessor complex. DGCR8 is essential to stabilize the hairpin structure and catalysis the activity of Drosha to cut the pri-miRNA into pre-miRNA. This process reduces the size of pri-miRNA (over 1k pair base (pb)) into pre-miRNA (approximative 65 pb) [129]. Afterward, Exportin 5 and RanGTP will bind to the pre-miRNA and assure the translocation of the miRNA into the cytoplasm for the second step of the biogenesis [128]. The second cut to produce the mature miRNA is mediated by the Dicer and TAR RNA-binding protein (TRBP). The function of TRBP regards the cutting site of Dicer and the final size of the double-strand mature miRNA. Finally, the miRNA is integrated into the Argonaut (Ago) protein, a subunit of the RNA-induced silencing complex (RISC) [128-130]. Most of the miRNA present in the RISC complex is the 5' arm of the precursor RNA, while the 3' arm of the precursor is liberated in the cytoplasm resulting in its degradation. -5p is added to the miRNA name such as miR-203-5p when the 5' arm of the precursor of miRNA is incorporated in RISC. However, some 3' arm of the precursor miRNA are incorporated in another RISC, they are identified as -3p, for example, miR-203-3p [130,131].

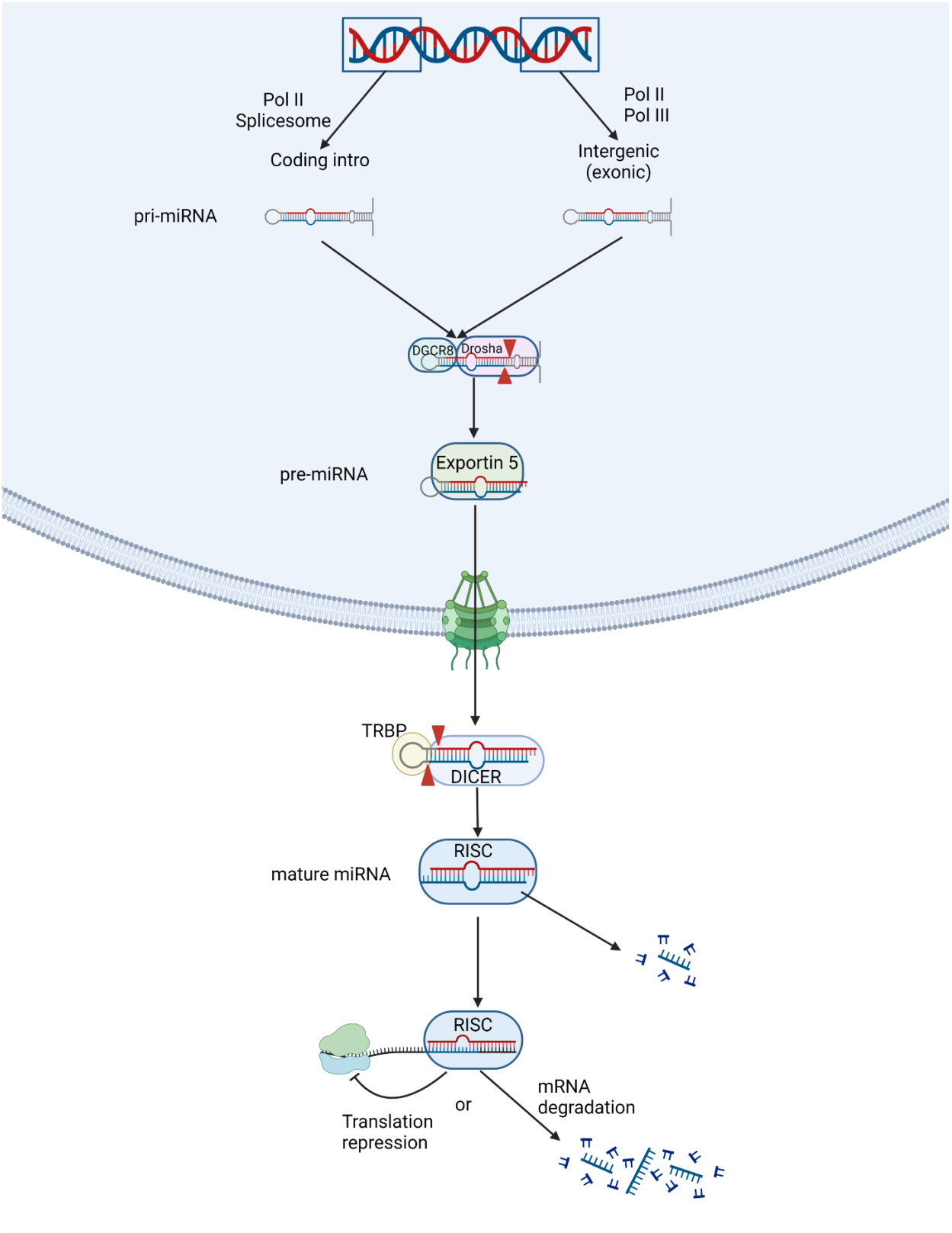

Created with BioRender.com

Figure 8: microRNA biogenesis

1.3.2 microRNA inhibitory mechanism

The inhibitory mechanism of miRNA is provided by the RISC complex and Protein Gawky (GW) 182. The interaction of miRNA to the target mRNA is mediated by the seed region (which has a length of 7 nucleotides) to the 3' Untranslated Transcribed Region (UTR) [130]. The inhibition is mediated through multiple mechanisms, some are unclear. One mechanism is the inhibition of the translation elongation or the premature removal of the ribosome from the mRNA (Fig. 9A). On the other hand, there is a possibility of the recruitment of proteolysis to degrade the nascent polypeptide. Although, the proteolysis is not yet identified nor is the recruitment process (Fig. 9B) [130,132]. The third mechanism is based on the competition of the 5'cap between AGO2 and eIF4E preventing the initiation of the translation (Fig 9C). The other mechanism to inhibit the initiation translation is the binding of eIF6 to AGO2 which prevents the formation of the initiation complex and the joining of the large subunit to the small subunit (Fig. 9D). The RISC complex accelerates the degradation of the mRNA by the recruitment of decapping enzyme, Decapping (DCP) 2 and decapping activation protein: DCP1, Ge-1, Enhancer of mRNA-decapping protein 3 (EDC3) and RCK/p54 (Fig. 9E). The decapping protein DCP2 increases the removal of the 5'cap and the mRNA vulnerability to XRN1 exoribonuclease. The RISC complex will augment the deadenylation of the mRNA through the Chromatin assembly factor 1 (CAF1) carbon catabolite repression 4–negative on TATA-less (CCR4-NOT) deadenylase complex. The recruitment process is still unclear, however, the P-body protein GW182 is essential (Fig. 9F) [132].

miRNA can inhibit the transcription of their target after their recruitment into the RNA-induced transcriptional silencing (RITS) complex. The complex will be translocated back into the nucleus to bind at pre-mRNA, resulting in the methylation of the histone and the repression of the transcription [133].

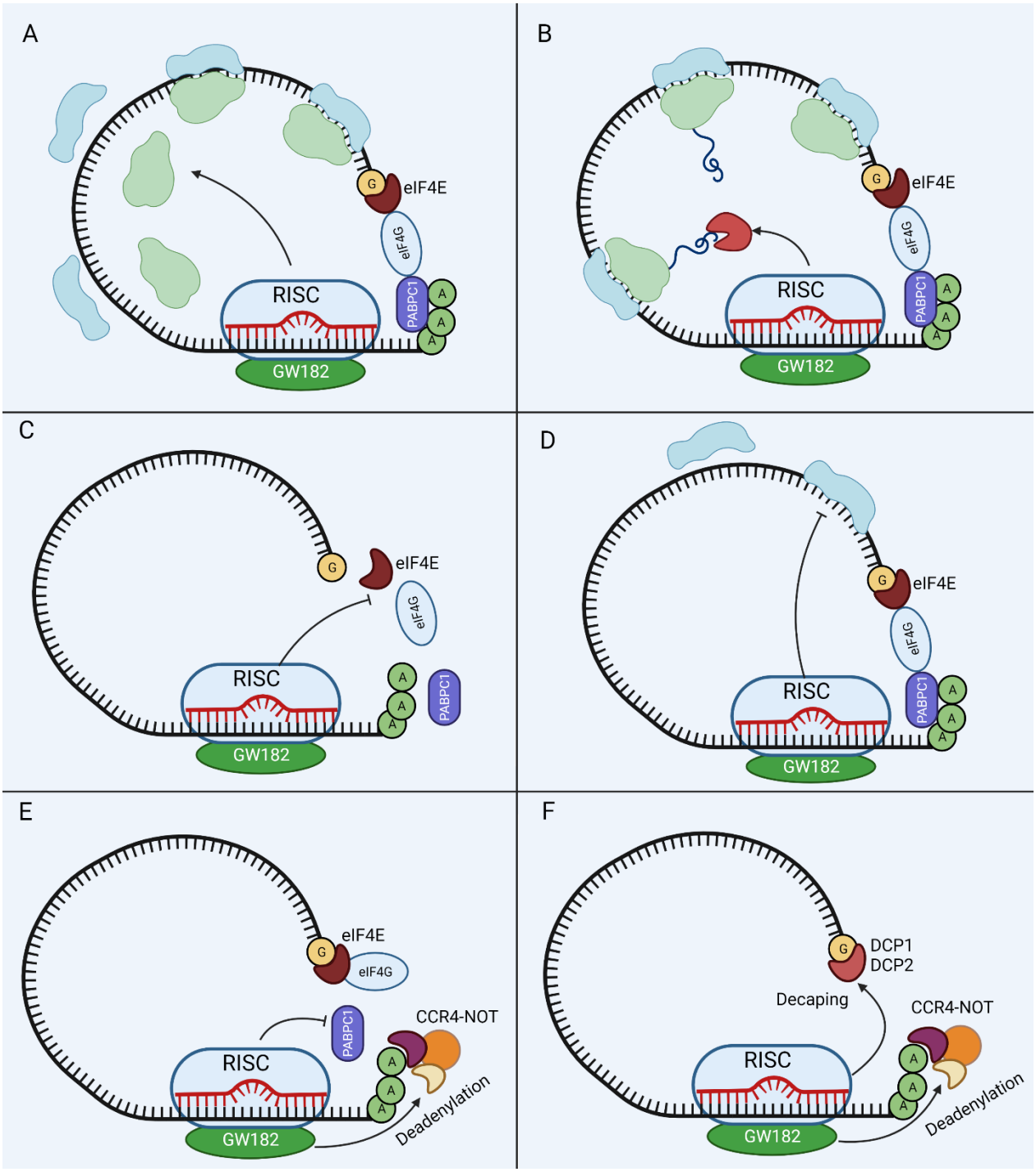

Created with BioRender.com

Figure 9: miRNA inhibitory mechanism. (A) Premature dissociation of the ribosome. (B) polypeptide degradation. (C) Repression of Cap-recognition. (D) Inhibition of large subunit recruitment to small subunit. (E), (F) Acceleration of mRNA degradation.

1.4. Immuno-miRNAs.

Multiple miRNAs have an important function in the immune cell's function development and signaling [134]. They are called immuno-miRNAs. In the $CD8^+$ T cells, some immuno-miRNAs are downregulated after activation while others are upregulated. Their function on their target; while some immuno-miRNA genes are involved in the signaling pathways regulating survival, other miRNA's targets affect the production of key effector molecules such as cytokines (IFN-γ, TNF-α, Il-2, Prf and GzmB)[135,136]. Furthermore, some miRNAs expressions are affected by the presence of certain cytokines, such as TGF-β1, or the environment they resided, such as TME. In the T cells, multiple immuno-miRNAs were identified as inhibitory functions, such as miR-23~27~24 cluster and miR-146a, or enhancer functions, such as miR-17~92 clusters, miR-181, miR-155 and miR-21a[136-140].

1.4.1 miR-23~27~24 cluster inhibitor effects on the $CD8^+$ T cells

This cluster is composed of miR-23a, miR24-2 and miR-27a. Depending on the stage of expression, the miRNAs target different genes[137]. In the early differentiation stage of lymphoid lineage, the three miRNAs promote the myeloid lineage and their proliferation by directly targeting Runx1, Satb1, Bach1 and Ikzf1. In the context of the $CD8^+$ T cells, the cluster expression is upregulated after the activation of the TGF-β/SMAD pathway and the suppression of c-Myc. Afterward, they target directly and indirectly IFN-γ.

1.4.2 miR-146a anti-inflammatory effects

miR-146a is an intergenic miRNA responsible to inhibit the NF-κB activation inside T cells and innate immune cells through different targets. This miRNA can target IRAK1/2, TRAF6, MyD88, TLRs, NOTCH1 and FADD[137]. Also, it is essential to prevent chronic inflammation and autoimmune disease as the KO mouse model has developed[136]. This miRNA could affect the AICD[137].

1.4.3 miR-17~92 clusters pro-inflammatory function in T cells

miR-17~92 clusters composed of those 6 miRNAs: miR-17, mir-18a, miR-19a/b, miR-20a and miR-92 is essential in the T cell activation as well as its effector function in either $CD4^+$ T cells or $CD8^+$ T cells. Due to its composition of multiple miRNAs, the

upregulation of the cluster increases the differentiation of the Th1 $CD4^+$ T cells and the effector $CD8^+$ T cells[137].

1.4.4 miR-181 essential function in TCR signaling and T cell activation.

In T cell activation, the upregulation of miR-181 decreases the TCR-threshold through its target, Dual specific phosphatase (DUSP) 6, DUSP5, PTPN22 and SHP-2 [136,137]. This inhibitor protein is responsible for the dephosphorylation and inhibition of the ERK signaling pathway increasing the sensitivity and power of the TCR signaling pathway [137]. Furthermore, miR-181 targets CTLA-4[136].

1.4.5 miR-155 increase the effector function of the $CD8^+$ T cells in the TME and chronic infection.

miR-155 has been identified to have a pivotal role in the cytotoxicity activity and IFN-γ and IL-2 production in the $CD8^+$ T cells in the tumor model as well as the chronic infection LCMV clone 13 models[138,139]. The increase of the miRNA expression was correlated with the rejection of the tumor as well as the clearance of the virus clone 13 [138,139,141]. To understand the reason for the pro-inflammatory function of miR-155, multiple inhibitory molecules were identified as a target of the miRNA. It includes SOCS1, CTLA-4, PTPN2, SHIP-2, TGFBR2, DUSP10, c-Maf, SMAD2 and GSK-3β[142-146]. Due to its different targets, the upregulation of miR-155 increases the TCR signaling sensitivity along with the cytokine signaling pathway[136,137,141].

1.4.6 miR-21a function on $CD8^+$ T cell activity.

Similar to miR-155, miR-21a is essential in the production of pro-inflammatory cytokines, such as IL-2 and IFN-γ and the effector function of the $CD8^+$ T cells. During T cell activation, miR-21a expression was found to be upregulated[147]. In the miR-21a knocked out mice model, the proliferation of the T cells was reduced compared to the WT mouse. These effects could be explained by the different targets[140]. Until now, miR-21a inhibits PTEN, Programmed Cell Death 4 (PDCD4), speedy/RINGO cell cycle regulator family member A (SPY) 1, SPY-2, FASL, Tipe2 and TGFBR2 expression[140,147-151].

1.5 Hypothesis and objective

In the TME, the inhibition of the $CD8^+$ T cell through different mechanisms has helped the tumor cell to invade any antitumoral immunity. One mechanism is the production of the anti-inflammatory cytokine, such as TGF-β [3,91]. The activation of the TGF-β /SMAD pathway affects the expression of multiple genes in the $CD8^+$ T cells decreasing their cytotoxicity activity. One process is the upregulation of PD-1 expression [93]. The activation of SMAD3 inhibits the transcription of SATB1 [92]. This TF recruits the DNA methyltransferase, DNMT3A/B through the NuRD complex to PD-1 promoter [95,96]. PD-1 is one marker of the exhausted $CD8^+$ T cells [106]. Furthermore, this receptor has a function in the inhibition of the TCR and CD28 signaling pathway [82,83]. Because of this function, the use of αPD-1 BCI increased the $CD8^+$ T cell's cytolytic activity [78].

The function of mir-21 in various types of cells has been pointed out in other research labs over time [140,147-151]. Interestingly, in two cancer cell lines, BPH-1 and PC-3, miR-21 targets TGFBR2, a receptor of the TGF-β /SMAD pathway [151].This work is based on the hypothesis that, by targeting this receptor in the $CD8^+$ T cells, miR-21a could decrease, indirectly, the expression of PD-1 and restimulated the $CD8^+$ T cells.

Our objective was to evaluate the capacity of miRNA in the $CD8^+$ T cell cytolytic activity. Firstly, the miRNA having an important function the $CD8^+$ T cells was identified in the B16-PD-L1 αPD-L1 treatment model. Secondly, the identification of target genes, including TGFBR2 and PD-1 from the selected miRNA, miR-21a, was performed after the transduction of the activated $CD8^+$ T cells as well as the measurement of the $CD8^+$ T cells cytotoxic activity. Furthermore, the potential of miR-21a in tumor rejection was tested in an ACT model.

Chapter 2: Materials and methods

2.1 *In vivo* studies

2.1.1 Mice

C57BL/6j, B6.SJL and OT-I Rag1 KO were used in different *in vivo* and *ex vivo* experiments. The mice were 7-9 weeks old during the experimentation. The breeding was realized in the animal facility of Centre de recherche de l'Hôpital Maisonneuve-Rosemont.

2.1.2 Tumor cell line

Two melanoma cells line were used in the implantation of tumors in the mice. They were B16-PD-L1, a murine melanoma cell line with overexpression of PD-L1, and B16-OVA, a murine melanoma expressing the ovalbumin (OVA) protein on its surface.

2.1.3 Tumor implantation & αPD-L1 treatment

4 days before the treatment, 50 000 cells in 50µL DMEM of B16-PD-L1 were implanted in the flank subcutaneous of the C57BL/6j. Following the tumor growth, each mouse was treated with 200µg/100µL phosphate-buffered saline (PBS) αPD-L1 (Clone 10F.9G2, Leinco) on days 4, 7, 11 and 14 through intraperitoneal (IP) injection.

2.1.4 Adoptive cell transfer

7-9 weeks old B6-SJL received 100 000 cells in 50 µL DMEM B16-OVA subcutaneous. 7 days after the implantation, 200 000 transduced OT-I were injected by IP injection in each mouse. The cells were washed twice and the concentration was adjusted in PBS for an injection of 100µL.

2.1.5 Isolation of tumor-infiltrating lymphocytes

The isolation of the TILs was realized with the density gradient. After the micing of the tumor, the tumor tissue is digested with 20µg of Liberase TL and 8µg DNase I enzyme each for 30min at 37°C. The cells were recuperated after straining

the digested tissue through a 70µm nylon cell strainer. The cells were resuspended in a PBS/10% Fetal bovine serum (FBS) before overlaying the cells mixture on the Lymphocyte separation medium (Corning). After the discontinuous gradient, the middle layer containing the TILs was removed followed by two washes in PBS/2%FBS. Afterward, the cells were ready for fluorescence-activated cell sorting (FACS) staining.

2.2 *In vitro* studies

2.2.1 Splenocytes isolation

The splenocytes were collected from OT-I Rag1 KO and C57BL/6j spleen. The spleen was homogenized and filtered through a 70µm nylon cell strainer. The removal of the red blood cells was done by the use of RBC lysis buffer (Biolegend). After the washing of the cells, they were counted on a hemocytometer.

2.2.2 Lymph node extraction

The isolation of the lymph node was collected from OT-I Rag1 KO and C57BL/6j spleen. The spleen was filtrated through the 70µm nylon cell strainer. After concentrating the cells, they were counted on a hemocytometer.

2.2.3 T cell isolation & activation

The purification of the $CD8^+$ T cells from the splenocytes and the lymph nodes was done using the EasySep™ Mouse CD8+ T cell isolation kit (Stemcell technologies). The cells were activated with αCD3 (Clone 2C11) and αCD28 (Clone: 37.51, Leinco). The C57BL/6j splenocytes were activated using 1 µg/ml of soluble αCD3 and αCD28. As for the T cells from the OT-I Rag1 KO, the plate was αCD3 coated at a concentration of 2,5 µg/ml. αCD28 and human recombinant (rh)IL-2 (StemCell technologies) were added to the cell's media at the concentration of 2 µg/ml and 72 UI/ml, respectively. The cells were activated for two days. After the transduction of the OT-I T cells, the cells were reactivated with soluble 1 µg/ml of αCD3 and 36 UI/ml of rhIL-2 for two days.

2.2.4. Retrovirus production

Each type of retrovirus was done with the transfection of HEK293T. 4×10^6 cells were plated in the 100 mm plate in DMEM 10%FBS. The following day, the cells were transfected with a solution of 54µg of Lipofectamine 2000 (ThermoFisher), 18ng of the transfer plasmid pMKO.1 GFP and 9µg of the pCL-ECO. pCL-Eco was a gift from Inder Verma (Addgene plasmid # 12371 ; http://n2t.net/addgene:12371 ; RRID:Addgene_12371). The next day, the media of the transfected cell was changed to RPMI 1640, 10% FBS, 1X MEM Non-Essential Amino Acids (Gibco™) and 1mM Sodium pyruvate (Gibco™). The retrovirus supernatant was collected the two following days after the switch of media from DMEM into RPMI. The virus was kept at 4°C for short terms use or at -80°C for long-term storage.

2.2.5 T cells transduction

After the activation of the T cells, they were transduced with the retrovirus supernatant. The cells were resuspended in 50% new media (RPMI) and 50% of the retrovirus supernatant at a final concentration of 10^6 cells/ml. 8ng/ml of Hexadimethrine bromide (Millipore Sigma) was added to the virus/cell solution. Then, the cells were divided into 6 wells plate. The plate was centrifuged for 90min at 2000rpm at 37°C, then placed in a 37°C 5% CO_2 incubator for 2 more hours before removing the virus media and replacing it with fresh RPMI 1640 10%FBS, 1% Penicillin/streptomycin media.

2.2.6 Cytotoxicity assay

The CytoTox 96® Non-Radioactive Cytotoxicity Assay (Promega) was used to measure the cytotoxic activity of the OT-I. The OT-I were priory activated with αCD3, αCD28 and rh-IL2, followed by their transduction with miR-21 mimic or pMKO.1 GFP (CTL). The assay was done as indicated by the manufacturer. The target used was EL4 pulsed with 10nM OVA peptide, SIINFELK, for 1 hour at 37°C. After the incubation, the pulsed EL4 was washed with red-phenol free RPMI 2%

FBS and 5 000 cells were distributed per well in a round-bottom 96-well plate. To respect the ratio effector:target (E:T), the quantity of OT-I was increased between the ratio. After adding the effector to the target, the plate was centrifuged at 150g for 4 min before its incubation for 4 hours at 37°C.

2.3 Molecular biology

2.3.1 Insertion of miRNA construct in a plasmid

The construction of the miRNA overexpression system was done in the retroviral plasmid pMKO.1 GFP. pMKO.1 GFP was a gift from William Hahn (Addgene plasmid # 10676 ; http://n2t.net/addgene:10676 ; RRID:Addgene_10676). The structure of the miRNA hairpin followed the method presented by Addgene regarding the shRNA construct. The construct has four sections: sense, loop, antisense and terminal. The loop and the terminal sequence were CTCGAG and TTTT in all the constructs. The sequence of miR-21 mimic and miR-155 mimic sense is the mature miRNA sequence of the mouse, while the miR-21 and miR-155 antagomir sense sequence is the antisense sequence of the mature miRNA (Table 1).

Table 1: miRNA construct sequence

miRNA construct name	Sequence (5'→ 3')
miR-21 mimic	TAGCTTATCAGACTGATGTTGACTCGAGTCAACATCAGTCTGATAAGCTATTTT
miR-21 antagomir	ATCGAATAGTCTGACTACAACTCTCGAGAGTTGTAGTCAGACTATTCGATTTTT
miR-155 mimic	TTAATGCTAATTGTGATAGGGGTCTCGAGACCCCTATCACAATTAGCATTAATTTT
miR-155 antagomir	AATTACGATTAACACTATCCCCACTCGAGTGGGGATAGTGTTAATCGTAATTTTTT

After the determination of the miRNA construct, the insertion inside the pMKO.1 GFP was done using the Q5 Site-Directed Mutagenesis kit (New England BioLabs) and the primer sequence was obtained on the NEBaseChanger website (Table 2) and synthesis by Invitrogen (ThermoFisher).

Table 2: Insertion miRNA construct primers

Primer name	Sequence (5'→3')
miR-21 mimic FORWARD	TCGAGCAACATCAGTCTGATAAGCTAGTCCTTTCCACAAGATATATAAAGCC
miR-21 mimic REVERSE	GCAACATCAGTCTGATAAGCTATTTTGAACACCGGTACGCGTAC
miR-21 antagomir FORWARD	TCGAGAGTTGTAGTCAGACTATTCGATGTCCTTTCCACAAGATATATAAAG
miR-21 antagomir REVERSE	GAGTTGTAGTCAGACTATTCGATTTTTGACCCTGTGGAATGTGTG
miR-155 mimic FORWARD	TCGAGACCCCTATCACAATTAGCATTAAGTCCTTTCCACAAGATATATAAAG
miR-155 mimic REVERSE	GACCCCTATCACAATTAGCATTAATTTTCCCTGTGGAATGTGTGTC
miR-155 antagomir FORWARD	TCGAGTGGGGATAGTGTTAATCGTAATTGTCCTTTCCACAAGATATATAAAG
miR-155 antagomir REVERSE	GTGGGGATAGTGTTAATCGTAATTTTTTCCCTGTGGAATGTGTGTC

The PCR reaction reagent composition followed the manufacture protocol. The PCR reaction extension was calculated to the size of the plasmid (Table 3).

Table 3: PCR reaction condition. (A) PCR tube composition. (B) PCR cycling program for pMKO.1 GFP.

(A)

	Quantity for 25 µl RXN
Q5 Hot Start High-Fidelity 2X Master Mix	12,5 µL
10 µM Forward Primer	1,25 µL
10 µM Reverse Primer	1,25 µL
Template DNA (plasmid)	15 ng
Nuclease-free water	9 µL

(B)

STEP	Temperature	Time	Nb cycle
Initial denaturation	98°C	30 sec	1
Denaturation	98°C	10 sec	25
Annealing	64°C	30 sec	
Extension	72°C	3 min 40 sec	
Final extension	72°C	2 min	1
Hold	4°C	infini	1

The PCR product ligation used the KLD reaction from the Q5 Site-Directed Mutagenesis kit (Table 4).

Table 4: Ligation reaction.

	Volume for 10 µL RXN
PCR product	1 µL
2X KLD Reaction Buffer	5 µL
10X KLD Enzyme Mix	1 µL
Nuclease-free water	3 µL

The extraction of the complete plasmid was done after the Escherichia coli DH5α transformation. For 50µL of chemically competent E. coli DH5α, 5µL of the ligation product was added. The mixture was incubated on ice for 20 min, followed by a heat shock at 42°C for 1minute and a second incubation on ice for 10 min. Luria Broth (LB) was added to the bacteria/plasmid mixture before placing the tube in an incubator shaker at 37°C for 1 hour. The bacteria were then spread on an LB-ampicillin plate and incubated overnight at 37°C.

The extraction of the plasmid was done by midi-prep using the NucleoBond® Xtra Midi EF kit (Macherey-Nagel; distributed by TAKARA).

2.3.2 Total RNA isolation

2.3.2.1 miRNeasy kit

The extraction of the miRNA from the $CD8^+$ TILs was realized with the miRNeasy kit (Qiagen) following the manufacturing procedures, except for two steps. The cells were resuspended in 200µL of QIAzol Reagent. And 70µL of chloroform was added after the lysis to separate the protein, DNA and RNA into three phases.

2.3.2.2 Trizol

The extraction of total RNA was done by Trizol. The T cells were resuspended in Trizol to lyse the cells and conserve the RNA stability. The isolation of the RNA was realized by adding chloroform to the Trizol, mixing the two phases by vortex and letting them incubate for 5 min at room temperature. The two phases were separated into three layers after centrifugation at 12000g for 15min at 4°C. The RNA was concentrated by precipitation after adding the 75% cold ethanol and incubating the solution for 10 min at room temperature. The RNA was pelleted after centrifugation of 7500g for 5 min at 4°C. Depending on the size of the pellet, it was resuspended at variate volumes in DEPC treated water (Invitrogen). Small size or invisible pellets were dissolved in 20µL of DEPC water. A large pellet was resuspended in 100µL of DEPC water.

2.3.3. Microarray analysis from Genome Québec

The miRNA extraction was realized on the mixture of all the $CD8^+$ T cells from within the same group, control and αPD-L1 treated mice. The extracted RNA was sent to Genome Québec to perform the microarray. The analysis was performed in the program Transcriptome Analysis Console (TAC).

2.3.4. Validation of miR-21 and miR-155 expression by Taqman qPCR

The validation of miR-21 and miR-155 overexpression was done using TaqMan miRNA assay quantitative polymerase chain reaction (qPCR)

(ThermoFisher). The miRNA assay was separated into two-step: Reverse Transcription (RT) and qPCR. The RT reaction mixture followed the manufacture protocol, except 5ng of total RNA was added to the reaction. The qPCR reaction mixture was reduced compared to the manufactured reaction mixture (Table 5). The cycling reaction was performed by the 7500 Real-Time PCR System using the cycling mode related to the machine.

Table 5: qPCR reaction mixture composition.

Component	Volume per reaction
TaqMan™ Small RNA Assay (20X)	0,5 µL
PCR Master Mix	5 µL
Nuclease–free water	2,5 µL
cDNA	2 µL

2.3.5 SYBR GREEN qPCR

The quantification of gene mRNA was realized using two-step RT-qPCR. The synthesis of complementary DNA (cDNA) was done using the All-In-One 5X RT MasterMix. For each sample, 1µg of total RNA was added to each reaction. The mixture composition followed the manufacturing protocol.

As for qPCR reaction, BlasTaq™ 2X qPCR MasterMix was used. The mastermix composition volume was changed compared to the manufacturing procedure (Table 6A). The PCR cycling program used was as described in the manufacturing procedure, the fast cycling.

Table 6: Mastermix Reaction and cycling program. (A) MasterMix composition. (B) qPCR cycling

(A)

Component	Volume per reaction
BlasTaq™ 2X qPCR MasterMix	5 µL
Forward Primer (10µM)	0,3 µL
Reverse Primer (10µM)	0,3 µL
Template cDNA	1 µL
Nuclease-free H_2O	3,4 µL
Final volume	10 µL

(B)

Step	Temperature	Duration	Cycle
Enzyme activation	95°C	3 min	1
Denaturation	95°C	1 sec	40
Annealing/Extension	60°C	10 sec	
Melting curve	Refer to specific guidelines for instrument used		

Table 7: qPCR primer sequence

Primer name	Sequence (5'→3')
GAPDH Forward	AGCTTGTCATCAACGGGAAG
GAPDH Reverse	TTTGATGTTAGTGGGGTCTCG
TGFBR2 Forward	CCTACTCTGTCTGTGGATGACC
TGFBR2 Reverse	GACATCCGTCTGCTTGAACGAC
PDCD1 Forward	TCAGTCAAGAGGAGCATGCA
PDCD1 Reverse	AGTCCCTAGAAGTGCCCAAC
SATB1 Forward	TGATAGAGATGGCGTTGCTG
SATB1 Reverse	TTTTGAGGGTGACCACATGA
CTLA4 Forward	GTACCTCTGCAAGGTGGAACTC
CTLA4 Reverse	CCAAAGGAGGAAGTCAGAATCCG
PRDM1 Forward	CATGGAGGACGCTGATATGAC
PRDM1 Reverse	ATGCCTCGGCTTGAACAGAAG
JAK1 Forward	CTGTCTACTCCATGAGCCAGCT
JAK1 Reverse	CCTCATCCTTGTAGTCCAGCAG

2.4 Flow Cytometry

The flow cytometry analysis was done using LSRFortessa X-20 (BD), or the Cytek Aurora (Cytek). As for the sorting of the TILs to isolate the $CD8^+$ T cells, FACSAria III Cell Sorter (BD) was used. For the sorting of the transduced OT-I before the ACT, SH800S cell sorter (Sony Biotechnology) was used.

2.4.1 Antibodies and reagents used

During the FACS staining of the TILs from the αPD-L1 treatment and αIgG isotype for the sorting of the $CD8^+$ TILs, the cells were stained with Fixable Viability Stain 510, CD8a PE-Cy7 and CD45-FITC from BD and CD11c-BV650 from Biolegend.

As for the ACT experimentation, the TILs were stained with Fixable Viability Dye eFluor™ 780 (ThermoFisher), CD3ε-Alexa Fluor 700, CD8α-BV650, CD4-

BV605, CD45-PerCp-Cy5.5, CD44-BUV395, pAKT-BV421, Satb1-Alexa Fluor 647 (BD), KLRG1-PE and CD62L-PE-Cy5 (Biolegend).

2.4.2. Viability and extracellular staining

To stain the viability with either Fixable Viability Stain 510 or Fixable Viability Dye eFluor™ 780, the cells were washed in PBS then incubated on ice with the viability dye diluted in PBS for 20 min.

As for the extracellular staining, the surface antibodies were mixed in PBS/2%FBS buffer at a dilution factor of 200:1. It was added to the cells for incubation on ice for 30 min.

2.4.3 Fixation and intracellular staining

The cells from the ACT experiment were fixed using a 1% Paraformaldehyde (PFA) solution for 15 min followed by two washes with PBS/2%FBS buffer. Then they were fixed using FoxP3 Transcription Factor Fixation/Permeabilization Concentrate and Diluent solutions. Afterward, the cells were permeabilized using Permeabilization Buffer (10X) solution. The intracellular antibodies were diluted in the Permeabilization Buffer before resuspending the TILs in the antibodies MasterMix. After the staining was complete, the cells were resuspended in PBS/2%FBS buffer.

2.4.4 Gating strategy

The gating strategy used started with the selection of lymphocytes followed by the single-cell population and the live cell population (**Fig. S1**). In the sorting of the $CD8^+$ tumor infiltrated cells (TIL), the $CD8^+$ T cells were obtained with the selection of the $CD45^+$ $CD8^+$ cells. Because the myeloid cells could express CD8, they were differentiated with the CD11b marker.

2.5 Statistical analysis

The statistical analysis was performed on GraphPad Prism 8. The significant analysis of the tumor growth and tumor weight was performed using multiple t-tests and the Holm-Sidak method. The analysis of the infiltrated $CD45^+$ T cells and $CD8^+$ T cells

was performed with two-way ANOVA and Sidak's multiple comparisons. The same analysis was applied to the miR-21 mimic adoptive cell transfer T cell infiltration characterization population.

Chapter 3: Results

3.1 The immune checkpoint block of PD-1 affects the microRNA expression in CD8$^+$ tumor-infiltrated lymphocytes.

The expression of PD-L1 on tumor cells was shown to be essential for the control of the tumor growth with the use of the αPD-L1 treatment [152,153]. The use of this model assured the response of the treated mice to αPD-L1 and the obtention of a miRNA signature in the condition of tumor control. To determine the effects of immunotherapy on the CD8$^+$ T cells and their miRNA signature, tumor-bearing mice were treated with αIgG isotype antibodies (CTL), αPD-L1 and αPD-1 (data not shown). The treatment of tumor-bearing mice with αPD-L1 had a significant reduction in the tumor growth compared to the CTL and αPD-1 treated mice (**Fig. 10A,B,C**) as well as significantly smaller tumor weight (**Fig. 10D**). The sorting of CD8$^+$ TILs and their FACS analysis showed that the proportion of CD45$^+$ immune cells population in the live cell population increased with the αPD-L1 treatment (average: 76.92%) compared to the CTL (average: 62.85%). Also, the infiltration of CD8$^+$ T cells was a significant increase in the αPD-L1 treated mice compared to the isotype treated mice (average: 32.28% vs 11.3%). This increase in infiltration is also seen in the viSNE analysis (**Fig.11**). These data showed that αPD-L1 treatment could limit the growth of B16 melanoma tumors in a manner accompanied by an increase in the presence of CD45 and CD8$^+$ TILs.

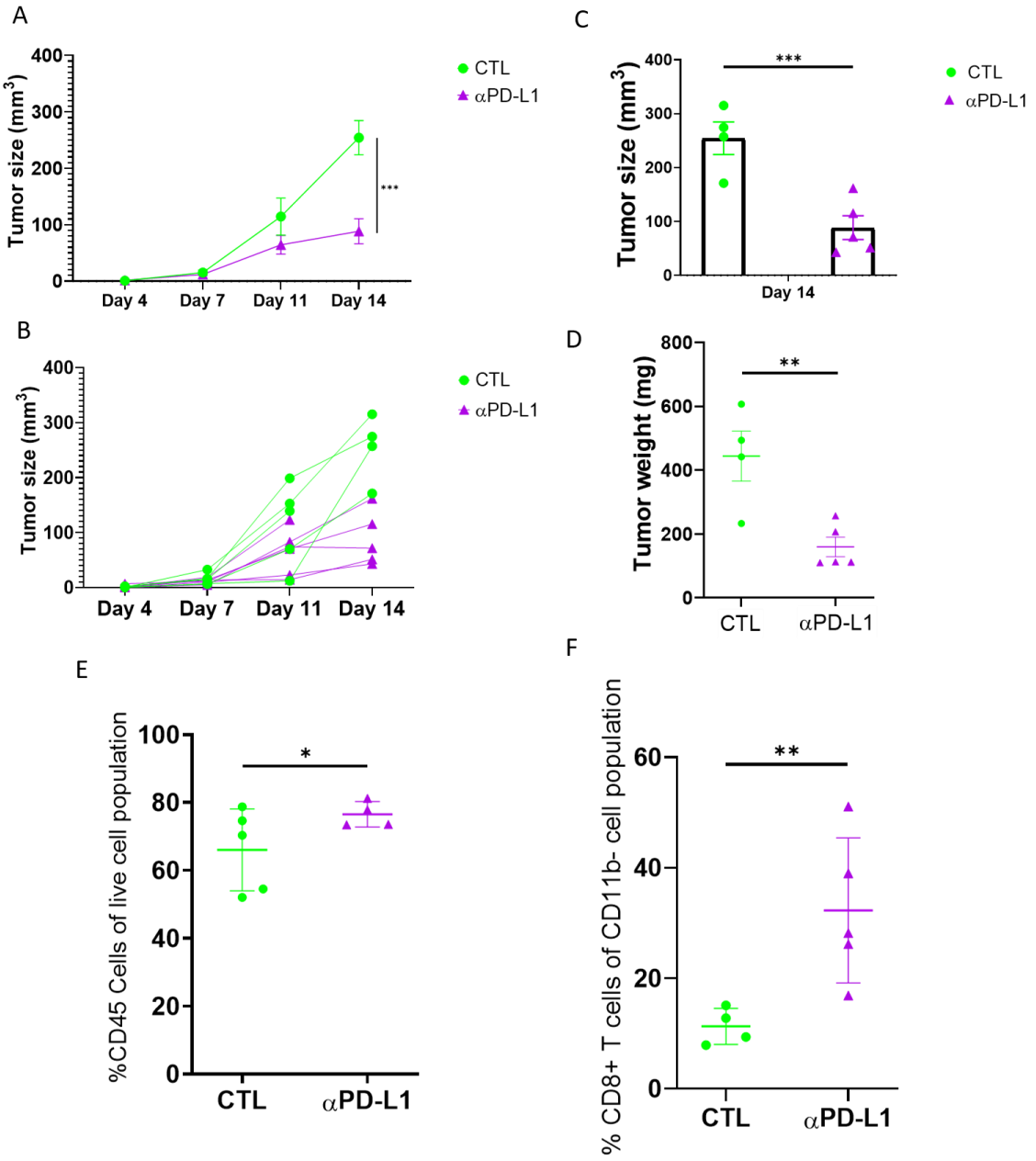

Figure 10: The treatment of αPD-L1 increased the infiltration of immune cells and CD8 $^{+}$ T cells in the tumor. The WT mice were implanted subcutaneously with B16-PD-L1. Then, they were treated on days 4, 7, 11 and 14 by IP injection before their sacrifice and the collection of the tumor. The mice in the CTL group were treated with IgG isotype control. The mice in the αPD-L1 were treated with αPDL1 (Clone 10F.9G2, Leinco). (A) The tumor growth average of each group (B) Individual mouse tumor growth in the CTL group (n=5) and αPD-L1 (n=5). (C) The final tumor size on day 14 of each mouse. (D) The tumor weight of each treatment group. (E) Percentage of CD45^{+} immune cells from the FACS sorting of the TILs. (F) Percentage of CD8^{+} T cells from the FACS sorting of the TILs. Statistical analysis: $p \leq 0,05$ *, $p \leq 0,01$ **, $p \leq 0,0001$ ***.

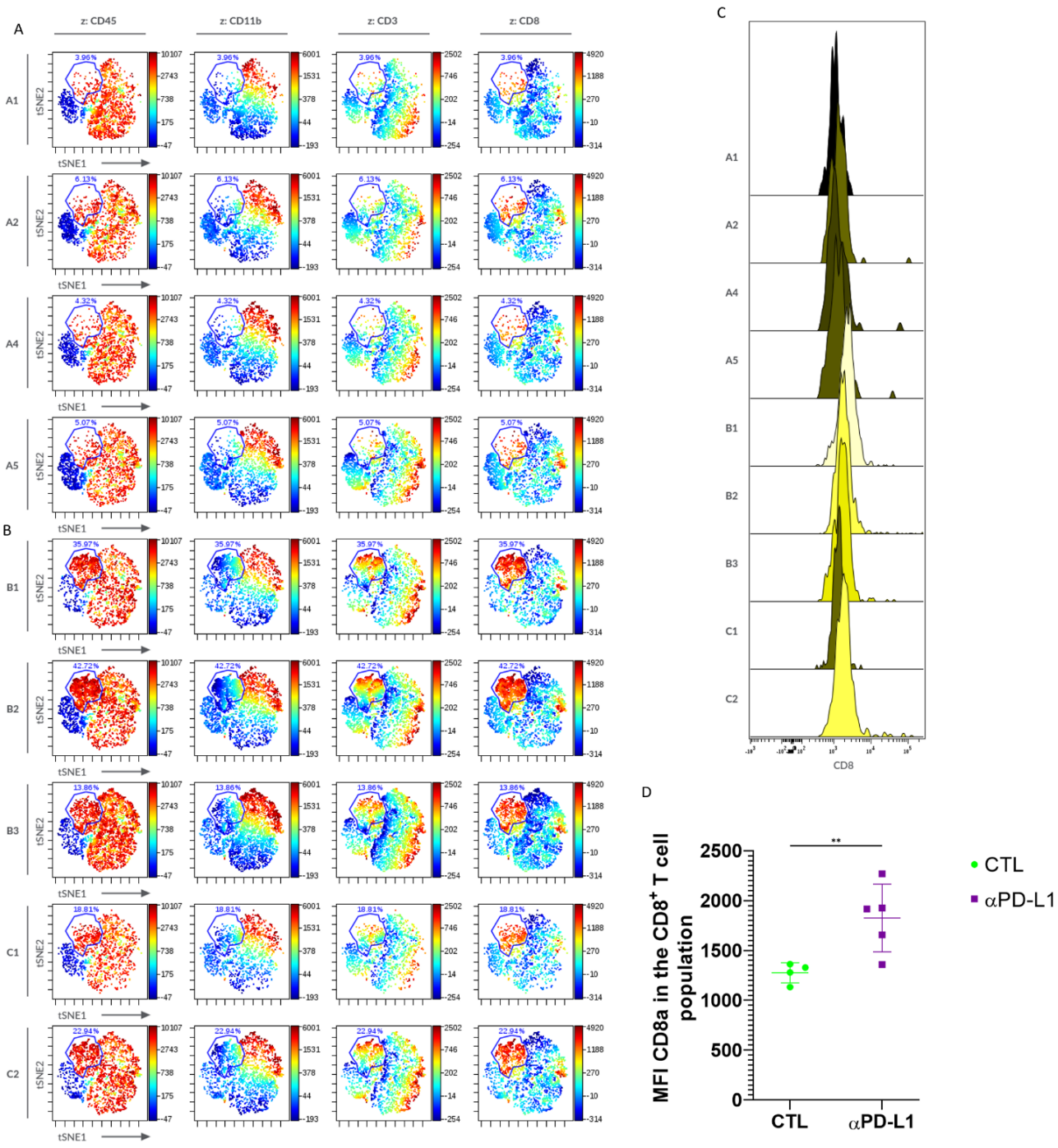

Figure 11: viSNE analysis of TILs from (A) the αIgG treated mice and (B) the αPD-L1 treated mice. (C) Histogram expression and (D) mean fluorescence of CD8a in the $CD8^+$ T cell population. (A) (B) The FACS sorting results were analyzed using the program viSNE from Cytobank. The analysis was done using proportional sampling events. The position of the cells was done by the viSNE algorithm to separate the different expressing populations. The gate selected the $CD8^+$ T cells. (C) (D) The CD8a mean fluorescence intensity (MFI) was obtained from the $CD8^+$ T cells population in Cytobank program. Statistical analysis: $p \leq 0,05$ *, $p \leq 0,01$ **, $p \leq 0,0001$ ***.

To identify the miRNA signature of the $CD8^+$ TILs, in collaboration with Dr. Catherine Menard in the Rudd lab, I next sorted by FACS followed by the extraction of total RNA. Due to restriction on the $CD8^+$ TILs number, the isolation was performed on the mixture of the $CD8^+$ TILs from each tumor within the same group of treatment. This combination was to assure enough miRNA during the microarray for detection. Interestingly, from the microarray run by Genome Quebec, 50 miRNAs expressions were affected between the two treatments. 27 miRNAs were upregulated in the $CD8^+$ T cells from the αPD-L1 treated mice compared to the CTL treated mice. While 23 miRNAs were downregulated in the same context (**Fig. 12**). In the list, we found that the miRNAs, miR-21a-5p and miR-155-5p were particularly interesting because of their conservation nature between the mouse and the human as well as their expression upregulation in the $CD8^+$ TILs from the αPD-L1 treated tumor, 2.47 and 3.6, respectively. Other interesting miRNAs included: mmu-miR-18b-5p, mmu-miR-181d-5p, mmu-miR-677-3p, mmu-miR-150-5p, mmu-miR-342-5p and mmu-miR-30d-5p (**Table 8,9,10,11)**.

Among the upregulated miRNAs, mmu-miR-18b-5p, mmu-miR-181d-5p and mmu-miR-677-3p are interesting miRNAs due to their conserved nature as well as their targets (**Table 8,9**). miR-18b-5p could be able to target inhibitory protein genes, such as SOCS5, SMAD2, PTPN13 and DUSP16. On the other hand, it can target important proteins in the main signaling pathway of T-cell activation, including HIF1α, FOSL2, ORAI3, MAPK4 and NFAT5. miR-181d targets the terminal exhaustion marker TOX, as well as other regulator proteins, TGFBR1, BCL6 and CREB1. Strikingly, miR-677-3p targets T-cell activation proteins, SOS1 and NFAT and co-receptor ICOS.

The downregulation of miR-342-5p is interesting because it inhibits CD3γ, IL6Rα and AKT1 and T-cell activation TFs, NFATC1, NFATC3, FOSL2 and IRF8. Regarding miR-150-5p, it is surprisingly a good immuno-miR due to its effects on T-cell activation key mediators. The miRNA could affect the expression of inhibitory receptors, BTLA, FZD4 and FZD1, and signaling pathway regulators, SOCS7, GSK3β and APC. miR-30d-5p targets essential signaling pathway protein, TRAF3, receptor NOTCH1 and TFs, NFAT5, NFATC3, IRF4 and SATB1. It can also, repress the expression of inhibitory proteins, JARID2, GSKIP and SOCS1/3 (**Table 10,11**).

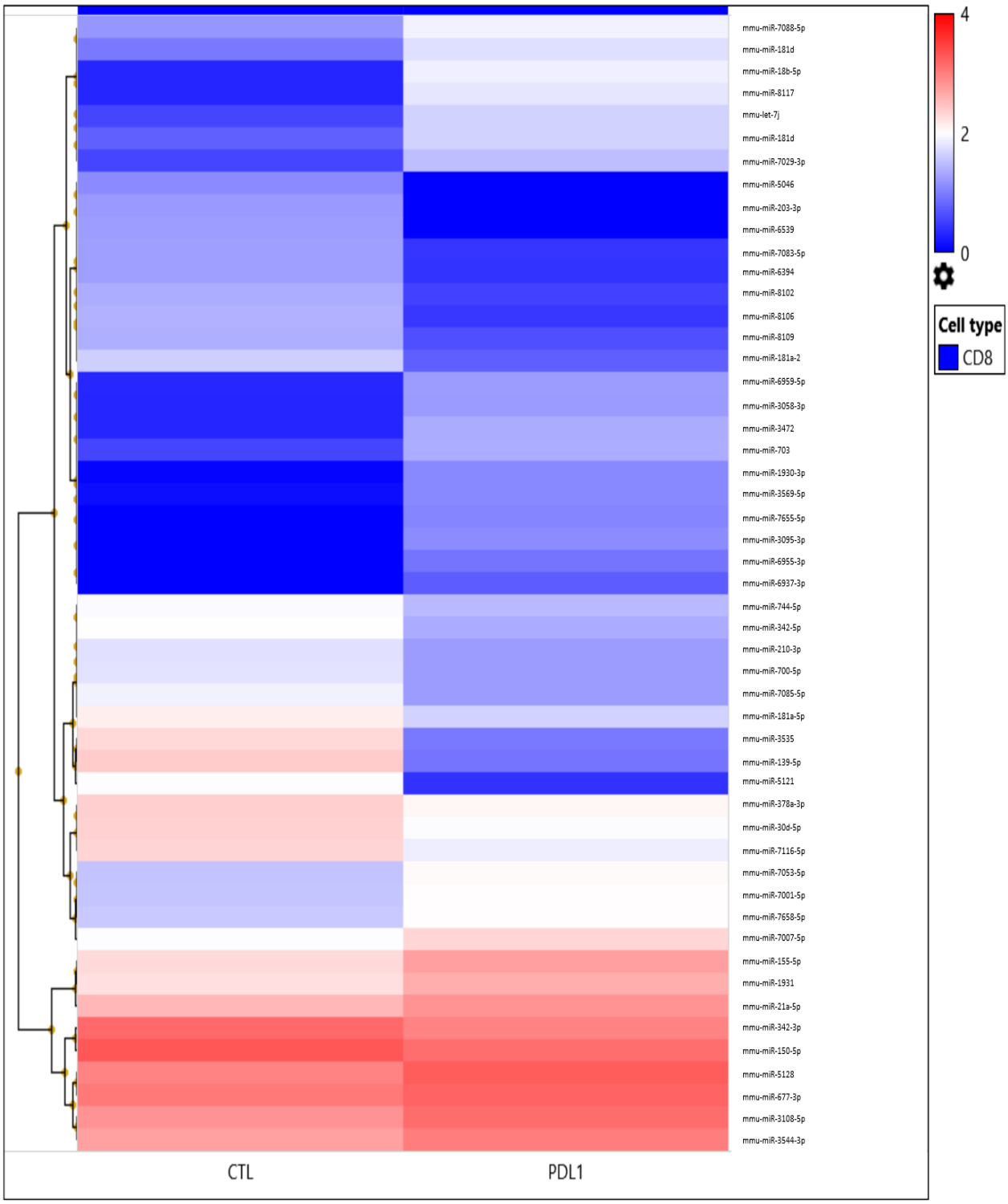

Figure 12: microRNA signal signature of the CD8⁺ tumor-infiltrated T cells. The microarray was run by Genome Québec. The heatmap was generated by TAC program. The clustering performed was the hierarchical clustering regrouping the miRNA based on their expression levels. The color scale is based on the signal (log2) of each miRNA detected in the sample. The red-colored tiles are the high expressed miRNA, while the blue-colored tiles are the low expressed miRNA.

Table 8: miRNA expression highly upregulated with the αPD-L1 treatment.

miRNA	Fold change	predicted target gene
mmu-miR-18b-5p	5,5	HIF1α, SMAD2, DUSP16, FOSL2, ORAI3, MAP3K1, KLF6, NFAT5, MAPK4, SOCS5, NOTCH2, SATB1, PTPN13
mmu-miR-8117	4,85	TOX4, ID2, Thy1, MAP3K4, IL10RA, IRAK3, HK2, SMAD3, IL22RA1, MAPK10, IL4RA
mmu-miR-5128	3,63	HDAC1, IL17RE, KLF6, TOX3, TOX4, CTLA4, MAPK10, SPRY4, IL12RB1, CD28, ORAI2, FZD8, DUSP19, STAT5A
mmu-miR-155-5p	3,6	**Table 12** listed in detail: SMAD5, TAB2, IKBKE, SOCS6, TRAF3
mmu-miR-3108-5p	3,26	STAT3, SATB1, EOMES, CD44, TGFBR1, TAB3, BCL2L11, SOCS5, GATA6, DUSP15, CREB1, CCR7, DUSP4, FADD
mmu-let-7j	3,23	DUSP1, FASL, ROCK1, TAB2, HK2, MAPK6, DUSP9, CCR7, PRDM1

Table 9: miRNA expression weakly upregulated with the αPD-L1 treatment.

miRNA	Fold change	predicted target gene
mmu-miR-1931	2,79	SMAD1, CASP3
mmu-miR-7088-5p	2,76	CEACAM18, IL12RB2, MAP3K3, CASP9, STAT3, SMAD9, DUSP6, FOSL2, BCL6B, IRF9, MAP2K4, HRK, LEF1
mmu-mir-181d	2,71	BCL6, CREB1, TOX, TGFBR1
mmu-miR-3544-3p	2,69	DUSP3, NFATC4, NFATC3, TRAF2, ITK, PIK3R3 (p55), ORAI2, BCL2, IL10RB, CCR4, SOCS3, CEACAM2, MAPK6, JAK1, CEACAM1
mmu-miR-7029-3p	2,56	CEACAM19, CEACAM2, STIM1, ORAI2, CCR9, TNFSF10, MAPK7, BCL2, ICOS, SMAD1, TAB3, IDO2, FOXO1, ITK, PDCD1, JARID2, TOX2, MTOR
mmu-miR-3472	2,51	DUSP7, CCR4, TNFRSF14, IL23R, TBX21, ICOS, SUZ12, DUSP4, BCL10, CCR6, MAPK1, SMAD2, FZD7, STAT1, CCR5
mmu-miR-21a-5p	2,47	**Table 12** listed in detail: PLEKHA1 (TAPP1), PELI1, HRK, FBXO11, PIK3R1 (p85α), EIF4EBP2
mmu-miR-7053-5p	2,31	ICOS, GRB2, GATAD2B, MAPK4, DUSP12, RUNX3, FZD8
mmu-miR-3095-3p	2,31	DUSP28, ITK, PTPN4, PRKCB, PTPN5, TAB2, DUSP3, SMAD2, IL9R, MAPK4, SOCS5, IKBKE
mmu-miR-7001-5p	2,22	FOXP4, CD276, NOS1, E2F2, IL2RB, LRP1, CAV1
mmu-mir-703	2,17	DNMT1, FZD7, NCK1, BCL6, ID2, FZD3, BCL2, MAP2K3, IL6RA, SMAD4, IL17RE, ITK
mmu-miR-6959-5p	2,15	CEACAM2, CEACAM1, IL12RB1, JARID2, DUSP10, TRAF6, FOSL2, TGFBR1, JAK1, SMAD4, SOCS7, LAIR1, CASP16, KLF9
mmu-miR-3058-3p	2,13	SMAD7, MAPK13
mmu-miR-6955-3p	2,13	IL2RA, DNMT3B, SOCS2, FOXO3, MAPK9, FZD3, DUSP4, TRAF3, IL17RD, ITK, STAT6, IL27RA, NFATC2, FADD, SOCS7
mmu-miR-1930-3p	2,11	CD69, ORAI3, HRK, DUSP22
mmu-miR-7655-5p	2,1	TNFRSF9, CREB, GSK3B, SMAD5, RUNX3, SMURF2, FZD3, GRB2, DUSP18, NCK1, IKBKG, PRF1, IL12RB
mmu-miR-7658-5p	2,09	TNFRSF8 [91], MAPK4, NFATC3, IKBKB, PIK3CG, LY6E, STAT5A, CAMK1D, DUSP18, SOX10, TBX21, CTLA2B, FOXP3, CD25, SOCS4, BTLA, ITK, CAMK4, NFATC2, TRAF3
mmu-miR-6937-3p	2,07	IL10RB, JAK1, ORAI3, DUSP4, PRDM1, TYK2, IL-2, DUSP7, JAK3, PIK3CB, TGFBR3, FOSL2
mmu-miR-3569-5p	2,07	SOCS3, JUND, MAPK4, DUSP19, DUSP7, MAP3K4, MAP2K4
mmu-miR-677-3p	2,06	NFAT5, ICOS, SOS1
mmu-miR-7007-5p	2,05	TOX2, DUSP1, SATB1, MAP3K4, TBX21, LEF1, IL17RD, LAT, ORAI1, CHD4, STAT6, DUSP11

Table 10: miRNA highly downregulated with the αPD-L1 treatment.

miRNA	Fold change	Target gene
mmu-miR-139-5p	-10,9	CXCR4, GALNT3, MAPK8, HK2, TRAF3, NOTCH1, SMAD4, SOCS2, SOCS7, FOXO1
mmu-miR-3535	-8,15	CASP12, IRAK2, HRK, MCL1, STAT3, MTOR, TAB3
mmu-miR-5121	-6,27	TNFRSF9, SPRY4, IL2RA, IKBKB, SMAD9, ORAI3, PRKCA, SMAD3, IL6RA, ICOS
mmu-miR-6539	-2,96	TGFBR1, SMAD9, IKBKE, SUZ12, TAB3, TRAF3, SOCS3, TRAF1
mmu-miR-342-5p	-2,8	CD3G, FOXP3, JARID2, GSK3A, TGFBR3, STAT6, NFATC1, NFATC3, FZD2, FZD8, FZD7, FOSL2, AKT1, SOCS3, TIFAB, IRF8, IL6RA

Table 11: miRNA weakly downregulated with the αPD-L1 treatment.

miRNA	Fold change	Target gene
mmu-miR-7116-5p	-2,64	LEF1, TGFBR3, IL13RA1, ITK, CASP9, NFAT5, CXCR5, TRAF3, GRB2, EIF4E, ILF3, RAF1, RAPH1, IRAK, MAPK9, EZH2, MAP3K12, NFRKB, TNFAIP8, CAMK1, CD28, BCL2L1, STAT3, TGFBR3, CAMK2D, CAMK2A
mmu-miR-7085-5p	-2,63	PECAM1, RASAL2, AGO1, IRF2, IRAK1
mmu-mir-181a-2 (precursor to miR-181a-5p)	-2,63	BCL-2, TGFBR1, PDCD4, DUSP10, CAMKK1, TGFBR2, SOCS2, NFATc2, PTEN, SOCS4, SMAD7, JARID2, NFAT5, TGFBR3, NOTCH2, STAT3
mmu-miR-203-3p	-2,46	RASAL2, GSKIP, MAPK8, DUSP19, SMAD1, SOCS2
mmu-miR-8106	-2,41	ITK, MCL1, KLF8, IL20RB, CEACEM1, SMURF1, SOCS5, IL2RB, EOMES, PTEN, IL12RB1, SMAD2, RUNX3, PRKCA, MAPK1, ZEB2, TRAF4, SPRY1, CCR9, NFATC4
mmu-miR-181a-5p	-2,38	BCL-2, TGFBR1, PDCD4, DUSP10, CAMKK1, TGFBR2, SOCS2, NFATc2, PTEN, SOCS4, SMAD7, JARID2, NFAT5, TGFBR3, NOTCH2, STAT3
mmu-miR-150-5p	-2,35	DUSP3, ZEB1, MAP3K3, BTLA, APC, FZD4, FOXO4, SOCS7, FZD1, GSK3B, PTPN6
mmu-miR-30d-5p	-2,27	NFAT5, SOCS1, NFATC3, SOCS3, JARID2, IRF4, GSKIP, SATB1, TRAF3, NOTCH1
mmu-miR-342-3p	-2,27	ARFGAP2, CASP2, PAK1, MAP2K3, FOSL2, PTPN14, TRAF1
mmu-miR-744-5p	-2,25	AKT1, JUNB
mmu-mir-5046	-2,2	ITK, FOXO4
mmu-miR-8102	-2,2	DUSP18, AKT1, CASP16, SMURF1, TRAF3, DUSP23
mmu-miR-700-5p	-2,16	AGO1, RAP1B, NFATC2, SOCS2
mmu-miR-210-3p	-2,09	TNFSF10, STAT6, LAIR1, ZEB2, MAPK6
mmu-miR-6394	-2,09	IRF4, CASP2, PTPN1, CEACAM1, IL6RA, STAT3, CEACAM2, TRAF6
mmu-miR-8109	-2,07	JUNB, FZD8
mmu-miR-7083-5p	-2,06	FOSL2, TBX21, SMAD7, MAPK3, AKT1, HRK, MAPK4, IL2RB, TGFBR3, ZAP70, IL22RA1, CASP9
mmu-miR-378a-3p	-2,02	GRB2, GATA6, MAPK1, MAP2K6, TNFRSF1B

3.2 miR-21a-5p and miR-155-5p affect multiple genes proven to increase the anti-tumoral response.

The prediction of miR-21 and miR-155 target genes was obtained with the TargetScan algorithm (**Table 12**) [154,155]. The two miRNAs were already known to have an essential function in the activation and the response of the $CD8^+$ T cells in the tumor, in the chronic infection model as well as in autoimmune disease and graft rejection [138,139,142-146,151,156-158]. For this reason, these two miRNAs were of particular interest as a starting point in my analysis. miR-21 targets also included key regulators such as PTEN, PDCD4, Sprouty1 (SPRY1) and Dual-specificity phosphatase 10 (DUSP10), which had been established in the tumor rejection to increase the antitumoral response of the $CD8^+$ T cells [156]. It also induces iTregs from the naïve $CD4^+$ T cells, through the suppression of SATB1 and the upregulation of FoxP3 [157]. Also, miR-21 is implicated in tumorigenesis. Where TGFBR2 and FASL have confirmed targets of miR-21 in the prostate cancer cell line, BPH-1 and PC-3, and the breast cancer cell line, MCF-7, respectively [151,159].

miR-155 function and target were even better known. In the tumor model, miR-155 targets have included SOCS1, Fos-related antigen 2 (FOSL2), Src homology 2 (SH2) domain containing inositol polyphosphate 5-phosphatase 1 (SHIP-1), CTLA-4, Protein Tyrosine Phosphatase Non-Receptor Type 2 (PTPN2), DUSP10 and SATB1 in the $CD8^+$ T cells, increasing the response in the rejection of the tumor [142,143,158,160]. In the context of the cell line, miR-155 targets TGFBR2 in the prostate cancer cell line [138,144]. The repression of SMAD2 expression occurs through miR-155 in the macrophage [158]. In the $CD4^+$ T cells, c-Maf and jumonji, AT rich interactive domain 2 (JARID2) are suppressed by miR-155 [144,145]. Further, the suppression of GSK3β is caused by miR-155 in the context of the graft-infiltrated lymphocytes [146]. The implication was that miR-21 and miR-155 repression of TGFBR2 expression could have an indirect effect on the expression of PD-1 permitting a reduction of the terminally exhausted $CD8^+$ T cells [93,94,143,151].

Table 12: miR-21 & miR-155 confirmed and predicted gene target.

miRNA	Target		
	Predicted [Score]	Confirmed	Cells studies
miR-21	PLEKHA1 (TAPP1) [97]	PTEN	$CD4^+$ T cell, $CD8^+$ T cell
	PELI1 [99]	PDCD4	$CD4^+$ T cell, $CD8^+$ T cell
	HRK [97]	FASL	MCF-7
	MAP2K3 [87]	TGFBR2	BPH-1, PC-3
	TIAM1 [92]	SATB1	Tregs
	MAP3K1 [97]	SPRY1	$CD4^+$ T cell
	FBXO11 [94]	DUSP10	$CD8^+$ T cells
	PIK3R1 (p85α) [77/70]		
	EIF4EBP2 [89]		
	KLF6 [91]		
miR-155	MAP3K10 [96]	SOCS1	$CD8^+$ T cell
	MAP3K14 [94]	FOSL2	CD8 $^+$ T cell
	SMAD5 [85]	SHIP-1	$CD8^+$ T cell
	TAB2 [94]	CTLA4	$CD8^+$ T cell
	IKBKE [92]	PTPN2	$CD8^+$ T cell
	SOCS6 [82]	c-Maf	$CD4^+$ T cells
	ITK [90]	GSK3B	graft-infiltrating lymphocytes
	RELA [89]	SMAD2	Macrophages
	RHOQ [84]	DUSP10	$CD8^+$ T cell
	TRAF3 [88]	TGFBR2	BPH-1, PC-3
	CREB1 [72]	SATB1	$CD8^+$ T cell
	MAP3K2 [65]	JARID2	Th17 $CD4^+$ T cell
	FZD5 [64]		

3.3 miR-21 and miR-155 target PD-1 expression and other inhibitor genes enhancing the activity of $CD8^+$ T cells.

To validate the importance of these miR-21 and miR-155 in the $CD8^+$ T cells as well as to increase the statistically significant difference between the two groups, the experiment was repeated and the miRNA expression was confirmed with the qPCR measurements (average fold change of 10.35 for miR-21 and 5.28 for miR-155 overexpression) (**Fig. 13**). These data confirmed the overexpression of these miRNAs in the context of αPD-L1 immunotherapy.

miRNA's sequence or anti-sense was inserted into the retrovirus transfer plasmid, pMKO.1 GFP. The miRNA mimic was overexpressed inside the cells with the retroviral transduction. In other words, the miRNA mimic increased the effects of the specific miRNA. For example, miR-21 mimic added to the expression of miR-21. By contrast, the miRNA antagomirs act as an inhibitor of the miRNA expression inside the cells since it is the anti-sense sequence of the mature miRNA. It acts to neutralize the effects of its target miRNA. Ideally, the sense and the anti-sense approaches should complement each and permits us to identify the identity and targeting of genes by the miRNA.

With this, it was next important to confirm the function of miRNAs in the regulation of T-cell function and tumor immunity. The determination of the different targets of miR-21 and miR-155 in $CD8^+$ T cells was shown in figure 14. The $CD8^+$ T cells were transduced with each retrovirus containing the miRNA mimic, antagomir and empty vector (CTL). The total RNA was extracted by Trizol for the two-step RT-qPCR. The determination of the fold change included the determination of dCT, ddCT and the fold change (log2). The calculation of dCT is the normalization of the gene expression to the housekeeping gene, GAPDH. The second calculation is the normalization of the difference between the mock-transduced cells and the miRNA transduced cells. Finally, the fold change was calculated by using the log2 fold change. Among targets, based on the previous paper, I expected miR-21 to target SATB1 and TGFBR2. Indeed, I saw effects on Tgfbr2 and not on Satb1 (**Fig.14A)**.

Similarly, in figure 14B, among targets based on previous papers, I expected miR-155 to target SATB1, TGFBR2, SOCS1, PRDM1 and CTLA4. Indeed, I saw effects on Tgfbr2, Ctla4, Prdm1 and not on Stab1 and Socs1 (**Fig.14B**).

miR-21 mimic, miR-155 mimic and miR-155 antagomir repress the transcription of PD-1 gene (PDCD1) and TGFBR2. Interestingly, unlike reported in other studies, we found that the miRNAs did not affect the expression of SATB1 or SOCS1 [138,160]. While miR-155 mimic suppressed the expression of CTLA-4, miR-155 antagomir has a higher effect in its suppression (-2,7 vs -170.6 fold change). The effects of miR-21 mimic and miR-21 antagomir on JAK1 were surprising due to the absence of a binding site on the mRNA for the miRNAs in different prediction sites (TargetScan, miRDB and RNA22). This suggested an indirect pathway. Because miR-155 and miR-21 target various genes, the miRNAs could target inhibitory TF of the JAK1, CTLA-4 and PRDM1. Interestingly, some genes target by miRNA mimic were also target by the antagomirs. This process could be explain the inhibitory effects of the miRNAs. The antagomir could increase the transcription of transcriptional repressor of those genes. This could result in the higher repression of the genes then the miRNA mimic. Additionally, miR-21 mimic effects on the expression of TGFBR2, SOCS1 and CTLA-4, well as miR-21 antagomir on CTLA4, cannot be determined in the qPCR due to their poor expression (**Fig 14**).

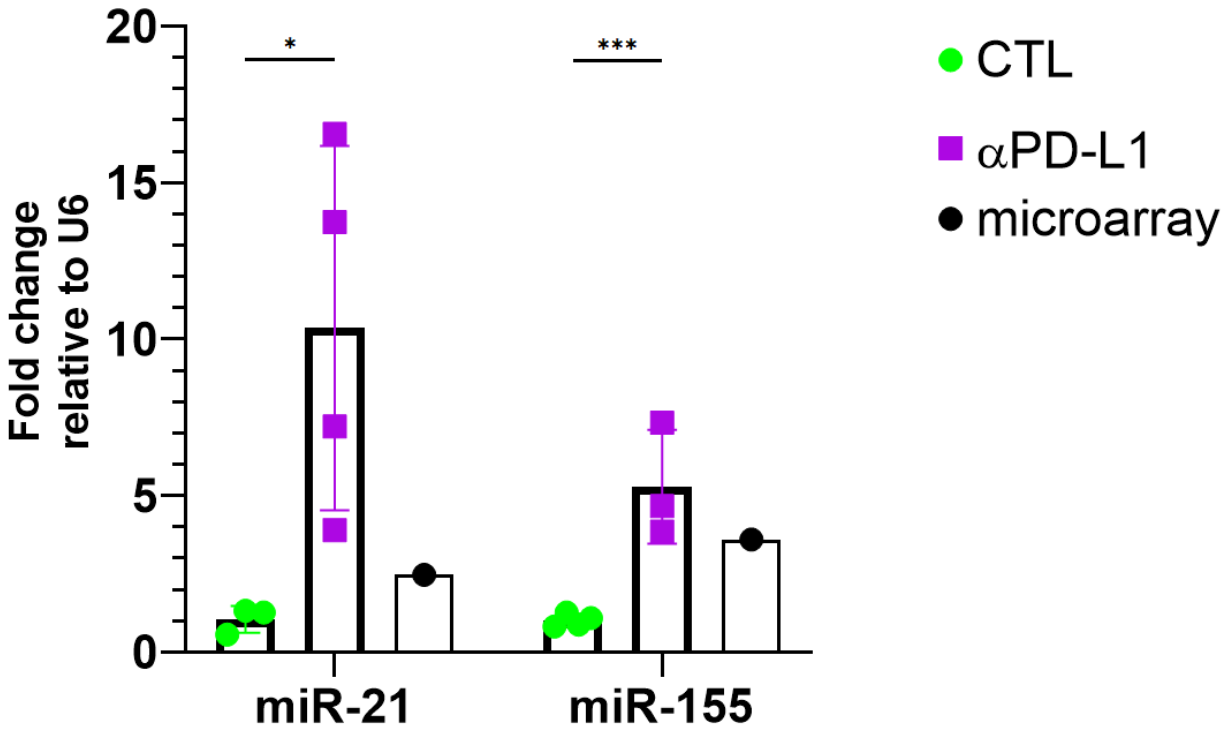

Figure 13: Validation and determination of the p-value of miR-21 & miR-155 expression in TILs CD8⁺ T cells. The validation of miR-21 and miR-155 was realized using TaqMan RT-qPCR. The tumoral infiltrated CD8⁺ T cells were isolated identically as in the initial experiment. The microarray results are the fold change calculated from the microarray. Statistical analysis: $p \leq 0,05$ *, $p \leq 0,01$ **, $p \leq 0,0001$ ***.

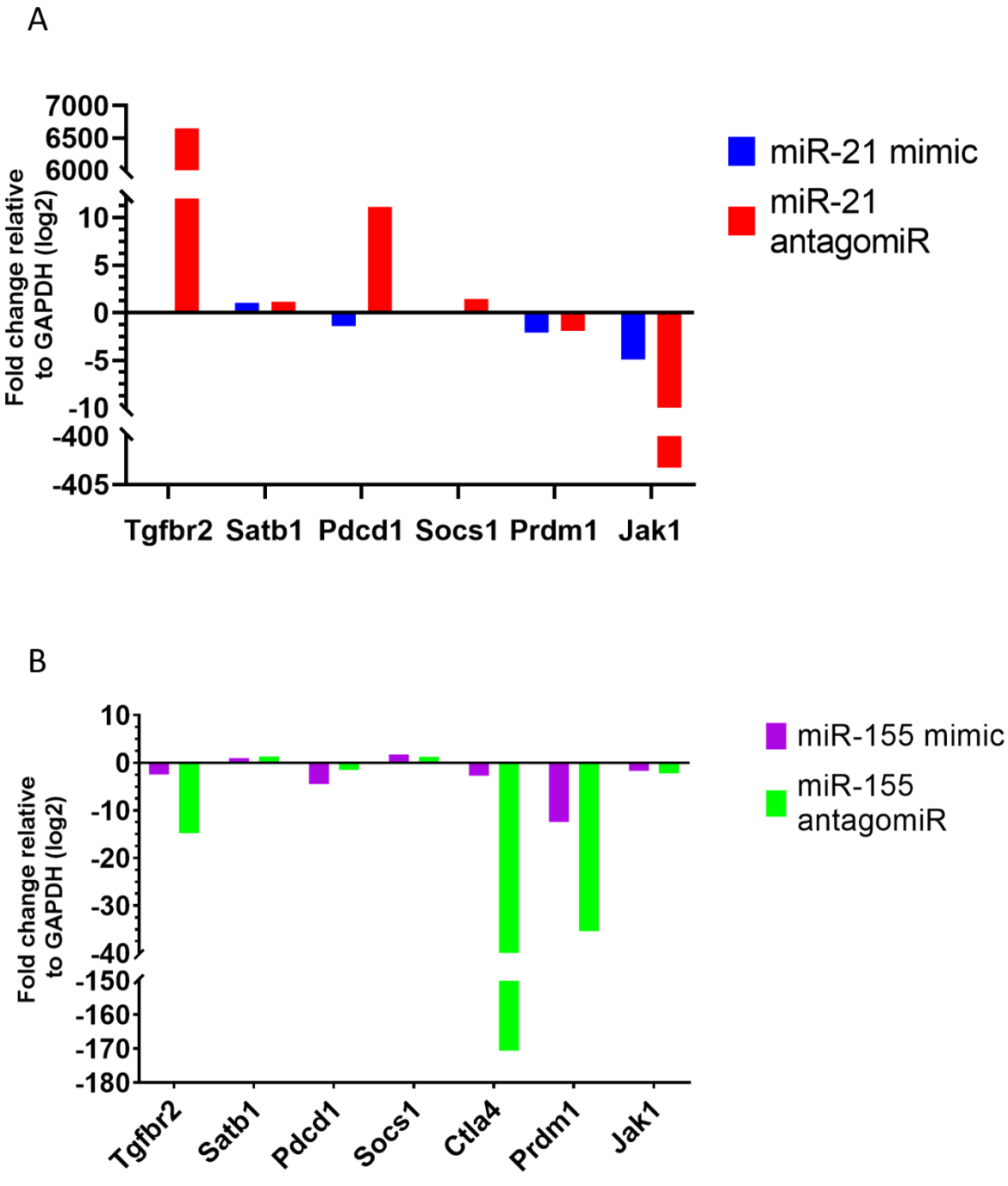

Figure 14: miR-21 mimic and miR-155 mimic target the expression of Pdcd1 and other genes in the CD8$^+$ T cells. CD8$^+$ T cells were isolated from C57BL/6j spleen. They were activated with αCD3 and αCD28 for two days before the transduction with pMKO.1 GFP (CTL), (A) pMKO.1 GFP miR-21 mimic and pMKO.1 GFP miR-21 antagomir, (B) pMKO.1 GFP miR-155 mimic and pMKO.1 GFP miR-155 antagomir. The expression was calculated from the CT, dCT, ddCT and log2 fold change between the CTL and the other transductions, after the normalization with GAPDH, the housekeeping gene.

3.4 miR-21 affects the cytotoxicity and cytokine production of $CD8^+$ T cells.

miR-21 was further analyzed in the potential regulation of tumor rejection using an adoptive cell transfer (ACT) model. This ACT model had been previously used by the Rudd lab to examine the GSK-3 pathway in the regulation of T-cell tumor rejection [161,162]. However, I initially began with an *in vitro* assay for OT-I T-cell killing of OVA carrying targets (**Fig.15**). This involved the activation of OT-I cells by use of OVA peptide ($OVA_{257-264}$), SIINFEKL, followed by incubation for 7 days followed by an assessment of CTL function using OVA expressing target cells [163]. A higher lactate dehydrogenase (LDH) release in the OT-I spontaneous LDH release was used to compare mixtures of target cells, EL4-OVA and effector cells (**Fig.15**). With this, in control samples, I observed an increase in killing with increasing ratios of T-cell to target from 2.5 to 25:1, although this was not optimal given a problem with the 5:1 ratio. Nevertheless, miR-21 mimic expression was found to increase the cytotoxicity activity of the OT-I $CD8^+$ T cells when comparing ratios 2.5 to 10:1 (with the outlier 5:1 expected). Given that an increase was observed at the other target ratios, these data suggested that the miR-21 mimic could augment $CD8^+$ T-cell function.

To understand the other effects on the immune response, the production of cytokine was determined. There was no change in the cytokine production between the control and miR-21 transduced $CD8^+$ T cells. Contrary to the qPCR results, the reduction of PD-1 expression wasn't detected at the protein level unlike at the mRNA level (**Fig. S2**).

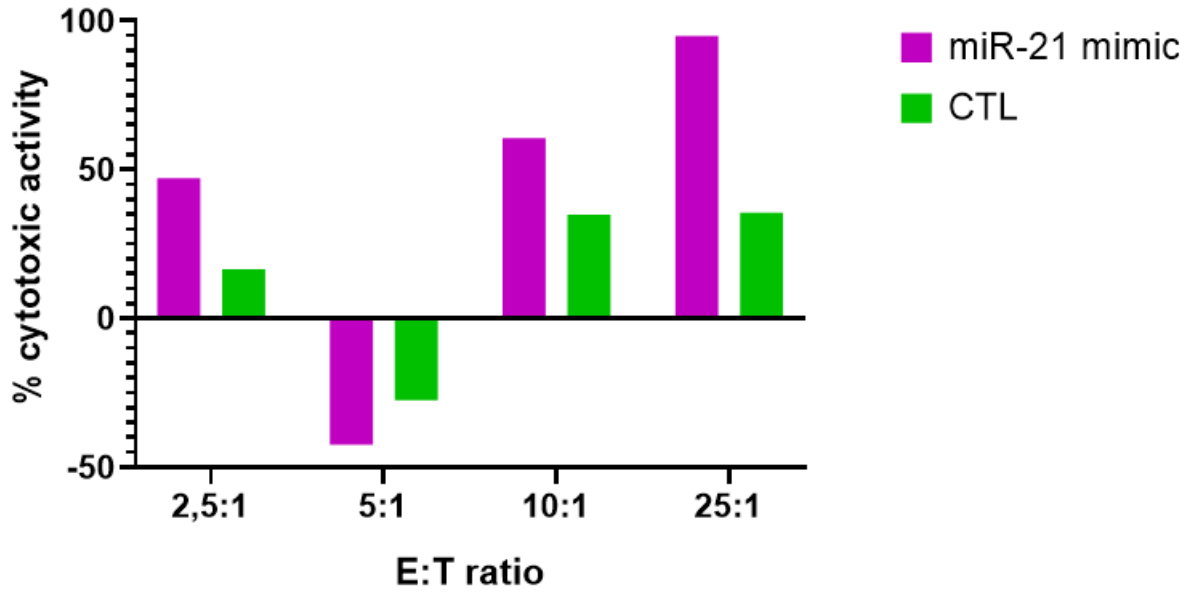

Figure 15: miR-21 overexpression increases the cytotoxic activity of the OT-I CD8⁺ T cells. The cytotoxicity assay measures the liberation of LDH in the media. The supernatant was transferred to a new plate before adding the reactive and the measurement of absorbance at 490nm in the TECAN plate reader (n=2).

3.5 miR-21 transduced OT-1 increases the control of tumor growth.

Next, to determine the effects of miR-21 on tumor growth, OT-I cells were transduced by miR-21 mimic or empty plasmid followed by their sorting by FACS and their transfer into B16-OVA bearing mice. The sorting showed an approximative 50% of transducing OT-I in the two groups (**Fig. 16**). The mice receiving the miR-21 OT-I had better control on the tumor growth (i.e. 278.5 mm^3 to 149.3 mm^3) than the CTL with a p-value of 0,001 (**Fig. 17A, B**). Also, see the spider graphs (**Fig.17B**). These data showed for the first time that the expression of miR-21 in T-cells could be used in ACT therapy to improve cytolytic T-cell functions against tumors.

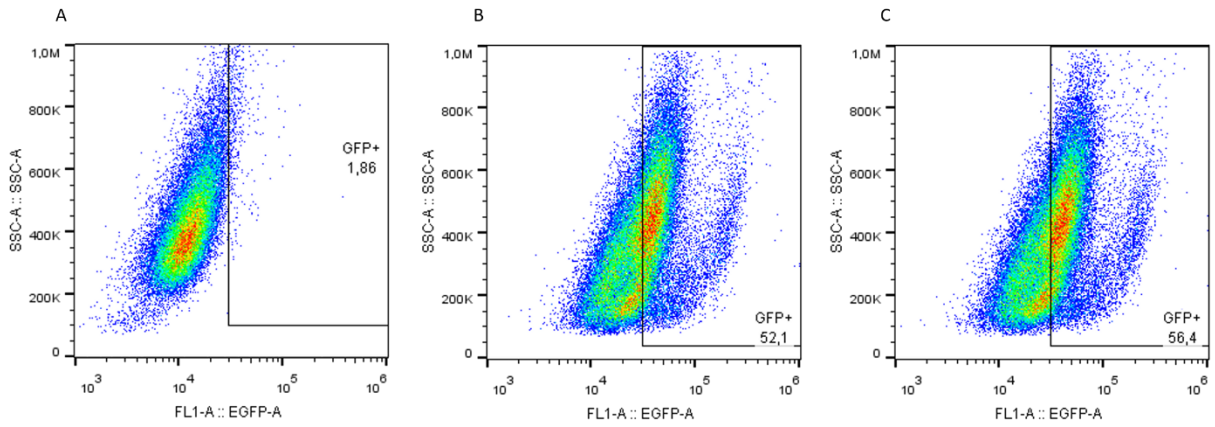

Figure 16: Transduced OT-I cells showed GFP$^+$ expression. (A) Non transduced control OT-I, (B) miR-21 mimic transduced OT-I, (C) pMKO.1 transduced OT-I. The cells were sorted using Sony SH8000S sorter.

After demonstrating the effect of miR-21 ACT on tumor growth, we wanted to understand the effects of the injection of miR-21 OT-I on the other infiltrated immune cells. From each tumor-bearing mouse, the TILs, the draining lymph node and the splenocytes were taken after 21 days after the tumor implantation. Because the injection was done by IP, the OT-I cells would tend to migrate toward the spleen. Because of the OT-I movement, multiple organs were removed to localize the transfer cells. Furthermore, to understand the full length of miR-21 OT-I injection effects in the two lymphoid organs, various markers were analyzed in the dLN and the spleen. In those organs, no major change was noticed between the groups regarding the presence of CD3$^+$, CD4$^+$ and CD8$^+$ T cells. The same change was observed in the CD3$^+$ TILs between the two groups (**Fig. 17C, D and E**). We observed that the smaller size tumor had the lowest infiltration of CD8$^+$ T cells. The efficient infiltration of OT-I in the tumor could reduced the infiltration of other CD8$^+$ T cells (**Fig. 17F**). As for the CD4$^+$ TILs, there is a small decrease in infiltration in the miR-21 mimic injected mice (**Fig. 17D**).

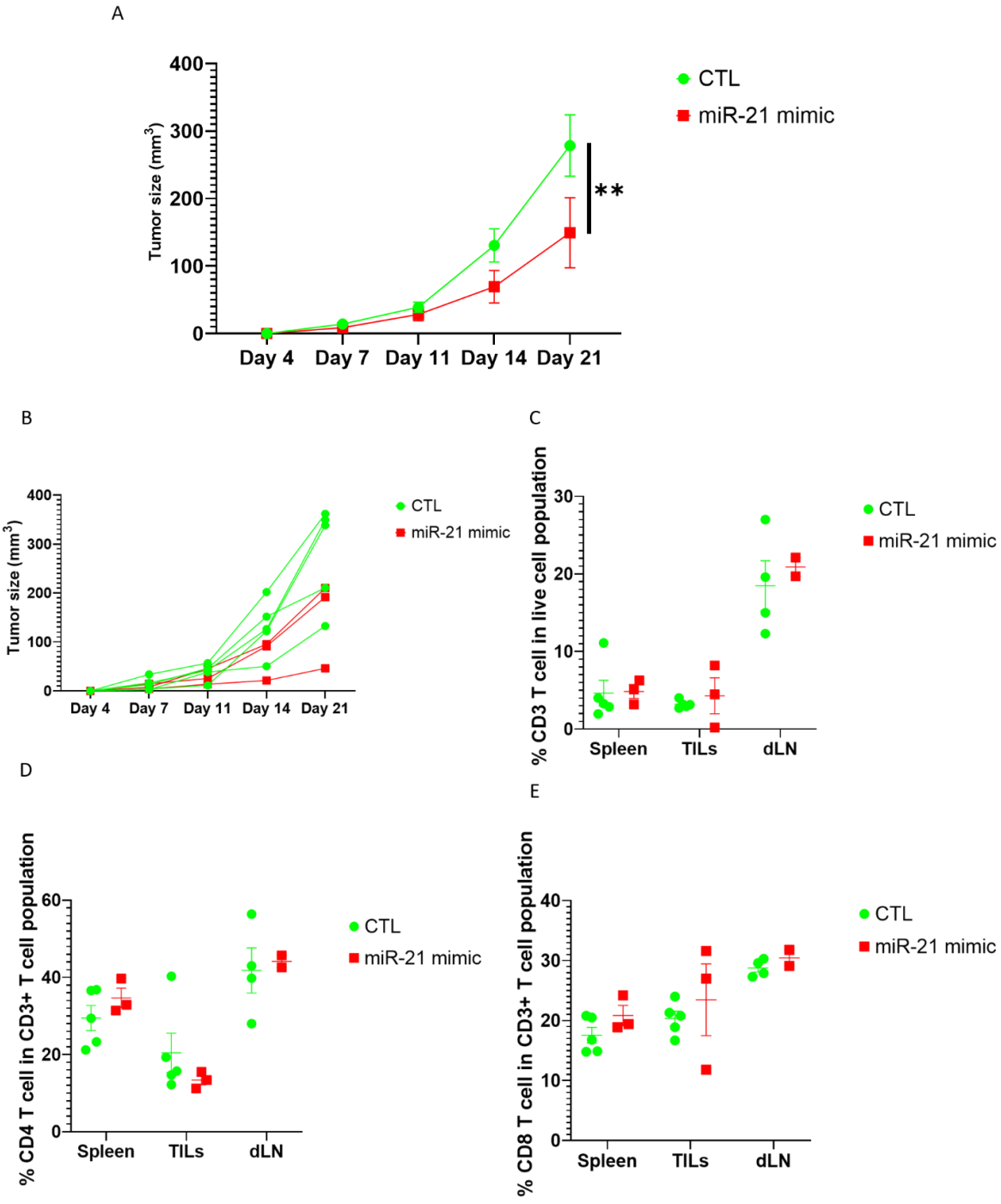

Figure 17: The cell transfer of miR-21 transduced OT-I in the B16-OVA bearing mice reduces the growth of the tumor. B6-SJL mice were implanted subcutaneously with B16-OVA. On day 7, the mice received the transduced OT-I. The tumor was measured on days 11, 14 and 21. The mice were sacrificed and the organ was collected on day 21. (A) The tumor growth curve between the two groups. (B) Individual mouse tumor growth in the CTL group (n=5) and miR-21 mimic (n=3). (C) Percentage of infiltration $CD3^+$ T cells. (D) Percentage of infiltration $CD4^+$ T cells. (E) Percentage of infiltration of $CD8^+$ T cells. Statistical analysis: $p \leq 0,05$ *, $p \leq 0,01$ **, $p \leq 0,0001$ ***.

Despite this, although the infiltration of $CD8^+$ T cells did not change between the CTL and miR-21, I found that the percentage of $CD44^+$, $CD62L^+$ memory T cells, $SATB1^+$ and Killer cell lectin-like receptor subfamily G member 1 $(KLRG1)^+$ effector T cells were lower in the miR-21 mimic group while the $PD\text{-}1^+$ T cells were significantly higher (**Fig. 18**). Interestingly, all the $CD8^+$ T cells were $CD45^+$ in the two groups (data not shown), but the mean fluorescence intensity (MFI) was higher in the miR-21 group (**Fig. 19A**). Also, the $CD44^+$ population was lower in the miR-21 group while the MFI increased significantly (**Fig. 18A and 19C**). The expression of CD45, CD44 and PD-1 shows the activated population in the $CD8^+$ T cell. The high expression of PD-1 on the $CD8^+$ T cell displays the exhausted T-cell population as well as their activation. The expression of PD-1 is upregulated after their activation, in other words, the higher the active T-cell the higher their PD-1 expression. These data corroborate the high expression of the activator marker CD44 as well as the high expression of CD45 on their surface. However, the effect of miR-21 wasn't detected in the $CD8^+$ T cells. Furthermore, the GFP^+ OT-I cells were not found in any of the collected organs. Either way, the transfer of miR-21 OT-I increased the activation of the $CD8^+$ T cells in the tumor, slowing their growth.

In the spleen, there were no changes between $PD\text{-}1^+$ and $SATB1^+$ populations in the two groups. The phenotype of the $CD8^+$ T cells changed with a decrease of $CD44^+$ T cells, the effector cells and an increase in the memory cells. In the draining lymph node (dLN), there was an increase in the effector T cells along with the $SATB1^+$ T cells (**Fig. 18**).

Therefore, from these, I observed an effect of miR-21 on the regression of B16 tumors with a trend to see an increase in $PD\text{-}1^+$ TILs in tumors. PD-1 expression is both an activation indicator when expressed at moderate levels and a marker for T-cell exhaustion when expressed at high levels [19].

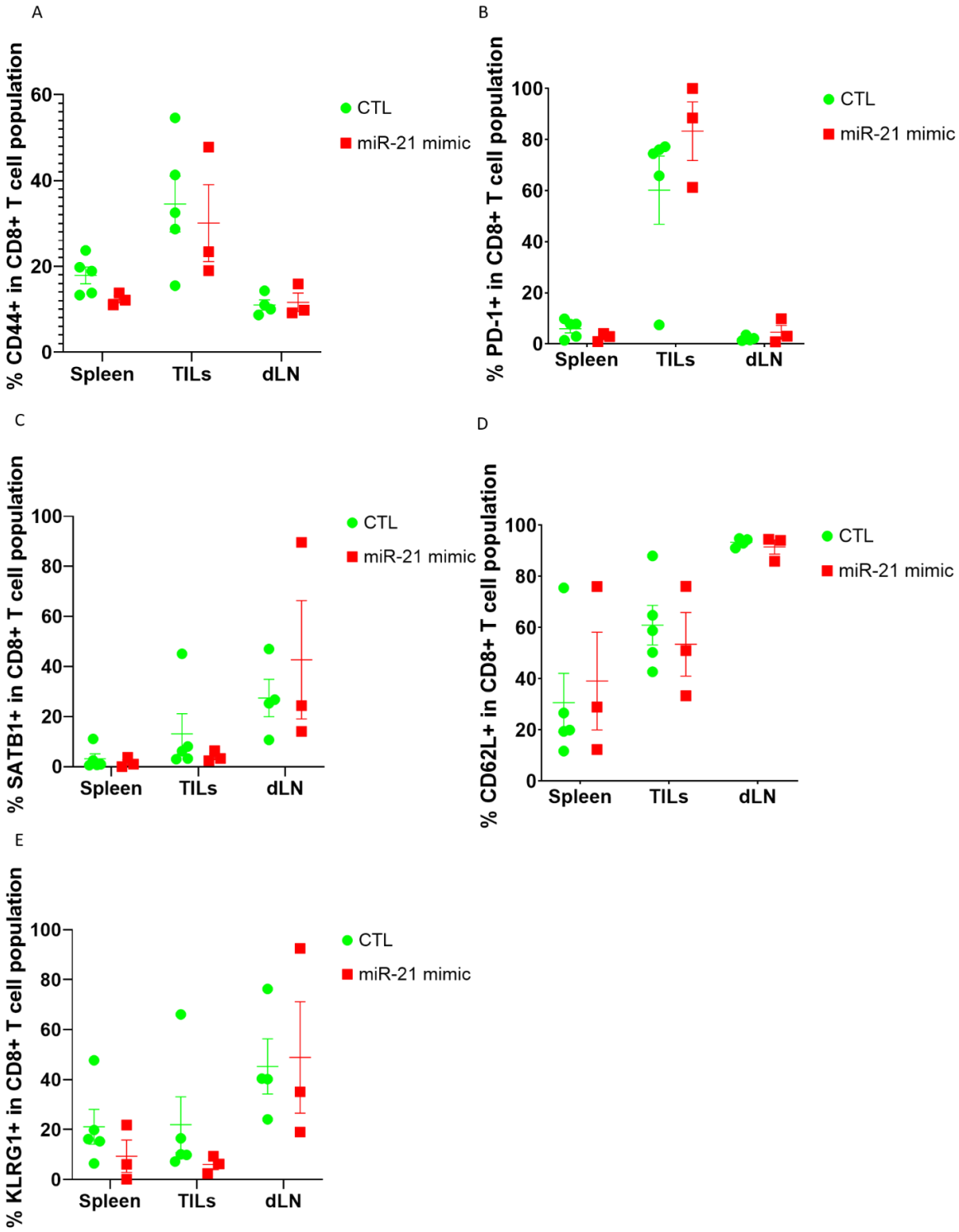

Figure 18: Population variation of effector, memory and exhausted CD8⁺ T cells after the cell transfer of OT-I transduced miR-21. The TILs, dLN and spleen of each tumor-bearing mice were collected on day 21 followed by their stained for (A) activation (CD44), (B) exhaustion (PD-1), (D) effector (KLRG1) and (E) memory (CD62L) marker, as well for (C) STAB1 expressing cells.

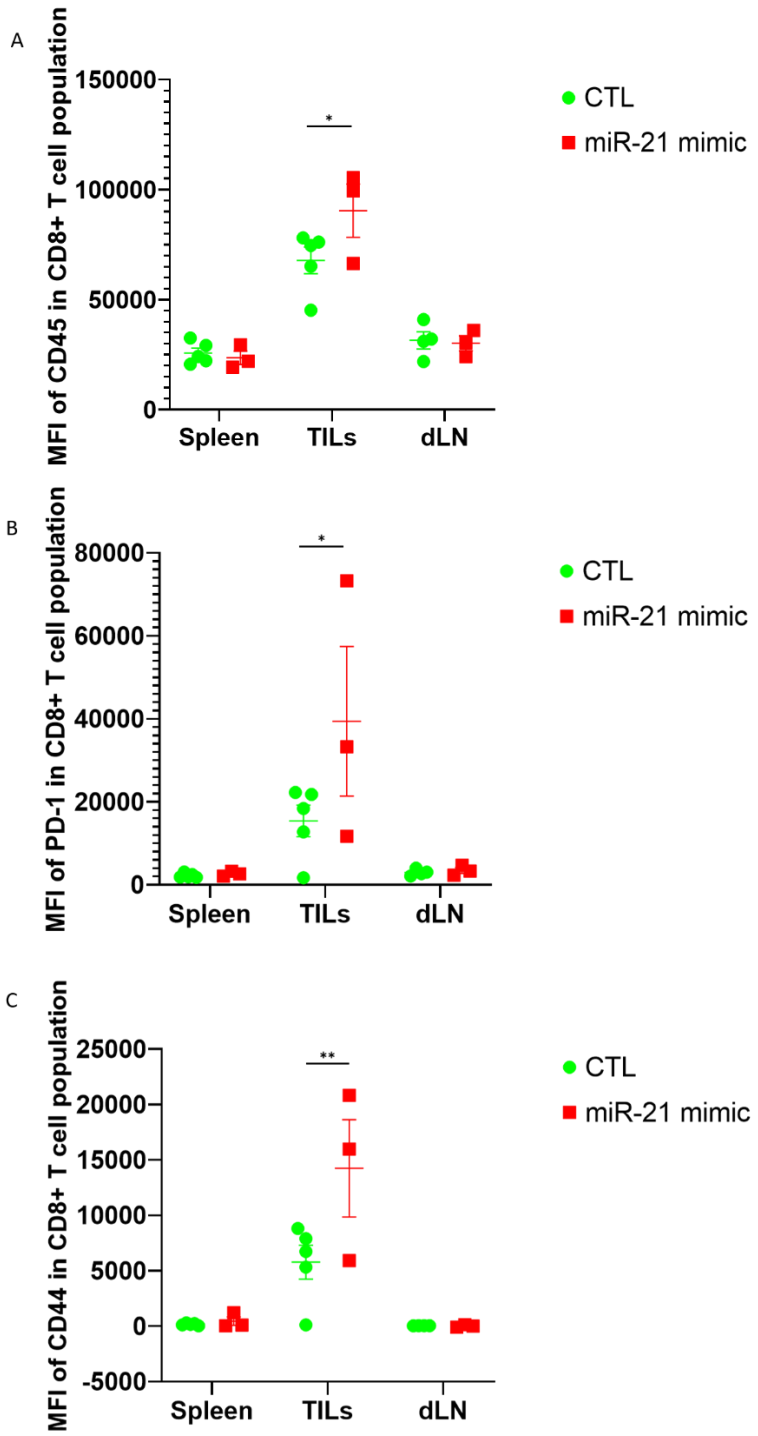

Figure 19: The transfer of miR-21 OT-I increases the expression (MFI) of CD44, PD-1 and CD45. The FACS analysis and obtention of the MFI were done on $CD8^+$ T cells. (A) MFI of CD45. (B) MFI of PD-1. (C) MFI of CD44. Statistical analysis: $p \leq 0,05$ *, $p \leq 0,01$ **, $p \leq 0,0001$ ***.

The viSNE analysis was done with proportional event sampling. There were multiple variations in the distribution of $CD3^+$ T cells between the mice within each group (**Fig. 20A**). The overall infiltration of the $CD3^+$ T cells was higher in the miR-21 OT-I transfer cells mice. The distribution of the $CD8^+$ T-cells shows a shift in the CD44 and PD-1^{hi} population in the miR-21 treated mice. Figure 20A presents a lower expression of PD-1 and CD44. Also, it is visible in the dLN (**Fig. 20B**).

By comparing the expression of the different markers in the $CD3^+$ T cells, it appears that the injection of OT-I miR-21 cells results in the decrease of the phosphorylated form of AKT and a decrease in SATB1 expression within the T cells. In the other markers, there was no major variation between the two groups in the whole T cell population except CD44 expression in the three miR-21 treated mice which were lower (**Fig. 20C**).

These data show the importance of T-cell infiltration in the tumor to increase tumor rejection. The high infiltration also reduces the exhaustion of the T cells.

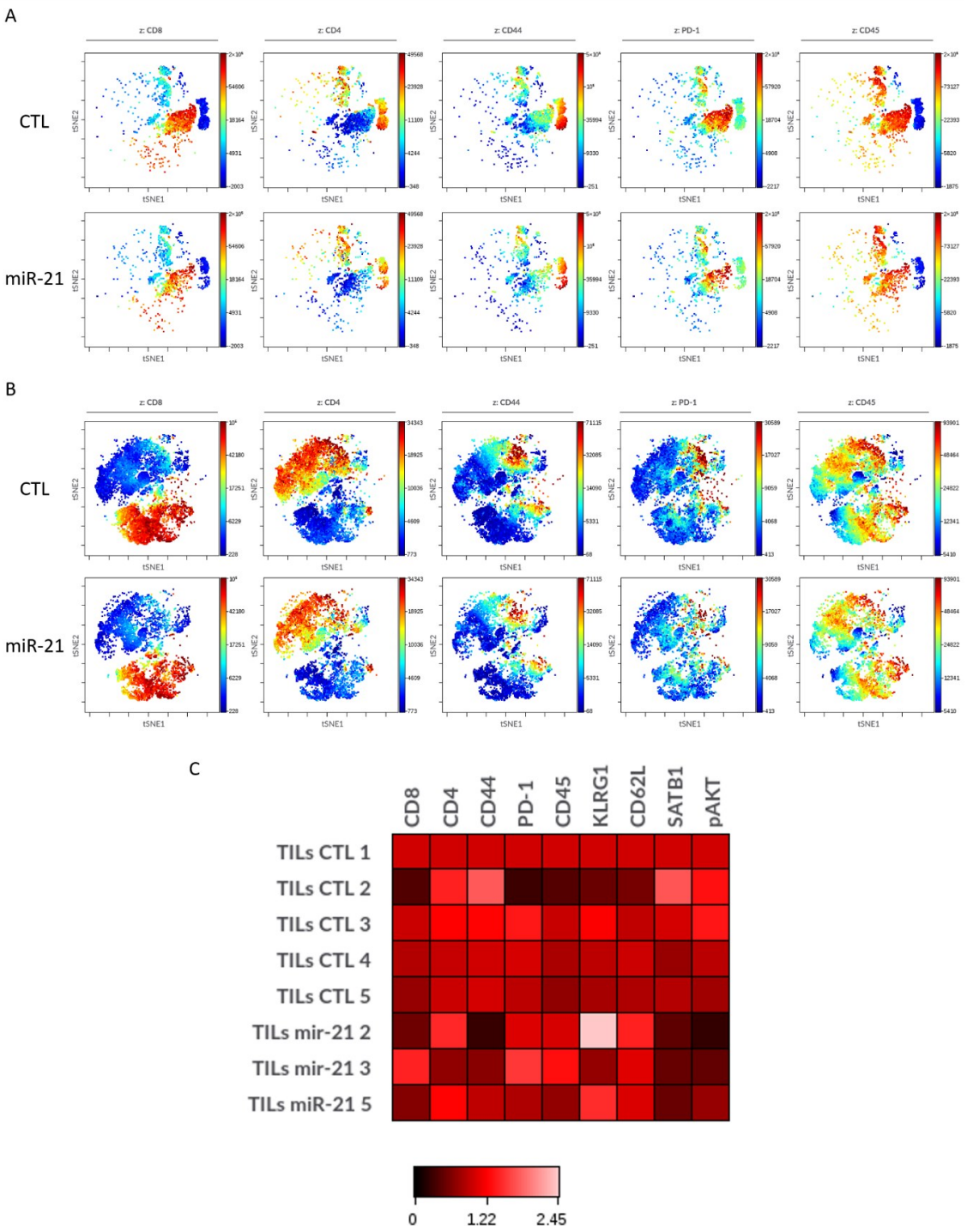

Figure 20: The variation of different markers on the CD3⁺ T cell between the transfer of miR-21 transduced OT-I and the CTL transduced OT-I. viSNE proportional analysis of the marker from the (A) TILs and (B) dLN. (C) Heatmap generated by Cytobank measuring the fold change between TILs CTL1 and the rest of all the markers.

Chapter 4: Discussion

The investigation of the expression of miRNAs in various diseases has increased over the last few years [164]. These regulators negatively regulate the expression of key modulators of cell function as demonstrated in many contexts. In this context, it has been unclear whether specific miRNAs are linked to the ability of checkpoint blockade in tumor rejection. This is the subject of my M. Sc. thesis where my work has identified several miRNAs which are upregulated or downregulated in TILs from B16 tumors successfully regressed by αPD-L1 immunotherapy. Amongst these, my thesis focussed on two of interest, miR-21 and miR-155 expression in the $CD8^+$ T cells since some pre-existing data was documenting their importance in T-cell biology. My work has contributed to the field by connecting miR-21 to αPD-L1 therapy as well as implicated the miRNA for the first time in the development of $CD8^+$ T-cell cytotoxic activity.

Previous work has implicated miR-21 and miR-155 expression in T-cell functions such as anti-tumoral response, T-cell apoptosis and autoimmune disease [140,149,156,165]. miR-21 and miR-155 has been seen in $CD8^+$ T-cell activation, in TILs and tumor cells [138,139,142,147,149,151,159,160]. Also, miR-155 has been seen in macrophages, Th17 cells and graft-infiltrated lymphocytes [145,146,158]. In my work, I found that the treatment with αPD-L1 caused an increase of miR-21 and miR-155 within the $CD8^+$ T cells. We observed a trend for an increase in CD3 and $CD8^+$ cells within the $CD3^+$ TIL population in the miR-21 mimic population as defined in adoptive cell therapy. In terms of receptor expression, the work showed an increase in the MFI of CD45, CD44 and PD-1 indicating that the $CD8^+$ subset likely underwent activation leading to an increase in the antigen-experienced TILs.

As indicated above and in **table 12,** miR-21 affects different genes in multiple cell types. Among them, TGFBR2 has been identified as a target in the cancer cell lines BPH-1 and PC-3, prostatic cancer cell lines [151]. The signaling pathway influences the expression of other genes, including SATB1 [93]. This TF increases the DNA methylation of the PD-1 promotor through the recruitment of DNMT3, a DNA methyltransferase [94]. With the upregulation of miR-21 expression, it should downregulate the expression of TGFBR2 increasing PD-1 methylation. Although, PD-1 expression is upregulated after T cell

activation by NFAT and AP-1 [166]. miR-21 overexpression could prevent the $CD8^+$ T cell to turn into terminally exhausted T cells in later T cell stages, such as inside the TME.

The expression of CD44 on the T cells is related to their activation and motility. CD44 is an adhesion receptor with a function in the rolling, arrest and transmigration of the T cells to the inflammation site. The receptor has a binding site for PI3K and Lck, each important for the cell spreading and the actin polymerization, respectively [167]. Interestingly, CD44 has the potential as a co-stimulatory receptor with the induction of CD69 and CD25. It has been reported that CD44 increases TCR signaling in the situation of low affinity between the TCR and the antigen [168]. Furthermore, the receptor protects the effector cells from apoptosis through the PI3K/AKT signaling pathway and the inhibition of Fas and Casp-8 signaling [167]. The expression of CD44 on the T cells is important to assure their migration toward the tumor. The adhesion receptor has an important role in the navigation of the killer T cells through the EMT [169]. However, the high CD44 expression is related to low phosphorylation of ZAP-70, PLC-γ1, Erk and LCK Y394, including Ca^{2+} influx. Although the $CD44^+$ $CD8^+$ T cell population was low, the expression on the surface shows the exhaustion of the T cells correlating with the expression of PD-1 on them. Paradoxically, in my work, the infiltration of T cells was reduced in the adoptive cell transfer while the expression of CD44 was increased. It could be possible that the CD44 marker has a higher influence on the activation and exhaustion of the $CD8^+$ T cells than their migration toward the tumor in this cell transfer model.

CD45 receptor has multiple functions in the T cells. Its main function in the T cell activation is the initiation of Lck activation. The transmembrane phosphatase dephosphorylates the inhibitor residue 7505. The full activation of Lck needs the autophosphorylation of residue Y394. However, CD45 can dephosphorylate the residue. So, the high expression of CD45 on the T cells reduces the phosphorylation of ZAP-70, PLC-γ1 and Erk and, overall, the activation of the T cells [5,170].

In my work, the downregulation of pAKT could correlate with the high expression of CD45. CD28 phosphorylation is mediated by Lck. The decrease of pAKT could explain a lower presence of the active form of Lck. pAKT regulates the survival of the T cells, so

a reduction of pAKT would increase the risk of T cell death. The correlation of CD44 expression and the $CD8^+$ T cell infiltration shows that the control of tumor size is mediated by the capacity of the T cell to travel into the TME. High expression of CD44 causes a higher infiltration in the tumor resulting in its control of growth (**Fig.17,18,19**).

The αPD-L1 treatment increase the infiltration of $CD45^+$ immune cells when it's compared to his control conditions (αPD-1 compared to αIgG). During analysis of the $CD45^+$ immune cells infiltration, the transfer of miR-21 OT-I didn't affects the migration when compared to CTL OT-I. In the αPD-L1 treatment, the influx of immune cells and $CD8^+$ T cells was higher between all the groups. Also, the tumor-bearing mice treated with αPD-L1 had the best control on the tumor growth and tumor weight. This experiment showed that the increase in the influx of $CD8^+$ T cells in the tumor could control tumor growth. Compared to the ACT of miR-21 OT-I, the transduced cells had a higher killing function that is not provided by the αPD-L1 treatment.

Having shown an effect of the αPD-L1 treatment, the next question will in the future be to determine whether αPD-1 can have any further effect on T-cells expressing the miR-21 mimic. If the induction of miR-21 is the principal pathway by which αPD-1 promotes T-cell function against tumor antigens, then the αPD-1 treatment in combination with miR-21 antagomirs transduced ACT will have no further effect. Results as such will be of great unexpected importance, firstly by showing for the first time that αPD-1 elicits protective immunity due to an effect on microRNAs and secondly by specifically identifying the main microRNA of importance, miR-21.

If αPD-1 has additional effects on miR-21 $mimic^+$ T-cells then this would implicate other microRNAs in the process. This is considered the most likely outcome but it is noteworthy that the level of miR-21 mimic effects on tumor growth is similar to what one generally sees for αPD-L1. Another approach therefore will be to transduce with miR-21 antagomir to see whether it blocks the ability of αPD-1 to regress tumors. The combination of approaches will likely provide the most accurate assessment.

On another level, my results are the first to show that miR-21 plays a role in tumor regression. Others had shown that miR-21 suppresses apoptosis in activated T cells [149],

while others have documented a direct role in the tumor growth itself [165]. This introduces the question, which of the various targets of miR-21 is responsible for these important effects on the tumor immunity? Previous studies have shown that miR-21 and miR-155 expression is mediated by the TF, AP-1, NF-κB and STATs, STAT3 for miR-21 and STAT5 for miR-155 [148].

The most striking downregulated target in my study was JAK1 in miR-21 antagomir transduced cells. This kinase has been connected to cytokine receptors and signaling pathways [171]. It binds to the pro-inflammatory cytokine receptor, such as IL-2, IL-21 and the IFN receptor, as well as an anti-inflammatory cytokine receptor, for example, IL-10. The implication of JAK1 in the $CD8^+$ T cells variates between their proliferation, the differentiation into memory phenotype and their inhibition [71]. The differentiation of the $CD8^+$ T cells into Tc2 has shown to have low effects on tumor growth compared to Tc1 cells [108]. The inhibition of JAK1 expression could change the polarization of the $CD8^+$ T cells into Tc1. The JAK isotype responsible for the Tc1 differentiation is JAK2 and Tyrosine kinase 2 (TYK2). The suppression of JAK1 expression wouldn't affect the Tc1 polarization only the Tc2 due to the interaction of the kinase to IL-4R. The production of IL-10 from the Tregs and macrophages M2 is a reason for the immune-suppressive environment of the TME. By targeting JAK1 in the $CD8^+$ T cells, it can be possible to prevent or inverse the inhibitory effects of the anti-inflammatory cytokine and re-establish its cytotoxicity activity. It would be interesting to see the effects of miR-21 antagomir and mimic in the presence of IL-10 and the polarization on the $CD8^+$ T cells in future studies. miR-21 increases amounts of IL-10 and prostaglandin E_2 (PGE_2) in the tumor microenvironment *in vivo* [172].

Another effect of miR-21 and miR-155 mimic would be the downregulation of the PDCD1 mRNA level. However, the protein level expression doesn't change between the GFP-transduced T cells and the miR-21 mimic transduced T cells. The conservation of the PDCD1 gene between the mouse and the human is very low. The comparison of the transcript from the two species by the program Basic Local Alignment Search Tool (BLAST) from the National Center for Biotechnology Information (NCBI) shows a similarity of 71%. To downregulate the expression of PD-1, reproducible between the mouse and the human, the effects have to be indirect. By targeting TGFBR2, SMAD2/3

phosphorylation is reduced preventing their translocalization in the nucleus [90]. The TF represses the expression of SATB1 [113].

Another study showed that SATB1 increases the DNA methylation of PD-1 promotor by recruiting the NuRD complex and the methyltransferase DNMT3A/B [94,96]. During the analysis of my ACT, SATB1 expression was reduced in $CD8^+$ T cells after the transfer of the miR-21 mimic transduced OT-I. This could explain the higher expression of PD-1 in the miR-21 group.

Also, miR-21 targets the expression of PTEN in the $CD8^+$ T cells. By measuring the phosphorylation of AKT, the level of PTEN could be determined as well as the overall expression of miR-21 in the cells. Due to the restrictive number of cells and the purity of the TILs during separation, the quantity of miR-21 could be determined. It would be the next step to understand the effects of the miRNA on the PD-1 expression through TGFBR2.

Lastly, an additional finding of my work was that miR-21 mimic increases the cytotoxic activity of the OT-I T cell shown by the cytotoxicity assay. There was an unusual result at a ratio of 5:1 effector while the other ratio showed an increase in cytotoxicity function (**Fig.15**). The overexpression of miR-21 mimic did influence the production of cytokine and the number of productive cells. Still, the increase was not major except for the intensity fluorescence of TNF-α (**Fig.S2**). The pro-inflammatory cytokine could be the cause of the high cytotoxic activity. However, the molecule does have effects on the target cells and the effector cells. It's responsible for the AICD [111,112]. It can trigger the apoptosis of cancer in the proximity of the producing cells. The use of the kit limits us to determine the cells affected by the cytotoxic molecules. With the present results, it's hard to conclude the mechanism of miR-21 mimic cytokine production. Other studies showed an increase in IL-2 and IFN-γ production in the $CD8^+$ T cells after their transduction with miR-21. Controversially, a group that used an inhibitor of miR-21 showed an increase of $IL\text{-}2^+$ and $TNF\text{-}\alpha^+$ T cells with a decrease of $GzmB^+$ T cells.

The regulation of the pro-inflammatory expression is mediated by four TFs: AP-1, NF-κB, NFAT and Runx3. This last TF mediated the expression of Prf1 [173]. Furthermore,

the expression of Runx3 is dependent on the $CD8^+$ T-cell activation [174]. Upon the activation of the $CD8^+$ T cells, IL-2, TNF-α and IFN-γ are upregulated through the interaction of their promotor with AP-1 and NFAT. Also, GzmB expression is regulated by NFAT. miR-21 targets PDCD4, a suppressor of AP-1 dimerization, another important target would be PTEN and its influence on the PI3K/AKT signaling pathway [156]. Due to the influence of miR-21 on the signaling pathway, it plays an important central role in the $CD8^+$ T cell activation and cytotoxic activity as shown by other papers and the results presented. The increase of miR-21 expression should improve the production of multiple cytokines while repressing the inhibitory signaling pathway. In the cytokine production, IFN-γ and TNF-α MFI and productive cells did augment after the transduction. Regarding the production of GzmB, Prf and IL-2, the expression of the protein reduces in the miR-21 mimic transduced T cells. However, the number of producing cells slightly increase when compared to the control. This could indicate the positive and negative effects of miR-21 against other targets, one of them being p85α, a subunit of PI3K. This protein is essential in the survival and proliferation of the $CD8^+$ T cells.

During the ACT experiment, the tumor growth was reduced after the transfer of miR-21 OT-I. To identify the effects of this transfer on the surrounding immune cells, there were changes in the type of infiltrated T cells. In the transfer OT-I miR-21 group, we noticed a lower population of $CD4^+$ T cells, while the $CD8^+$ T cell population was separated into two groups: high infiltration of $CD8^+$ T cell versus low migration of $CD8^+$ T cell (**Fig.17**). Regarding the phenotype markers, the exhausted T cells were more prevalent in the miR-21 mimic injected mice compared to the control. It is also seen that the overall expression of PD-1 was higher. The other effects of miR-21 ACT are seen to reduce the effector population and the memory population inside the TME as well as to reduce the $CD44^+$ population. Surprisingly, although the $CD44^+$ cells number was reduced, the overall intensity of their expression was increased in the $CD8^+$ T cells (**Fig.18,19**). Furthermore, the expression of CD45 augmented after the transfer even though all the $CD8^+$ T cells expressed CD45 at their surface, in either group (**Fig.19**). In the condition of HIV infection, the $CD45^{high}$ $CD8^+$ T cell express a high level of activation marker (CD38 and HLA-DR) and proliferation marker (Ki-67), as well as a high level of PD-1, which collaborates with the cell transfer [175]. The migration of OT-I miR-21 to the tumor may increase the activation

of the already present $CD8^+$ TILs, enhancing tumor rejection. Though, the mechanism is still unclear. It would be interesting to incorporate the αPD-1 treatment with the ACT to reject completely the tumor in the long term.

The results show the importance of miR-21 and miR-155 in the rejection or control of the tumor. The overexpression of the miR-21 in the $CD8^+$ T cells increases their cytotoxic activity by targeting inhibitor proteins as well as controlling the tumor growth after the transfer. The miRNA influences the production of the pro-inflammatory cytokine and the inhibitor signaling pathway. Because miR-21 targets TGFBR2, the expression of PD-1 should be decreased, as related to the qPCR. On the other hand, the protein level increased on the surface of the miR-21 transduced cells. This indicates the influence of other TFs regulating the exhaustion of the $CD8^+$ T cells.

Reference

1. Gorentla, B.K., and Zhong, X.P. (2012). T cell Receptor Signal Transduction in T lymphocytes. J Clin Cell Immunol *2012*, 5. 10.4172/2155-9899.S12-005.
2. Courtney, A.H., Lo, W.L., and Weiss, A. (2018). TCR Signaling: Mechanisms of Initiation and Propagation. Trends Biochem Sci *43*, 108-123. 10.1016/j.tibs.2017.11.008.
3. Labani-Motlagh, A., Ashja-Mahdavi, M., and Loskog, A. (2020). The Tumor Microenvironment: A Milieu Hindering and Obstructing Antitumor Immune Responses. Frontiers in Immunology *11*. 10.3389/fimmu.2020.00940.
4. Rudd, C.E., Trevillyan, J.M., Dasgupta, J.D., Wong, L.L., and Schlossman, S.F. (1988). The CD4 receptor is complexed in detergent lysates to a protein-tyrosine kinase (pp58) from human T lymphocytes. Proceedings of the National Academy of Sciences *85*, 5190-5194. doi:10.1073/pnas.85.14.5190.
5. Rudd, C.E. (2021). How the Discovery of the CD4/CD8-p56(lck) Complexes Changed Immunology and Immunotherapy. Front Cell Dev Biol *9*, 626095. 10.3389/fcell.2021.626095.
6. Rudd, C.E. (1990). CD4, CD8 and the TCR-CD3 complex: a novel class of protein-tyrosine kinase receptor. Immunology today *11*, 400-406. 10.1016/0167-5699(90)90159-7.
7. Veillette, A., Bolen, J.B., and Bookman, M.A. (1989). Alterations in tyrosine protein phosphorylation induced by antibody-mediated cross-linking of the CD4 receptor of T lymphocytes. Molecular and Cellular Biology *9*, 4441-4446. doi:10.1128/mcb.9.10.4441-4446.1989.
8. Nika, K., Soldani, C., Salek, M., Paster, W., Gray, A., Etzensperger, R., Fugger, L., Polzella, P., Cerundolo, V., Dushek, O., Hofer, T., et al. (2010). Constitutively active Lck kinase in T cells drives antigen receptor signal transduction. Immunity *32*, 766-777. 10.1016/j.immuni.2010.05.011.
9. Wei, Q., Brzostek, J., Sankaran, S., Casas, J., Hew, L.S., Yap, J., Zhao, X., Wojciech, L., and Gascoigne, N.R.J. (2020). Lck bound to coreceptor is less active than free Lck. Proc Natl Acad Sci U S A *117*, 15809-15817. 10.1073/pnas.1913334117.
10. Xu, C., Gagnon, E., Call, M.E., Schnell, J.R., Schwieters, C.D., Carman, C.V., Chou, J.J., and Wucherpfennig, K.W. (2008). Regulation of T cell receptor activation by dynamic membrane binding of the CD3epsilon cytoplasmic tyrosine-based motif. Cell *135*, 702-713. 10.1016/j.cell.2008.09.044.
11. Zimmermann, K., Eells, R., Heinrich, F., Rintoul, S., Josey, B., Shekhar, P., Losche, M., and Stern, L.J. (2017). The cytosolic domain of T-cell receptor zeta associates with membranes in a dynamic equilibrium and deeply penetrates the bilayer. J Biol Chem *292*, 17746-17759. 10.1074/jbc.M117.794370.
12. Hwang, J.R., Byeon, Y., Kim, D., and Park, S.G. (2020). Recent insights of T cell receptor-mediated signaling pathways for T cell activation and development. Exp Mol Med *52*, 750-761. 10.1038/s12276-020-0435-8.
13. Rudd, C.E. (1999). Adaptors and Molecular Scaffolds in Immune Cell Signaling. Cell *96*, 5-8. https://doi.org/10.1016/S0092-8674(00)80953-8.

14. Zhang, W., Sommers, C.L., Burshtyn, D.N., Stebbins, C.C., DeJarnette, J.B., Trible, R.P., Grinberg, A., Tsay, H.C., Jacobs, H.M., Kessler, C.M., Long, E.O., et al. (1999). Essential Role of LAT in T Cell Development. Immunity *10*, 323-332. https://doi.org/10.1016/S1074-7613(00)80032-1.
15. Rossy, J., Williamson, D.J., and Gaus, K. (2012). How does the kinase Lck phosphorylate the T cell receptor? Spatial organization as a regulatory mechanism. Front Immunol *3*, 167. 10.3389/fimmu.2012.00167.
16. Wang, H., Kadlecek, T.A., Au-Yeung, B.B., Goodfellow, H.E., Hsu, L.Y., Freedman, T.S., and Weiss, A. (2010). ZAP-70: an essential kinase in T-cell signaling. Cold Spring Harb Perspect Biol *2*, a002279. 10.1101/cshperspect.a002279.
17. Balagopalan, L., Coussens, N.P., Sherman, E., Samelson, L.E., and Sommers, C.L. (2010). The LAT story: a tale of cooperativity, coordination, and choreography. Cold Spring Harb Perspect Biol *2*, a005512. 10.1101/cshperspect.a005512.
18. Zhang, E.Y., Parker, B.L., and Yankee, T.M. (2011). Gads regulates the expansion phase of CD8+ T cell-mediated immunity. J Immunol *186*, 4579-4589. 10.4049/jimmunol.1001604.
19. Balagopalan, L., Kortum, R.L., Coussens, N.P., Barr, V.A., and Samelson, L.E. (2015). The linker for activation of T cells (LAT) signaling hub: from signaling complexes to microclusters. J Biol Chem *290*, 26422-26429. 10.1074/jbc.R115.665869.
20. Koretzky, G.A., Abtahian, F., and Silverman, M.A. (2006). SLP76 and SLP65: complex regulation of signalling in lymphocytes and beyond. Nat Rev Immunol *6*, 67-78. 10.1038/nri1750.
21. Sela, M., Bogin, Y., Beach, D., Oellerich, T., Lehne, J., Smith-Garvin, J.E., Okumura, M., Starosvetsky, E., Kosoff, R., Libman, E., Koretzky, G., et al. (2011). Sequential phosphorylation of SLP-76 at tyrosine 173 is required for activation of T and mast cells. EMBO J *30*, 3160-3172. 10.1038/emboj.2011.213.
22. Lettau, M., Pieper, J., and Janssen, O. (2009). Nck adapter proteins: functional versatility in T cells. Cell Commun Signal *7*, 1. 10.1186/1478-811X-7-1.
23. Gaylo, A., Schrock, D.C., Fernandes, N.R., and Fowell, D.J. (2016). T Cell Interstitial Migration: Motility Cues from the Inflamed Tissue for Micro- and Macro-Positioning. Front Immunol *7*, 428. 10.3389/fimmu.2016.00428.
24. Muller, W.A. (2011). Mechanisms of leukocyte transendothelial migration. Annu Rev Pathol *6*, 323-344. 10.1146/annurev-pathol-011110-130224.
25. Shim, E.K., Jung, S.H., and Lee, J.R. (2011). Role of two adaptor molecules SLP-76 and LAT in the PI3K signaling pathway in activated T cells. J Immunol *186*, 2926-2935. 10.4049/jimmunol.1001785.
26. Song, G., Ouyang, G., and Bao, S. (2005). The activation of Akt/PKB signaling pathway and cell survival. Journal of Cellular and Molecular Medicine *9*, 59-71. https://doi.org/10.1111/j.1582-4934.2005.tb00337.x.
27. Andreotti, A.H., Schwartzberg, P.L., Joseph, R.E., and Berg, L.J. (2010). T-cell signaling regulated by the Tec family kinase, Itk. Cold Spring Harb Perspect Biol *2*, a002287. 10.1101/cshperspect.a002287.
28. Davis, R.J. (2000). Signal Transduction by the JNK Group of MAP Kinases. Cell *103*, 239-252. https://doi.org/10.1016/S0092-8674(00)00116-1.

29. Papavassiliou, A.G., and Musti, A.M. (2020). The Multifaceted Output of c-Jun Biological Activity: Focus at the Junction of CD8 T Cell Activation and Exhaustion. Cells *9*. 10.3390/cells9112470.
30. Park, Y.J., Yoo, S.A., Kim, M., and Kim, W.U. (2020). The Role of Calcium-Calcineurin-NFAT Signaling Pathway in Health and Autoimmune Diseases. Front Immunol *11*, 195. 10.3389/fimmu.2020.00195.
31. Putney, J.W., and Tomita, T. (2012). Phospholipase C signaling and calcium influx. Adv Biol Regul *52*, 152-164. 10.1016/j.advenzreg.2011.09.005.
32. Haaning Andersen, A.D., Lange, M., and Lillevang, S.T. (2003). Allelic variation of the inducible costimulator (ICOS) gene: detection of polymorphisms, analysis of the promoter region, and extended haplotype estimation. Tissue Antigens *61*, 276-285. https://doi.org/10.1034/j.1399-0039.2003.00019.x.
33. Lopez-Cabrera, M., Munoz, E., Blazquez, M.V., Ursa, M.A., Santis, A.G., and Sanchez-Madrid, F. (1995). Transcriptional regulation of the gene encoding the human C-type lectin leukocyte receptor AIM/CD69 and functional characterization of its tumor necrosis factor-alpha-responsive elements. J Biol Chem *270*, 21545-21551. 10.1074/jbc.270.37.21545.
34. Hinz, M., Lemke, P., Anagnostopoulos, I., Hacker, C., Krappmann, D., Mathas, S., Dorken, B., Zenke, M., Stein, H., and Scheidereit, C. (2002). Nuclear factor kappaB-dependent gene expression profiling of Hodgkin's disease tumor cells, pathogenetic significance, and link to constitutive signal transducer and activator of transcription 5a activity. J Exp Med *196*, 605-617. 10.1084/jem.20020062.
35. Walling, B.L., and Kim, M. (2018). LFA-1 in T Cell Migration and Differentiation. Front Immunol *9*, 952. 10.3389/fimmu.2018.00952.
36. Bierer, B.E., and Burakoff, S.J. (1988). T cell adhesion molecules. FASEB journal : official publication of the Federation of American Societies for Experimental Biology *2*, 2584-2590. 10.1096/fasebj.2.10.2838364.
37. Esensten, J.H., Helou, Y.A., Chopra, G., Weiss, A., and Bluestone, J.A. (2016). CD28 Costimulation: From Mechanism to Therapy. Immunity *44*, 973-988. 10.1016/j.immuni.2016.04.020.
38. Casar, B., Arozarena, I., Sanz-Moreno, V., Pinto, A., Agudo-Ibanez, L., Marais, R., Lewis, R.E., Berciano, M.T., and Crespo, P. (2009). Ras subcellular localization defines extracellular signal-regulated kinase 1 and 2 substrate specificity through distinct utilization of scaffold proteins. Mol Cell Biol *29*, 1338-1353. 10.1128/MCB.01359-08.
39. Thome, M., Charton, J.E., Pelzer, C., and Hailfinger, S. (2010). Antigen receptor signaling to NF-kappaB via CARMA1, BCL10, and MALT1. Cold Spring Harb Perspect Biol *2*, a003004. 10.1101/cshperspect.a003004.
40. David, L., Li, Y., Ma, J., Garner, E., Zhang, X., and Wu, H. (2018). Assembly mechanism of the CARMA1-BCL10-MALT1-TRAF6 signalosome. Proc Natl Acad Sci U S A *115*, 1499-1504. 10.1073/pnas.1721967115.
41. Bai, D., Ueno, L., and Vogt, P.K. (2009). Akt-mediated regulation of NFkappaB and the essentialness of NFkappaB for the oncogenicity of PI3K and Akt. Int J Cancer *125*, 2863-2870. 10.1002/ijc.24748.
42. Kim, E.H., and Suresh, M. (2013). Role of PI3K/Akt signaling in memory CD8 T cell differentiation. Front Immunol *4*, 20. 10.3389/fimmu.2013.00020.

43. Manning, B.D., and Toker, A. (2017). AKT/PKB Signaling: Navigating the Network. Cell *169*, 381-405. 10.1016/j.cell.2017.04.001.
44. Porta, C., Paglino, C., and Mosca, A. (2014). Targeting PI3K/Akt/mTOR Signaling in Cancer. Front Oncol *4*, 64. 10.3389/fonc.2014.00064.
45. Liu, Y., Liu, S., Wu, C., Huang, W., Xu, B., Lian, S., Wang, L., Yue, S., Chen, N., and Zhu, Z. (2020). PD-1-Mediated PI3K/Akt/mTOR, Caspase 9/Caspase 3 and ERK Pathways Are Involved in Regulating the Apoptosis and Proliferation of CD4(+) and CD8(+) T Cells During BVDV Infection in vitro. Front Immunol *11*, 467. 10.3389/fimmu.2020.00467.
46. Wang, Z., Cui, X., Hao, G., and He, J. (2021). Aberrant expression of PI3K/AKT signaling is involved in apoptosis resistance of hepatocellular carcinoma. Open Life Sci *16*, 1037-1044. 10.1515/biol-2021-0101.
47. Slomp, A., and Peperzak, V. (2018). Role and Regulation of Pro-survival BCL-2 Proteins in Multiple Myeloma. Front Oncol *8*, 533. 10.3389/fonc.2018.00533.
48. Shamas-Din, A., Kale, J., Leber, B., and Andrews, D.W. (2013). Mechanisms of action of Bcl-2 family proteins. Cold Spring Harb Perspect Biol *5*, a008714. 10.1101/cshperspect.a008714.
49. Basu, S., Totty, N.F., Irwin, M.S., Sudol, M., and Downward, J. (2003). Akt Phosphorylates the Yes-Associated Protein, YAP, to Induce Interaction with 14-3-3 and Attenuation of p73-Mediated Apoptosis. Molecular Cell *11*, 11-23. https://doi.org/10.1016/S1097-2765(02)00776-1.
50. Burgering, B.M.T., and Medema, R.H. (2003). Decisions on life and death: FOXO Forkhead transcription factors are in command when PKB/Akt is off duty. Journal of Leukocyte Biology *73*, 689-701. https://doi.org/10.1189/jlb.1202629.
51. Zhang, X., Tang, N., Hadden, T.J., and Rishi, A.K. (2011). Akt, FoxO and regulation of apoptosis. Biochim Biophys Acta *1813*, 1978-1986. 10.1016/j.bbamcr.2011.03.010.
52. Johnstone, R.W., Frew, A.J., and Smyth, M.J. (2008). The TRAIL apoptotic pathway in cancer onset, progression and therapy. Nat Rev Cancer *8*, 782-798. 10.1038/nrc2465.
53. Chibaya, L., Karim, B., Zhang, H., and Jones, S.N. (2021). Mdm2 phosphorylation by Akt regulates the p53 response to oxidative stress to promote cell proliferation and tumorigenesis. Proc Natl Acad Sci U S A *118*. 10.1073/pnas.2003193118.
54. Wang, H., Xu, J., Lazarovici, P., Quirion, R., and Zheng, W. (2018). cAMP Response Element-Binding Protein (CREB): A Possible Signaling Molecule Link in the Pathophysiology of Schizophrenia. Front Mol Neurosci *11*, 255. 10.3389/fnmol.2018.00255.
55. Li, X.Y., Zhan, X.R., Liu, X.M., and Wang, X.C. (2011). CREB is a regulatory target for the protein kinase Akt/PKB in the differentiation of pancreatic ductal cells into islet beta-cells mediated by hepatocyte growth factor. Biochem Biophys Res Commun *404*, 711-716. 10.1016/j.bbrc.2010.12.048.
56. Wen, A.Y., Sakamoto, K.M., and Miller, L.S. (2010). The role of the transcription factor CREB in immune function. J Immunol *185*, 6413-6419. 10.4049/jimmunol.1001829.
57. Pugazhenthi, S., Nesterova, A., Sable, C., Heidenreich, K.A., Boxer, L.M., Heasley, L.E., and Reusch, J.E.B. (2000). Akt/Protein Kinase B Up-regulates Bcl-

2 Expression through cAMP-response Element-binding Protein*. Journal of Biological Chemistry *275*, 10761-10766. https://doi.org/10.1074/jbc.275.15.10761.
58. Gautrey, H.L., and Tyson-Capper, A.J. (2012). Regulation of Mcl-1 by SRSF1 and SRSF5 in cancer cells. PLoS One *7*, e51497. 10.1371/journal.pone.0051497.
59. Chou, C.H., Lai, S.L., Chen, C.N., Lee, P.H., Peng, F.C., Kuo, M.L., and Lai, H.S. (2013). IL-6 regulates Mcl-1L expression through the JAK/PI3K/Akt/CREB signaling pathway in hepatocytes: implication of an anti-apoptotic role during liver regeneration. PLoS One *8*, e66268. 10.1371/journal.pone.0066268.
60. Shaw, R.J., Bardeesy, N., Manning, B.D., Lopez, L., Kosmatka, M., DePinho, R.A., and Cantley, L.C. (2004). The LKB1 tumor suppressor negatively regulates mTOR signaling. Cancer Cell *6*, 91-99. 10.1016/j.ccr.2004.06.007.
61. Iwenofu, O.H., Lackman, R.D., Staddon, A.P., Goodwin, D.G., Haupt, H.M., and Brooks, J.S. (2008). Phospho-S6 ribosomal protein: a potential new predictive sarcoma marker for targeted mTOR therapy. Mod Pathol *21*, 231-237. 10.1038/modpathol.3800995.
62. Chauvin, C., Koka, V., Nouschi, A., Mieulet, V., Hoareau-Aveilla, C., Dreazen, A., Cagnard, N., Carpentier, W., Kiss, T., Meyuhas, O., and Pende, M. (2014). Ribosomal protein S6 kinase activity controls the ribosome biogenesis transcriptional program. Oncogene *33*, 474-483. 10.1038/onc.2012.606.
63. Biever, A., Valjent, E., and Puighermanal, E. (2015). Ribosomal Protein S6 Phosphorylation in the Nervous System: From Regulation to Function. Front Mol Neurosci *8*, 75. 10.3389/fnmol.2015.00075.
64. Qin, X., Jiang, B., and Zhang, Y. (2016). 4E-BP1, a multifactor regulated multifunctional protein. Cell Cycle *15*, 781-786. 10.1080/15384101.2016.1151581.
65. Papadopoli, D., Pollak, M., and Topisirovic, I. (2021). The role of GSK3 in metabolic pathway perturbations in cancer. Biochim Biophys Acta Mol Cell Res *1868*, 119059. 10.1016/j.bbamcr.2021.119059.
66. Szwed, A., Kim, E., and Jacinto, E. (2021). Regulation and metabolic functions of mTORC1 and mTORC2. Physiol Rev *101*, 1371-1426. 10.1152/physrev.00026.2020.
67. Tan, V.P., and Miyamoto, S. (2015). HK2/hexokinase-II integrates glycolysis and autophagy to confer cellular protection. Autophagy *11*, 963-964. 10.1080/15548627.2015.1042195.
68. Momcilovic, M., Bailey, S.T., Lee, J.T., Fishbein, M.C., Braas, D., Go, J., Graeber, T.G., Parlati, F., Demo, S., Li, R., Walser, T.C., et al. (2018). The GSK3 Signaling Axis Regulates Adaptive Glutamine Metabolism in Lung Squamous Cell Carcinoma. Cancer Cell *33*, 905-921 e905. 10.1016/j.ccell.2018.04.002.
69. Tran, C.W., Saibil, S.D., Le Bihan, T., Hamilton, S.R., Lang, K.S., You, H., Lin, A.E., Garza, K.M., Elford, A.R., Tai, K., Parsons, M.E., et al. (2017). Glycogen Synthase Kinase-3 Modulates Cbl-b and Constrains T Cell Activation. J Immunol *199*, 4056-4065. 10.4049/jimmunol.1600396.
70. Hermida, M.A., Dinesh Kumar, J., and Leslie, N.R. (2017). GSK3 and its interactions with the PI3K/AKT/mTOR signalling network. Adv Biol Regul *65*, 5-15. 10.1016/j.jbior.2017.06.003.
71. Seif, F., Khoshmirsafa, M., Aazami, H., Mohsenzadegan, M., Sedighi, G., and Bahar, M. (2017). The role of JAK-STAT signaling pathway and its regulators in

the fate of T helper cells. Cell Commun Signal *15*, 23. 10.1186/s12964-017-0177-y.
72. St Paul, M., and Ohashi, P.S. (2020). The Roles of CD8(+) T Cell Subsets in Antitumor Immunity. Trends in cell biology *30*, 695-704. 10.1016/j.tcb.2020.06.003.
73. Salas, A., Hernandez-Rocha, C., Duijvestein, M., Faubion, W., McGovern, D., Vermeire, S., Vetrano, S., and Vande Casteele, N. (2020). JAK-STAT pathway targeting for the treatment of inflammatory bowel disease. Nat Rev Gastroenterol Hepatol *17*, 323-337. 10.1038/s41575-020-0273-0.
74. Ruiz-Medina, B.E., Ross, J.A., and Kirken, R.A. (2015). Interleukin-2 Receptor beta Thr-450 Phosphorylation Is a Positive Regulator for Receptor Complex Stability and Activation of Signaling Molecules. J Biol Chem *290*, 20972-20983. 10.1074/jbc.M115.660654.
75. Rawlings, J.S., Rosler, K.M., and Harrison, D.A. (2004). The JAK/STAT signaling pathway. J Cell Sci *117*, 1281-1283. 10.1242/jcs.00963.
76. Steelman, L.S., Pohnert, S.C., Shelton, J.G., Franklin, R.A., Bertrand, F.E., and McCubrey, J.A. (2004). JAK/STAT, Raf/MEK/ERK, PI3K/Akt and BCR-ABL in cell cycle progression and leukemogenesis. Leukemia *18*, 189-218. 10.1038/sj.leu.2403241.
77. Yoshimura, A., Naka, T., and Kubo, M. (2007). SOCS proteins, cytokine signalling and immune regulation. Nat Rev Immunol *7*, 454-465. 10.1038/nri2093.
78. Seidel, J.A., Otsuka, A., and Kabashima, K. (2018). Anti-PD-1 and Anti-CTLA-4 Therapies in Cancer: Mechanisms of Action, Efficacy, and Limitations. Front Oncol *8*, 86. 10.3389/fonc.2018.00086.
79. Boussiotis, V.A., Chatterjee, P., and Li, L. (2014). Biochemical signaling of PD-1 on T cells and its functional implications. Cancer J *20*, 265-271. 10.1097/PPO.0000000000000059.
80. Frearson, J.A., and Alexander, D.R. (1998). The phosphotyrosine phosphatase SHP-2 participates in a multimeric signaling complex and regulates T cell receptor (TCR) coupling to the Ras/mitogen-activated protein kinase (MAPK) pathway in Jurkat T cells. The Journal of experimental medicine *187*, 1417-1426. 10.1084/jem.187.9.1417.
81. Wei, F., Zhong, S., Ma, Z., Kong, H., Medvec, A., Ahmed, R., Freeman, G.J., Krogsgaard, M., and Riley, J.L. (2013). Strength of PD-1 signaling differentially affects T-cell effector functions. Proc Natl Acad Sci U S A *110*, E2480-2489. 10.1073/pnas.1305394110.
82. Mizuno, R., Sugiura, D., Shimizu, K., Maruhashi, T., Watada, M., Okazaki, I.M., and Okazaki, T. (2019). PD-1 Primarily Targets TCR Signal in the Inhibition of Functional T Cell Activation. Front Immunol *10*, 630. 10.3389/fimmu.2019.00630.
83. Hui, E., Cheung, J., Zhu, J., Su, X., Taylor, M.J., Wallweber, H.A., Sasmal, D.K., Huang, J., Kim, J.M., Mellman, I., and Vale, R.D. (2017). T cell costimulatory receptor CD28 is a primary target for PD-1-mediated inhibition. Science (New York, N.Y.) *355*, 1428-1433. 10.1126/science.aaf1292.
84. Patsoukis, N., Wang, Q., Strauss, L., and Boussiotis, V.A. (2020). Revisiting the PD-1 pathway. Sci Adv *6*. 10.1126/sciadv.abd2712.
85. Marasco, M., Berteotti, A., Weyershaeuser, J., Thorausch, N., Sikorska, J., Krausze, J., Brandt, H.J., Kirkpatrick, J., Rios, P., Schamel, W.W., Köhn, M., et al.

(2020). Molecular mechanism of SHP2 activation by PD-1 stimulation. Sci Adv *6*, eaay4458-eaay4458. 10.1126/sciadv.aay4458.
86. Chemnitz, J.M., Parry, R.V., Nichols, K.E., June, C.H., and Riley, J.L. (2004). SHP-1 and SHP-2 associate with immunoreceptor tyrosine-based switch motif of programmed death 1 upon primary human T cell stimulation, but only receptor ligation prevents T cell activation. J Immunol *173*, 945-954. 10.4049/jimmunol.173.2.945.
87. Nguyen, T.V., Ke, Y., Zhang, E.E., and Feng, G.S. (2006). Conditional deletion of Shp2 tyrosine phosphatase in thymocytes suppresses both pre-TCR and TCR signals. J Immunol *177*, 5990-5996. 10.4049/jimmunol.177.9.5990.
88. Celis-Gutierrez, J., Blattmann, P., Zhai, Y., Jarmuzynski, N., Ruminski, K., Gregoire, C., Ounoughene, Y., Fiore, F., Aebersold, R., Roncagalli, R., Gstaiger, M., et al. (2019). Quantitative Interactomics in Primary T Cells Provides a Rationale for Concomitant PD-1 and BTLA Coinhibitor Blockade in Cancer Immunotherapy. Cell Rep *27*, 3315-3330 e3317. 10.1016/j.celrep.2019.05.041.
89. Rota, G., Niogret, C., Dang, A.T., Barros, C.R., Fonta, N.P., Alfei, F., Morgado, L., Zehn, D., Birchmeier, W., Vivier, E., and Guarda, G. (2018). Shp-2 Is Dispensable for Establishing T Cell Exhaustion and for PD-1 Signaling In Vivo. Cell Rep *23*, 39-49. 10.1016/j.celrep.2018.03.026.
90. Travis, M.A., and Sheppard, D. (2014). TGF-beta activation and function in immunity. Annu Rev Immunol *32*, 51-82. 10.1146/annurev-immunol-032713-120257.
91. Bai, X., Yi, M., Jiao, Y., Chu, Q., and Wu, K. (2019). Blocking TGF-beta Signaling To Enhance The Efficacy Of Immune Checkpoint Inhibitor. Onco Targets Ther *12*, 9527-9538. 10.2147/OTT.S224013.
92. Handy, D.E., Castro, R., and Loscalzo, J. (2011). Epigenetic modifications: basic mechanisms and role in cardiovascular disease. Circulation *123*, 2145-2156. 10.1161/CIRCULATIONAHA.110.956839.
93. Park, B.V., Freeman, Z.T., Ghasemzadeh, A., Chattergoon, M.A., Rutebemberwa, A., Steigner, J., Winter, M.E., Huynh, T.V., Sebald, S.M., Lee, S.J., Pan, F., et al. (2016). TGFbeta1-Mediated SMAD3 Enhances PD-1 Expression on Antigen-Specific T Cells in Cancer. Cancer Discov *6*, 1366-1381. 10.1158/2159-8290.CD-15-1347.
94. Stephen, T.L., Payne, K.K., Chaurio, R.A., Allegrezza, M.J., Zhu, H., Perez-Sanz, J., Perales-Puchalt, A., Nguyen, J.M., Vara-Ailor, A.E., Eruslanov, E.B., Borowsky, M.E., et al. (2017). SATB1 Expression Governs Epigenetic Repression of PD-1 in Tumor-Reactive T Cells. Immunity *46*, 51-64. 10.1016/j.immuni.2016.12.015.
95. Lai, A.Y., and Wade, P.A. (2011). Cancer biology and NuRD: a multifaceted chromatin remodelling complex. Nat Rev Cancer *11*, 588-596. 10.1038/nrc3091.
96. Cai, Y., Geutjes, E.J., de Lint, K., Roepman, P., Bruurs, L., Yu, L.R., Wang, W., van Blijswijk, J., Mohammad, H., de Rink, I., Bernards, R., et al. (2014). The NuRD complex cooperates with DNMTs to maintain silencing of key colorectal tumor suppressor genes. Oncogene *33*, 2157-2168. 10.1038/onc.2013.178.
97. Derynck, R., and Zhang, Y.E. (2003). Smad-dependent and Smad-independent pathways in TGF-beta family signalling. Nature *425*, 577-584. 10.1038/nature02006.

98. Batlle, E., and Massague, J. (2019). Transforming Growth Factor-beta Signaling in Immunity and Cancer. Immunity *50*, 924-940. 10.1016/j.immuni.2019.03.024.
99. Zhang, Y.E. (2017). Non-Smad Signaling Pathways of the TGF-beta Family. Cold Spring Harb Perspect Biol *9*. 10.1101/cshperspect.a022129.
100. Chaplin, D.D. (2010). Overview of the immune response. The Journal of allergy and clinical immunology *125*, S3-23. 10.1016/j.jaci.2009.12.980.
101. Verbsky, J.W., and Routes, J.R. (2018). 41 - Recurrent Fever, Infections, Immune Disorders, and Autoinflammatory Diseases. In Nelson Pediatric Symptom-Based Diagnosis, R.M. Kliegman, P.S. Lye, B.J. Bordini, H. Toth, and D. Basel, eds. (Elsevier), pp. 746-773.e741. https://doi.org/10.1016/B978-0-323-39956-2.00041-8.
102. Sugimoto, M.A., Vago, J.P., Perretti, M., and Teixeira, M.M. (2019). Mediators of the Resolution of the Inflammatory Response. Trends in immunology *40*, 212-227. 10.1016/j.it.2019.01.007.
103. Germain, R.N. (2002). T-cell development and the CD4–CD8 lineage decision. Nature Reviews Immunology *2*, 309-322. 10.1038/nri798.
104. Kurts, C., Robinson, B.W.S., and Knolle, P.A. (2010). Cross-priming in health and disease. Nature Reviews Immunology *10*, 403-414. 10.1038/nri2780.
105. Zhang, N., and Bevan, M.J. (2011). CD8(+) T cells: foot soldiers of the immune system. Immunity *35*, 161-168. 10.1016/j.immuni.2011.07.010.
106. Reiser, J., and Banerjee, A. (2016). Effector, Memory, and Dysfunctional CD8(+) T Cell Fates in the Antitumor Immune Response. Journal of immunology research *2016*, 8941260. 10.1155/2016/8941260.
107. Kalia, V., and Sarkar, S. (2018). Regulation of Effector and Memory CD8 T Cell Differentiation by IL-2-A Balancing Act. Front Immunol *9*, 2987. 10.3389/fimmu.2018.02987.
108. Kemp, R.A., and Ronchese, F. (2001). Tumor-specific Tc1, but not Tc2, cells deliver protective antitumor immunity. J Immunol *167*, 6497-6502. 10.4049/jimmunol.167.11.6497.
109. Mittrücker, H.W., Visekruna, A., and Huber, M. (2014). Heterogeneity in the differentiation and function of $CD8^+$ T cells. Archivum immunologiae et therapiae experimentalis *62*, 449-458. 10.1007/s00005-014-0293-y.
110. Rudd, C.E. (1996). Upstream-downstream: CD28 cosignaling pathways and T cell function. Immunity *4*, 527-534. 10.1016/s1074-7613(00)80479-3.
111. Jorgovanovic, D., Song, M., Wang, L., and Zhang, Y. (2020). Roles of IFN-γ in tumor progression and regression: a review. Biomarker Research *8*, 49. 10.1186/s40364-020-00228-x.
112. Ye, L.L., Wei, X.S., Zhang, M., Niu, Y.R., and Zhou, Q. (2018). The Significance of Tumor Necrosis Factor Receptor Type II in CD8(+) Regulatory T Cells and CD8(+) Effector T Cells. Front Immunol *9*, 583. 10.3389/fimmu.2018.00583.
113. Mehta, A.K., Gracias, D.T., and Croft, M. (2018). TNF activity and T cells. Cytokine *101*, 14-18. 10.1016/j.cyto.2016.08.003.
114. Kim, E.Y., and Teh, H.-S. (2001). TNF Type 2 Receptor (p75) Lowers the Threshold of T Cell Activation. The Journal of Immunology *167*, 6812. 10.4049/jimmunol.167.12.6812.
115. Twu, Y.-C., Gold, M.R., and Teh, H.-S. (2011). TNFR1 delivers pro-survival signals that are required for limiting TNFR2-dependent activation-induced cell

death (AICD) in CD8+ T cells. European Journal of Immunology *41*, 335-344. https://doi.org/10.1002/eji.201040639.
116. Obar, J.J., and Lefrançois, L. (2010). Memory CD8+ T cell differentiation. Annals of the New York Academy of Sciences *1183*, 251-266. 10.1111/j.1749-6632.2009.05126.x.
117. Youngblood, B., Wherry, E.J., and Ahmed, R. (2012). Acquired transcriptional programming in functional and exhausted virus-specific CD8 T cells. Current opinion in HIV and AIDS *7*, 50-57. 10.1097/COH.0b013e32834ddcf2.
118. Lucey, D.R., Clerici, M., and Shearer, G.M. (1996). Type 1 and type 2 cytokine dysregulation in human infectious, neoplastic, and inflammatory diseases. Clinical microbiology reviews *9*, 532-562. 10.1128/cmr.9.4.532.
119. Kurachi, M. (2019). CD8(+) T cell exhaustion. Seminars in immunopathology *41*, 327-337. 10.1007/s00281-019-00744-5.
120. Dolina, J.S., Van Braeckel-Budimir, N., Thomas, G.D., and Salek-Ardakani, S. (2021). CD8+ T Cell Exhaustion in Cancer. Frontiers in Immunology *12*. 10.3389/fimmu.2021.715234.
121. Philip, M., and Schietinger, A. (2019). Heterogeneity and fate choice: T cell exhaustion in cancer and chronic infections. Current opinion in immunology *58*, 98-103.
122. Ma, J., Zheng, B., Goswami, S., Meng, L., Zhang, D., Cao, C., Li, T., Zhu, F., Ma, L., Zhang, Z., Zhang, S., et al. (2019). PD1(Hi) CD8(+) T cells correlate with exhausted signature and poor clinical outcome in hepatocellular carcinoma. Journal for immunotherapy of cancer *7*, 331-331. 10.1186/s40425-019-0814-7.
123. Ando, M., Ito, M., Srirat, T., Kondo, T., and Yoshimura, A. (2020). Memory T cell, exhaustion, and tumor immunity. Immunological Medicine *43*, 1-9. 10.1080/25785826.2019.1698261.
124. Zhang, J., Lyu, T., Cao, Y., and Feng, H. (2021). Role of TCF-1 in differentiation, exhaustion, and memory of CD8+ T cells: A review. The FASEB Journal *35*, e21549. https://doi.org/10.1096/fj.202002566R.
125. Radoja, S., Saio, M., Schaer, D., Koneru, M., Vukmanovic, S., and Frey, A.B. (2001). CD8(+) tumor-infiltrating T cells are deficient in perforin-mediated cytolytic activity due to defective microtubule-organizing center mobilization and lytic granule exocytosis. J Immunol *167*, 5042-5051. 10.4049/jimmunol.167.9.5042.
126. Monu, N., and Frey, A.B. (2007). Suppression of proximal T cell receptor signaling and lytic function in CD8+ tumor-infiltrating T cells. Cancer research *67*, 11447-11454. 10.1158/0008-5472.Can-07-1441.
127. Macfarlane, L.-A., and Murphy, P.R. (2010). MicroRNA: Biogenesis, Function and Role in Cancer. Curr Genomics *11*, 537-561. 10.2174/138920210793175895.
128. Ha, M., and Kim, V.N. (2014). Regulation of microRNA biogenesis. Nature Reviews Molecular Cell Biology *15*, 509-524. 10.1038/nrm3838.
129. O'Brien, J., Hayder, H., Zayed, Y., and Peng, C. (2018). Overview of MicroRNA Biogenesis, Mechanisms of Actions, and Circulation. Frontiers in Endocrinology *9*. 10.3389/fendo.2018.00402.
130. Vimalraj, S., and Selvamurugan, N. (2012). MicroRNAs: Synthesis, Gene Regulation and Osteoblast Differentiation. Current issues in molecular biology *15*, 7-18.

131. Ambros, V., Bartel, B., Bartel, D.P., Burge, C.B., Carrington, J.C., Chen, X., Dreyfuss, G., Eddy, S.R., Griffiths-Jones, S., Marshall, M., Matzke, M., et al. (2003). A uniform system for microRNA annotation. RNA (New York, N.Y.) *9*, 277-279. 10.1261/rna.2183803.
132. Eulalio, A., Huntzinger, E., and Izaurralde, E. (2008). Getting to the root of miRNA-mediated gene silencing. Cell *132*, 9-14. 10.1016/j.cell.2007.12.024.
133. Khraiwesh, B., Arif, M.A., Seumel, G.I., Ossowski, S., Weigel, D., Reski, R., and Frank, W. (2010). Transcriptional control of gene expression by microRNAs. Cell *140*, 111-122. 10.1016/j.cell.2009.12.023.
134. Mehta, A., and Baltimore, D. (2016). MicroRNAs as regulatory elements in immune system logic. Nature Reviews Immunology *16*, 279-294. 10.1038/nri.2016.40.
135. Yang, N., Zhu, S., Lv, X., Qiao, Y., Liu, Y.-J., and Chen, J. (2018). MicroRNAs: Pleiotropic Regulators in the Tumor Microenvironment. Frontiers in Immunology *9*. 10.3389/fimmu.2018.02491.
136. Rodríguez-Galán, A., Fernández-Messina, L., and Sánchez-Madrid, F. (2018). Control of Immunoregulatory Molecules by miRNAs in T Cell Activation. Frontiers in immunology *9*, 2148-2148. 10.3389/fimmu.2018.02148.
137. Hirschberger, S., Hinske, L.C., and Kreth, S. (2018). MiRNAs: dynamic regulators of immune cell functions in inflammation and cancer. Cancer Letters *431*, 11-21. https://doi.org/10.1016/j.canlet.2018.05.020.
138. Dudda, J.C., Salaun, B., Ji, Y., Palmer, D.C., Monnot, G.C., Merck, E., Boudousquie, C., Utzschneider, D.T., Escobar, T.M., Perret, R., Muljo, S.A., et al. (2013). MicroRNA-155 is required for effector CD8+ T cell responses to virus infection and cancer. Immunity *38*, 742-753. 10.1016/j.immuni.2012.12.006.
139. Stelekati, E., Chen, Z., Manne, S., Kurachi, M., Ali, M.A., Lewy, K., Cai, Z., Nzingha, K., McLane, L.M., Hope, J.L., Fike, A.J., et al. (2018). Long-Term Persistence of Exhausted CD8 T Cells in Chronic Infection Is Regulated by MicroRNA-155. Cell Rep *23*, 2142-2156. 10.1016/j.celrep.2018.04.038.
140. He, W., Wang, C., Mu, R., Liang, P., Huang, Z., Zhang, J., and Dong, L. (2017). MiR-21 is required for anti-tumor immune response in mice: an implication for its bi-directional roles. Oncogene *36*, 4212-4223. 10.1038/onc.2017.62.
141. Monnot, G.C., Martinez-Usatorre, A., Lanitis, E., Lopes, S.F., Cheng, W.-C., Ho, P.-C., Irving, M., Coukos, G., Donda, A., and Romero, P. (2020). miR-155 Overexpression in OT-1 CD8⁺ T Cells Improves Anti-Tumor Activity against Low-Affinity Tumor Antigen. Molecular Therapy - Oncolytics *16*, 111-123. 10.1016/j.omto.2019.12.008.
142. Martinez-Usatorre, A., Sempere, L.F., Carmona, S.J., Carretero-Iglesia, L., Monnot, G., Speiser, D.E., Rufer, N., Donda, A., Zehn, D., Jandus, C., and Romero, P. (2019). MicroRNA-155 Expression Is Enhanced by T-cell Receptor Stimulation Strength and Correlates with Improved Tumor Control in Melanoma. Cancer immunology research *7*, 1013-1024. 10.1158/2326-6066.Cir-18-0504.
143. Liu, X., Li, Y., Li, Z., and Hou, T. (2021). miR-155 promotes proliferation and epithelial-mesenchymal transition of MCF-7 cells. Exp Ther Med *21*, 218-218. 10.3892/etm.2021.9650.
144. Rodriguez, A., Vigorito, E., Clare, S., Warren, M.V., Couttet, P., Soond, D.R., van Dongen, S., Grocock, R.J., Das, P.P., Miska, E.A., Vetrie, D., et al. (2007).

Requirement of bic/microRNA-155 for normal immune function. Science (New York, N.Y.) *316*, 608-611. 10.1126/science.1139253.
145. Escobar, T.M., Kanellopoulou, C., Kugler, D.G., Kilaru, G., Nguyen, C.K., Nagarajan, V., Bhairavabhotla, R.K., Northrup, D., Zahr, R., Burr, P., Liu, X., et al. (2014). miR-155 activates cytokine gene expression in Th17 cells by regulating the DNA-binding protein Jarid2 to relieve polycomb-mediated repression. Immunity *40*, 865-879. 10.1016/j.immuni.2014.03.014.
146. Feng, Z., Xia, Y., Zhang, M., and Zheng, J. (2013). MicroRNA-155 regulates T cell proliferation through targeting GSK3β in cardiac allograft rejection in a murine transplantation model. Cellular immunology *281*, 141-149. 10.1016/j.cellimm.2013.04.001.
147. Carissimi, C., Carucci, N., Colombo, T., Piconese, S., Azzalin, G., Cipolletta, E., Citarella, F., Barnaba, V., Macino, G., and Fulci, V. (2014). miR-21 is a negative modulator of T-cell activation. Biochimie *107 Pt B*, 319-326. 10.1016/j.biochi.2014.09.021.
148. Kroesen, B.J., Teteloshvili, N., Smigielska-Czepiel, K., Brouwer, E., Boots, A.M., van den Berg, A., and Kluiver, J. (2015). Immuno-miRs: critical regulators of T-cell development, function and ageing. Immunology *144*, 1-10. 10.1111/imm.12367.
149. Ruan, Q., Wang, P., Wang, T., Qi, J., Wei, M., Wang, S., Fan, T., Johnson, D., Wan, X., Shi, W., Sun, H., et al. (2014). MicroRNA-21 regulates T-cell apoptosis by directly targeting the tumor suppressor gene Tipe2. Cell Death & Disease *5*, e1095-e1095. 10.1038/cddis.2014.47.
150. Wang, S., Wan, X., and Ruan, Q. (2016). The MicroRNA-21 in Autoimmune Diseases. Int J Mol Sci *17*, 864. 10.3390/ijms17060864.
151. Mishra, S., Deng, J.J., Gowda, P.S., Rao, M.K., Lin, C.L., Chen, C.L., Huang, T., and Sun, L.Z. (2014). Androgen receptor and microRNA-21 axis downregulates transforming growth factor beta receptor II (TGFBR2) expression in prostate cancer. Oncogene *33*, 4097-4106. 10.1038/onc.2013.374.
152. Lin, H., Wei, S., Hurt, E.M., Green, M.D., Zhao, L., Vatan, L., Szeliga, W., Herbst, R., Harms, P.W., Fecher, L.A., Vats, P., et al. (2018). Host expression of PD-L1 determines efficacy of PD-L1 pathway blockade-mediated tumor regression. J Clin Invest *128*, 805-815. 10.1172/JCI96113.
153. Ji, S., Lee, J., Lee, E.S., Kim, D.H., and Sin, J.-I. (2021). B16 melanoma control by anti-PD-L1 requires CD8+ T cells and NK cells: application of anti-PD-L1 Abs and Trp2 peptide vaccines. Hum Vaccin Immunother *17*, 1910-1922. 10.1080/21645515.2020.1866951.
154. McGeary, S.E., Lin, K.S., Shi, C.Y., Pham, T.M., Bisaria, N., Kelley, G.M., and Bartel, D.P. (2019). The biochemical basis of microRNA targeting efficacy. Science (New York, N.Y.) *366*. 10.1126/science.aav1741.
155. Agarwal, V., Bell, G.W., Nam, J.-W., and Bartel, D.P. (2015). Predicting effective microRNA target sites in mammalian mRNAs. eLife *4*, e05005. 10.7554/eLife.05005.
156. Kim, C., Hu, B., Jadhav, R.R., Jin, J., Zhang, H., Cavanagh, M.M., Akondy, R.S., Ahmed, R., Weyand, C.M., and Goronzy, J.J. (2018). Activation of miR-21-Regulated Pathways in Immune Aging Selects against Signatures Characteristic of Memory T Cells. Cell Rep *25*, 2148-2162.e2145. 10.1016/j.celrep.2018.10.074.

157. Beyer, M., Thabet, Y., Müller, R.-U., Sadlon, T., Classen, S., Lahl, K., Basu, S., Zhou, X., Bailey-Bucktrout, S.L., Krebs, W., Schönfeld, E.A., et al. (2011). Repression of the genome organizer SATB1 in regulatory T cells is required for suppressive function and inhibition of effector differentiation. Nat Immunol *12*, 898-907. 10.1038/ni.2084.
158. Louafi, F., Martinez-Nunez, R.T., and Sanchez-Elsner, T. (2010). MicroRNA-155 targets SMAD2 and modulates the response of macrophages to transforming growth factor-{beta}. The Journal of biological chemistry *285*, 41328-41336. 10.1074/jbc.M110.146852.
159. Wu, M.F., Yang, J., Xiang, T., Shi, Y.Y., and Liu, L.J. (2014). miR-21 targets Fas ligand-mediated apoptosis in breast cancer cell line MCF-7. Journal of Huazhong University of Science and Technology. Medical sciences = Hua zhong ke ji da xue xue bao. Yi xue Ying De wen ban = Huazhong keji daxue xuebao. Yixue Yingdewen ban *34*, 190-194. 10.1007/s11596-014-1257-5.
160. Brown, C.Y., Dayan, S., Wong, S.W., Kaczmarek, A., Hope, C.M., Pederson, S.M., Arnet, V., Goodall, G.J., Russell, D., Sadlon, T.J., and Barry, S.C. (2018). FOXP3 and miR-155 cooperate to control the invasive potential of human breast cancer cells by down regulating ZEB2 independently of ZEB1. Oncotarget *9*, 27708-27727. 10.18632/oncotarget.25523.
161. Rudd, C.E., Chanthong, K., and Taylor, A. (2020). Small Molecule Inhibition of GSK-3 Specifically Inhibits the Transcription of Inhibitory Co-receptor LAG-3 for Enhanced Anti-tumor Immunity. Cell Rep *30*, 2075-2082.e2074. 10.1016/j.celrep.2020.01.076.
162. Taylor, A., Rothstein, D., and Rudd, C.E. (2018). Small-Molecule Inhibition of PD-1 Transcription Is an Effective Alternative to Antibody Blockade in Cancer Therapy. Cancer research *78*, 706-717. 10.1158/0008-5472.Can-17-0491.
163. Taylor, A., Harker, J.A., Chanthong, K., Stevenson, P.G., Zuniga, E.I., and Rudd, C.E. (2016). Glycogen Synthase Kinase 3 Inactivation Drives T-bet-Mediated Downregulation of Co-receptor PD-1 to Enhance CD8(+) Cytolytic T Cell Responses. Immunity *44*, 274-286. 10.1016/j.immuni.2016.01.018.
164. Bonneau, É., Neveu, B., Kostantin, E., Tsongalis, G.J., and de Guire, V. (2019). How close are miRNAs from clinical practice? A perspective on the diagnostic and therapeutic market. EJIFCC *30*, 114 - 127.
165. Asangani, I.A., Rasheed, S.A., Nikolova, D.A., Leupold, J.H., Colburn, N.H., Post, S., and Allgayer, H. (2008). MicroRNA-21 (miR-21) post-transcriptionally downregulates tumor suppressor Pdcd4 and stimulates invasion, intravasation and metastasis in colorectal cancer. Oncogene *27*, 2128-2136. 10.1038/sj.onc.1210856.
166. Bally, A.P.R., Austin, J.W., and Boss, J.M. (2016). Genetic and Epigenetic Regulation of PD-1 Expression. Journal of immunology (Baltimore, Md. : 1950) *196*, 2431-2437. 10.4049/jimmunol.1502643.
167. Baaten, B.J., Li, C.R., and Bradley, L.M. (2010). Multifaceted regulation of T cells by CD44. Communicative & integrative biology *3*, 508-512. 10.4161/cib.3.6.13495.
168. Baaten, B., Tinoco, R., Chen, A., and Bradley, L. (2012). Regulation of Antigen-Experienced T Cells: Lessons from the Quintessential Memory Marker CD44. Frontiers in Immunology *3*. 10.3389/fimmu.2012.00023.

169. Mrass, P., Kinjyo, I., Ng, L.G., Reiner, S.L., Puré, E., and Weninger, W. (2008). CD44 mediates successful interstitial navigation by killer T cells and enables efficient antitumor immunity. Immunity *29*, 971-985. 10.1016/j.immuni.2008.10.015.
170. Cho, J.-H., Kim, H.-O., Ju, Y.-J., Kye, Y.-C., Lee, G.-W., Lee, S.-W., Yun, C.-H., Bottini, N., Webster, K., Goodnow, C.C., Surh, C.D., et al. (2016). CD45-mediated control of TCR tuning in naïve and memory CD8+ T cells. Nature Communications *7*, 13373. 10.1038/ncomms13373.
171. Lippitz, B.E. (2013). Cytokine patterns in patients with cancer: a systematic review. The Lancet. Oncology *14*, e218-228. 10.1016/s1470-2045(12)70582-x.
172. De Melo, P., Pineros Alvarez, A.R., Ye, X., Blackman, A., Alves-Filho, J.C., Medeiros, A.I., Rathmell, J., Pua, H., and Serezani, C.H. (2021). Macrophage-Derived MicroRNA-21 Drives Overwhelming Glycolytic and Inflammatory Response during Sepsis via Repression of the PGE(2)/IL-10 Axis. J Immunol *207*, 902-912. 10.4049/jimmunol.2001251.
173. Pipkin, M.E., Rao, A., and Lichtenheld, M.G. (2010). The transcriptional control of the perforin locus. Immunological reviews *235*, 55-72. 10.1111/j.0105-2896.2010.00905.x.
174. Shan, Q., Zeng, Z., Xing, S., Li, F., Hartwig, S.M., Gullicksrud, J.A., Kurup, S.P., Van Braeckel-Budimir, N., Su, Y., Martin, M.D., Varga, S.M., et al. (2017). The transcription factor Runx3 guards cytotoxic CD8+ effector T cells against deviation towards follicular helper T cell lineage. Nat Immunol *18*, 931-939. 10.1038/ni.3773.
175. Petkov, S., Bekele, Y., Lakshmikanth, T., Hejdeman, B., Zazzi, M., Brodin, P., and Chiodi, F. (2020). High CD45 expression of CD8+ and CD4+ T cells correlates with the size of HIV-1 reservoir in blood. Scientific Reports *10*, 20425. 10.1038/s41598-020-77433-z.

Supplementary figures

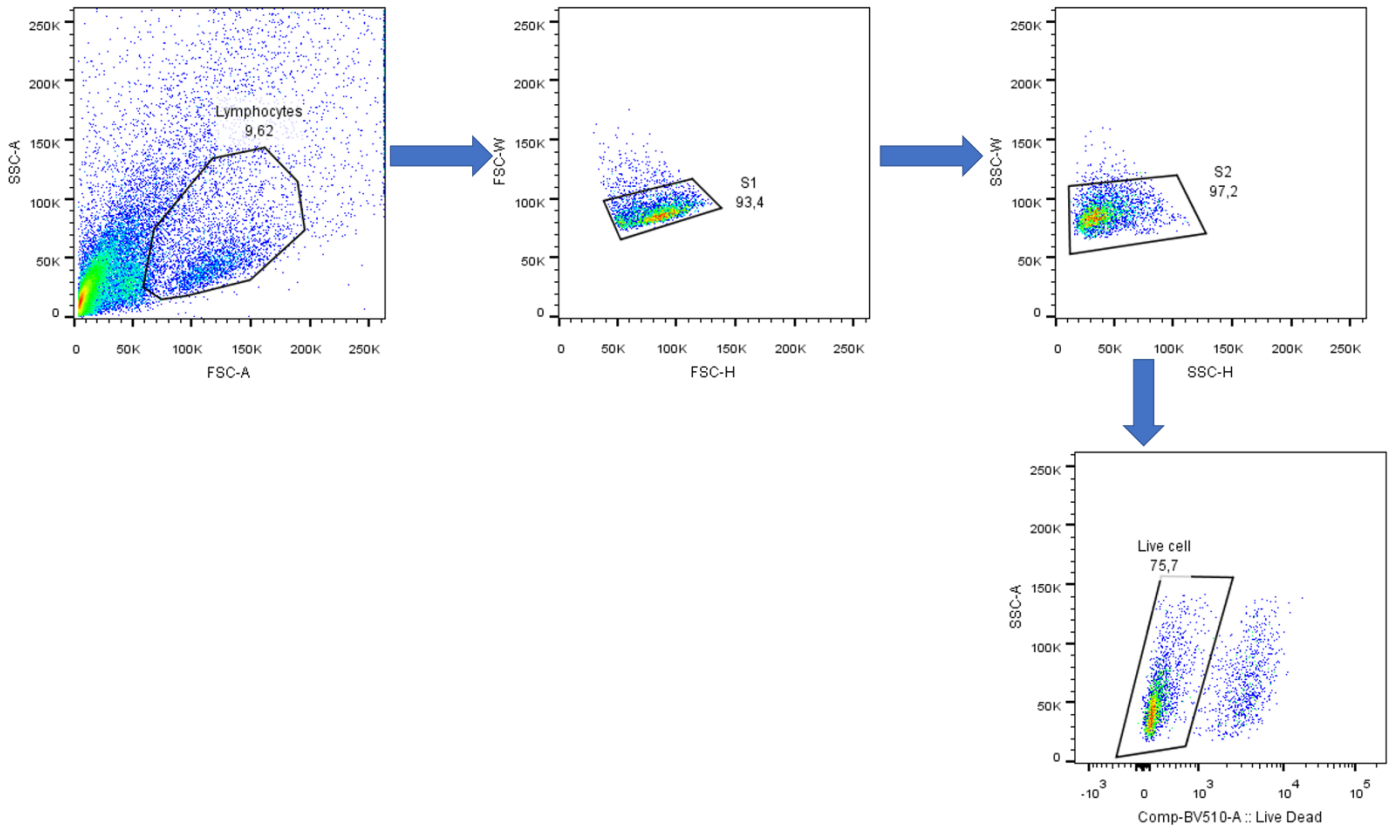

Figure S1: Gating strategy of the viSNE analysis from the tumor-bearing mice treated with αPD-L1 or αIgG isotype control. The FACS analysis and selection of the population were done by FlowJo. The method starts with the isolation of the lymphocytes from the tumor cells followed by the selection of single cells. During the sorting, some cells can be attached. So, only the single cells are selected. Finally, the live cells were selected (BV510- population).

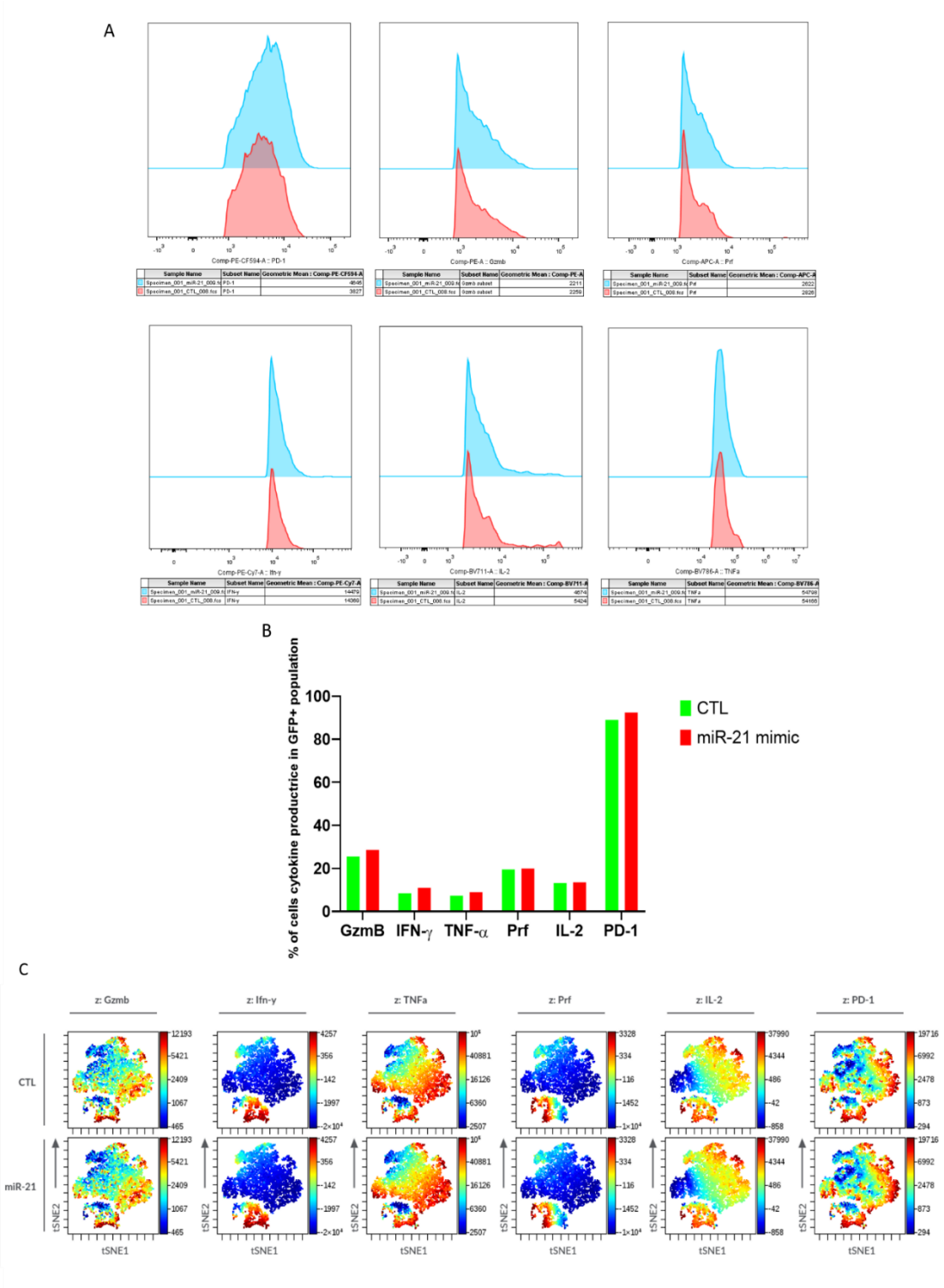

Figure S2: Cytokine production of miR-21 transduced CD8⁺ T cells. The CD8⁺ T cells were activated and transduced before the FACS and viSNE analysis. Before the staining, the cells were treated with BFA for 4 hours. All the analyses were done on the GFP⁺ population between the CTL and miR-21 mimic. (A) The histogram and MFI of each cytokine from CTL (Red) and miR-21 mimic (Blue). (B) Percentage of expressing population. (C) viSNE analysis of the cytokine production.

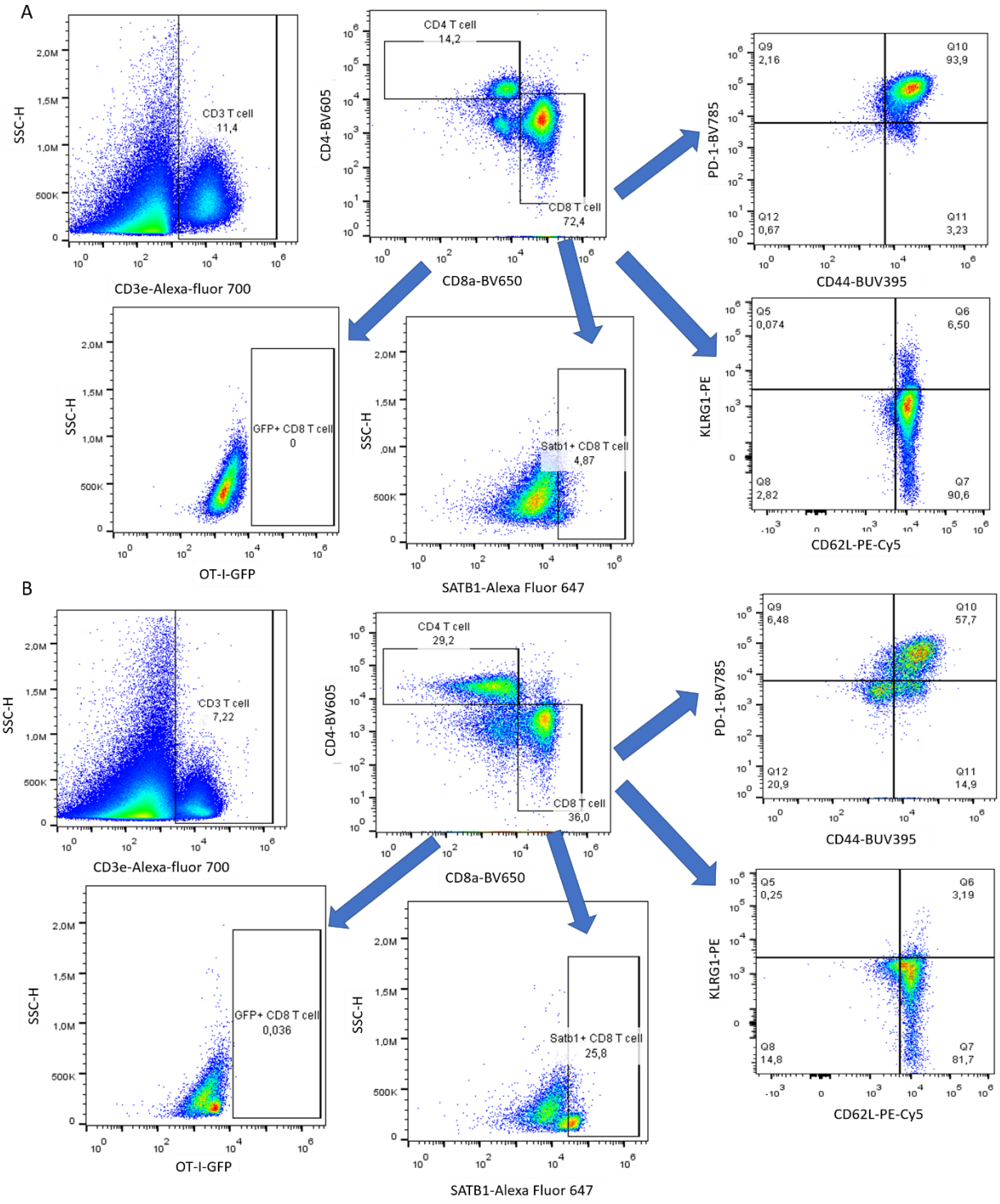

Figure S3: FACS graph of the CD8⁺ T cell phenotyping population after the transfer of (A) miR-21 mimic transduced OT-I and (B) mock-transduced OT-I. The FACS data file were concatenated in the program FlowJo between each group. The gating strategy used is the same as shown in fig. S1. The lymphocyte was isolated followed by the selection of singles cells and the live cells.